Development of Intrinsic Motoneuron Properties in Humans

by

Ghazaleh Mohammadalinejad

A thesis submitted in partial fulfillment of the requirements for the degree of

Master of Science

Neuroscience

University of Alberta

Abstract

Motoneuron properties and their firing patterns undergo significant changes throughout development and in response to neuromodulators like serotonin. In this thesis we examined intrinsic motoneuron properties in 50 typically developing participants ranging in age from 7 to 53 years. The primary objective was to investigate the age-related development of persistent inward currents (PICs) and spike frequency adaptation in a young development group (aged 7 to 17 years), a young adult group (aged 18 to 28 years) and an older adult group (aged 32 to 53 years). PICs are predominantly mediated by voltage- and calcium-dependent calcium and sodium ions, and they provide a long-lasting intrinsic depolarization to the motoneuron to help amplify and prolong synaptic inputs. To assess the contribution of the PIC to the self-sustained firing of motoneurons, we identified the spike times of multiple single motor units from the tibialis anterior (TA) muscle, an ankle dorsiflexor, using a 64-electrode surface electromyography (EMG) grid. The firing frequency (F) profiles of low threshold motor units were used to estimate the synaptic input to the TA motoneuron pool given their linear response to synaptic inputs. The contribution of the PIC to self-sustained firing was estimated based on the estimated synaptic input required to de-recruit the motor unit compared to the input needed for recruitment (ΔF) during a slowly increasing and then decreasing isometric dorsiflexion. ΔF was larger in the young development group (~ 5.8 Hz, n = 20) compared to the young (~ 4.9 Hz, n = 13) and older (~ 4.8 Hz, n = 8) adult groups, consistent with a developmental decrease in PIC-mediated self-sustained firing. ΔF was also larger in a subset of participants taking selective serotonin reuptake inhibitors (SSRIs: ~ 6.5 Hz, 11 to 28 years old, n = 9) compared to their age-matched controls (~ 5.3 Hz, n = 26), consistent with increased levels of spinal serotonin facilitating the motoneuron PIC.

We also investigated how potential intrinsic conductances may affect the nonlinear firing behaviour of the motor units (motoneurons) in response to a presumed linear increase

in synaptic drive by quantifying the slope and duration of three iteratively joined lines fit to the ascending firing rate profile. We proposed that the firing rate acceleration at the onset of motor unit discharge reflects the acceleration in membrane depolarization during the onset of PIC activation (termed secondary range) and the shallower increase in firing that follows this reflects motoneuron discharge during full PIC activation (termed tertiary range). In some motor units, firing rates also decreased before peak torque was reached (termed tertiary sag range) and we proposed this reflects spike frequency adaptation, another intrinsic property of the motoneuron. Participants in the young development and SSRI groups had steeper secondary range slopes (~ 5.7 and 7.2 Hz/s, respectively) compared to the young and older adult groups (both ~ 4.3 Hz/s), consistent with the PIC in the former two groups producing a steeper acceleration in membrane depolarization at the onset of motoneuron firing. In contrast, there were no changes in the slope or duration of the tertiary range between the different age groups or in response to SSRI intake. The slope of the tertiary sag range also decreased with age across the young development and young adult groups (r = -0.38, n = 33) and was steeper in the SSRI group (-2.9 Hz/s) compared to the age-matched controls (-1.7 Hz/s), an unexpected finding considering that large PICs are associated with reduced spike frequency adaptation. Moreover, both the young development and SSRI groups exhibited higher start, maximum and/or end firing rates, potentially due to higher synaptic drives in the young development group and from increases in motoneuron excitability in the SSRI group. In summary, both the young development and SSRI groups exhibited increased intrinsic motoneuron excitability compared to the young and older adults which may have been balanced by an increase in spike frequency adaptation. The increased motoneuron excitability in the young development group was also associated with a larger unsteadiness in the dorsiflexion torque profiles. We propose several intrinsic and extrinsic factors that affect both

motoneuron PICs and cell discharge that vary during development with a similar time course

to the changes in motoneuron firing behaviour observed in this thesis.

Preface

This thesis is an original work by Ghazaleh Mohammadalinejad. The studies of which this thesis is a part have received research ethics approval from the Health Research Ethics Board of the University of Alberta (Protocol 00076790) and conformed to the Declaration of Helsinki.

All electrophysiology experiments were performed in Dr. Monica Gorassini's laboratory, and she was the supervising author on all manuscripts. Ghazaleh Mohammadalinejad and Dr. Gorassini were responsible for the study design, electrophysiological data collection and analysis and manuscript composition of the studies presented in *Chapters 1-4*. The programs and codes utilized for data analysis were developed by Ghazaleh Mohammadalinejad, Dr. Babak Afsharipour and Dr. David Bennett. Dr. Alexandra Yacyshyn and Jack Basuk analyzed the torque data. Jennifer Duchcherer provided valuable assistance with data collection and analysis.

Chapters 1-4 are original work done by Ghazaleh Mohammadalinejad with Dr. Gorassini's supervision. *Chapters 2 & 3* of this thesis may be modified and submitted for publication.

Acknowledgement

First and foremost, I would like to acknowledge and thank my supervisor, Dr Monica Gorassini, for her support, encouragement, kindness and advice in helping me succeed in my studies. Her vast wisdom and wealth of experience have inspired me throughout my studies and inspired me to think outside the box. Despite coming from an Electrical Engineering background, Dr. Gorassini patiently assisted me in grasping complex concepts and fostered a genuine passion for my research. Her influence has shaped the scientist and individual I have become, leaving an indelible mark on my life.

I extend my sincere thanks to my thesis committee members, Dr. Kelvin Jones and Dr. Keith Fenrich, for graciously accepting their roles, providing valuable assessments of my work, and offering insightful feedback that has greatly enhanced the quality of my research. Additionally, I am grateful to Jennifer Duchcherer, a remarkable colleague, whose accommodating and supportive nature has made my work environment even more enjoyable and fulfilling.

I am immensely grateful to my family and friends who have stood by me throughout my academic pursuits, despite the distance that separated us. Their unwavering love, support, and encouragement have been constant sources of strength, motivating me to overcome challenges and hardships. I would like to extend a special appreciation to my life partner, Ramin Rasoulinezhad, for his unconditional love, boundless patience, and unwavering belief in my abilities.

I am truly blessed to have had such a remarkable support system, and I am forever indebted to all those who have contributed to my success.

Table of Contents

List of Tables

Chapter 3

List of Figures

Chapter 3

Chapter 4

List of Symbols and Abbreviations

5HT –Serotonin

ALS – Amyotrophic lateral sclerosis

Ca – Calcium

Cl – Chloride

CMoD – Control Modulation Depth

CNS – Central Nervous System

Dev – Development

ΔF – Delta F

EMG – Electromyography

FDI – first dorsal interosseous muscle

GABA – gamma aminobutyric acid

HDsEMG – High Density Surface Electromyography

ICaN – Calcium activated sodium current

IH – Hyperpolarization activated current

Kv1.2 – Voltage-activated Potassium Channel

MVC – Maximum Voluntary Contraction

Na – Sodium

NE – Noradrenergic

PIC – Persistent Inward Currents

PKC – Protein Kinase C

RT – Recruitment Threshold

SIL – Silhouette Value

SK – Calcium Activated Potassium Currents

SOL – Soleus muscle

SSD – Self Sustained Duration

SSRI – Selective Serotonin Reuptake Inhibitor

TA – Tibialis Anterior muscle

TRPM5 – Thermosensitive Transient Receptor Potential Melastatin 5 channel

Chapter 1

Introduction

The main goal of this thesis is to examine the changes in spinal motoneuron properties during human development. We examine this by measuring the firing behaviour of single motor units during isometric contractions. Because a motoneuron and the muscle fibers they innervate fire in a one-to-one manner, we can infer the discharge behaviour of single motoneurons by measuring the firing behaviour of single motor units. A motor unit consists of a single motoneuron and all the muscle fibers it innervates. Muscle fibers within the motor unit are classified as either type I (slow and fatigue resistant), type IIA (fast and fatigue resistance), and type IIB (fast and fatigable) (Scott *et al.*, 2001). Motor units with slow muscle fibers are innervated by small motoneurons and produce less twitch contraction forces compared to fast fibers that are innervated by large motoneurons and produce larger forces (Thorstensson *et al.*, 1976). Increases in muscle force can occur either by increasing the discharge rate of the motor units or by recruiting new motor units. According to the size principle, the smallest motoneurons are recruited first with larger motoneurons recruited later as the force progressively increases (Gregory & Bickel, 2005). As we describe below, we use the firing rate profiles of multiple single motor units with different recruitment thresholds obtained from high-density surface EMG (HDsEMG) (Del Vecchio *et al.*, 2020a) to assess changes in the intrinsic properties of motoneurons during development.

Early postnatal development of spinal motoneurons

Rodent studies

Spinal motoneurons that innervate limb muscles are the final processing site for the more than 30,000 descending, spinal and peripheral synaptic inputs each motoneuron receives (Ulfhake & Cullheim, 1988; Rose & Neuber-Hess, 1991) and they undergo significant changes in both anatomical and electrical properties during postnatal development. In rodents during the first three weeks after birth, soma size and the dendritic length and arborization of spinal motoneurons increase along with accompanying changes in passive and active electrical membrane properties [reviewed in (Jean-Xavier *et al.*, 2018)]. In cats, although the number of primary dendritic branches is established at birth (~12), the total length of the dendritic tree increases with the increasing size of the spinal cord, along with remodeling of its branch structure in the first few months postnatally (Ulfhake *et al.*, 1988). In rodents, the developmental changes in motoneurons coincide with the progression from immobility to full weight bearing locomotion, and differentially affect how slow and fast motoneurons respond to synaptic inputs to produce trains of action potentials needed for coordinated muscle activation and movement.

As rodent motoneurons lose their poly-innervation of muscle fibres two weeks after birth (Brown *et al.*, 1976), their ability to fire trains of action potentials at progressively higher rates increases. At two weeks, an increase in the density and maturation of voltage-dependent Na^+ and K^+ channels produce a more narrow and larger action potential to facilitate repetitive firing (Vinay *et al.*, 2000; Nakanishi & Whelan, 2010; Quinlan *et al.*, 2011; Jean-Xavier *et al.*, 2018; Smith & Brownstone, 2020). The shortening of the medium afterhyperpolarization, resulting from faster activation and inactivation times of Ca^{++}-activated K^+ currents, may also facilitate faster repetitive firing (Gao & Ziskind-Conhaim, 1998). At three weeks after birth, the amplitude of the delayed depolarization and corresponding high-frequency initial spikes (doublets) increases, potentially from an increased activation of high voltage-activated Ca^{++} channels (Smith & Brownstone, 2020).

Initial doublets increase and help maintain enhanced motor unit force during prolonged contractions (Parmiggiani & Stein, 1981). Postnatally at three weeks there is also a larger dispersion in recruitment thresholds between slow and fast motoneurons that is not solely dependent on cell size but also due to differences in the development of intrinsic conductances (Sharples & Miles, 2021). For example, at three weeks after birth, fast motoneurons have a larger hyperpolarization-activated inward current (IH) than slow motoneurons, where IH is thought to help maintain a more depolarized resting potential but may also increase the recruitment threshold of the motoneuron by shunting excitatory synaptic currents (Sharples & Miles, 2021). In addition, at three weeks after birth the threshold of low voltage-activated Na^+ and Ca^{++}-mediated persistent inward currents (PIC, see below) become more hyperpolarized compared to at one week, specifically in slow motoneurons where PICs activated near recruitment help to boost initial cell firing and reduce recruitment thresholds (Sharples & Miles, 2021). Thus, during a slowly increasing synaptic input, the lower threshold PICs in slow motoneurons helps to recruit them first before fast motoneurons whereas the larger IH in fast motoneurons delays their recruitment compared to slow motoneurons.

Although motoneurons can fire trains of action potentials more readily at three weeks after birth, their excitability (or gain), as measured by the slope of the firing rate response of the motoneuron to a ramp or stepwise increase in current injected into the soma (F/I slope), is lower compared to the first week after birth (Smith & Brownstone, 2020; Sharples & Miles, 2021). The shallower F/I slope is mediated by a decrease in cell resistance as the size of the motoneuron increases, first leading to an increase in the minimum current needed to depolarize and fire the motoneuron (higher rheobase) and a lower firing rate in response to subsequent increases in somatic current injection (Nakanishi & Whelan, 2010; Jean-Xavier *et al.*, 2018; Smith & Brownstone, 2020). Although increases in soma size during early post-

natal development results in decreasing the gain or excitability of the motoneuron, increases in the activation of other intrinsic conductances helps to counteract this and facilitate the firing response of the motoneuron to synaptic inputs. For example, the amplitude of voltage-dependent Ca^{++} and Na^+-mediated PICs increases during the first three weeks after birth (Quinlan *et al.*, 2011; Jean-Xavier *et al.*, 2018; Sharples & Miles, 2021) to help amplify synaptic inputs by providing an additional intrinsic depolarization (plateau potential) of the motoneuron. Although PICs in motoneurons of adult animals also produce self-sustained firing, where the motoneuron continues to fire at levels of injected current or synaptic input below that needed to recruit the motoneuron, at postnatal week three motoneurons exhibit small amounts of self-sustained firing (Quinlan *et al.*, 2011; Sharples & Miles, 2021), suggesting that PICs continue to increase in size or become more persistent into adulthood. Because it is difficult for rodent cervical and lumbar spinal cords to survive *in vitro* past 3 weeks postnatally beyond the juvenile stage, little is known about how PICs continue to develop from this stage to adulthood. Typically, spinal motoneurons in adult animals have been studied *in vivo* at 12 - 20 weeks, either in deeply anaesthetized animals where PICs are suppressed or in decerebrate preparations without anesthesia (Button *et al.*, 2006; Meehan *et al.*, 2010). Thus, the presence of self-sustained firing in adult motoneurons, especially those recorded in decerebrate preparations, may be produced by the presence of intact neuromodulatory inputs such as serotonin and noreadrenaline that originate from brainstem (D'Amico *et al.*, 2013).

Human studies

Human motoneurons also show developmental changes after birth. Although it is not possible to perform invasive intracellular studies in humans, one study has compared anatomical and electrophysiological properties of embryonic stem cells harvested between 31

to 44 days post-conception that were converted to motoneurons and further grown in culture for another 13 days (Takazawa *et al.*, 2012). Similar to animal studies during the first 3 weeks after birth, over the 13 days in culture the number of dendritic branches and soma size increased, the latter resulting in a decreased input resistance of the motoneuron. In older cells, action potential half-width decreased and maximum firing rates increased, which facilitated repetitive firing. Spike frequency adaptation (SFA), defined as a reduction in firing frequency in response to a sustained suprathreshold input, also developed over time to reveal that some properties of motoneuron firing behaviour measured *in vivo* can be replicated in motoneurons grown in culture.

In vivo studies in humans have used the firing rate properties of single motor units to estimate developmental changes of motoneuron firing behaviour given the 1:1 discharge of the muscle fibre and its innervating motoneuron. A non-invasive method using high-density surface EMG (HDsEMG) with 128 sensors to isolate the activity of single motor units was used to compare the firing rate patterns of tibialis anterior (TA) motor units between newborns and adults (Del Vecchio *et al.*, 2020a). The motor unit firing rates of newborns were modulated together and displayed a higher degree of synchronization compared to adults when performing both slow and fast, ballistic movements. As newborns predominantly have slow-type motor units (Buller *et al.*, 1960), synchronization of multiple units is likely needed to perform fast, large movements of the whole limb (Del Vecchio *et al.*, 2020b). Five-sensor surface EMG has also been used to non-invasively isolate single motor unit activity in three recent studies where differences in motor unit firing behaviour have been examined between children (7 to 11 years) and young adults (early twenties). Similar to adults, firing rates of motor units recorded in children increased with contraction effort and mean firing rates were higher in children in the first dorsal interosseous (Miller *et al.*, 2019) but not in the knee extensors (Chalchat *et al.*, 2019; Parra *et al.*, 2020). However, as discussed in *Chapter*

3, the low number of surface EMG electrodes (sensors) in these studies make accurate isolation of single motor units difficult (Farina & Enoka, 2011), especially in large muscles like the knee extensors.

Muscle and motor unit properties during pre- and postpubescent development

The increase in muscle strength and power (work/time) with age is a well-documented phenomenon (Larsson *et al.*, 1979). Specific force, which is the force generated per unit of muscle cross-sectional area (CSA) and reflects the force-generating capacity of individual muscle fibres, is lower in prepubescent children compared to adults (Belanger & McComas, 1989; Kanehisa *et al.*, 1994; O'Brien *et al.*, 2010; Bouchant *et al.*, 2011). While factors like muscle mass, CSA, and muscle fibre composition contribute to lower strength and power in children compared to adults, they cannot account for all the differences. One theory proposes that the lower muscle force and power in children are due to the inability to activate fast motor units with type IIB fibers (Dotan *et al.*, 2012; O'Brien *et al.*, 2012), evidenced by the fact that children have lower maximal voluntary isometric force (MVIF) at high contraction velocities (Falk *et al.*, 2009), and generally have lower muscle power output (Lloyd *et al.*, 2014). One of the factors that contribute to the lower power output in children is the slower rate of force development during the initial phase of the muscle contraction (Maffiuletti *et al.*, 2016), which could be due to the reduced ability to activate fast fatigable motor units. The voluntary activation ratio, a measure of how many motor units out of the total available are recruited during a voluntary contraction, is also compared between children and adults (Kluka *et al.*, 2015; Martin *et al.*, 2015). The twitch interpolation technique is used to assess the voluntary activation ratio, whereby a supramaximal electrical stimulus is applied during a maximum voluntary contraction. If the supramaximal electrical stimulus applied during a maximum voluntary contraction recruits additional motor units and muscle force, this

indicates the voluntary drive did not recruit all available motor units (Merton, 1954; Shield & Zhou, 2004). The lower voluntary activation ratio in children compared to adults (Grosset *et al.*, 2008; O'Brien *et al.*, 2010; Kluka *et al.*, 2015; Martin *et al.*, 2015) suggests a reduced ability to activate all available motor units during a maximal contraction, especially the fast, type II motor units. In line with the reduced ability to activate all available motor units, mean firing rates in the FDI are higher in children (age 9-12 years) than in adults (age of 21-26 years) at matched levels of force (as a percentage of maximum), suggesting that children need a greater neural drive to maintain the same relative contraction force (Kluka *et al.*, 2015; Martin *et al.*, 2015; Miller *et al.*, 2019; Parra *et al.*, 2020). However, as mentioned above in knee extensors, (Chalchat *et al.*, 2019) reported that there is no difference in mean firing rates and motor unit recruitment parameters at matched contraction levels between 20-80% of MVC between boys (age 9-11) and men (age 18-30), suggesting that the activation profile of motor units is similar to adults by prepubescence and may be muscle specific.

In summary, while children generally exhibit lower absolute force production compared to adults, it remains unclear whether this difference solely arises from differences in muscle mass and motor unit composition or if it also involves the inability to recruit fast fatigable motor units. In addition, there is a lack of information concerning the firing behaviour and intrinsic properties of *in vivo* human motoneurons during development from early after birth to adulthood. Below, we summarize some of the known firing behaviour and intrinsic properties of motoneurons measured in adults which we also investigate in children, adolescents and young adults in this thesis.

Investigating intrinsic motoneuron properties in humans

Self-sustained firing

The higher synchronization and firing rates of motor units in babies and children, respectively, compared to adults are likely due to differences in both the synaptic inputs to the motoneuron and how intrinsic conductances within the motoneuron contribute to the transduction of these inputs to produce cell firing. We define intrinsic conductances as those being activated by the internal voltage of the neuron or from the activation of internally released ions such as calcium, rather than from the activation of postsynaptic receptors from the presynaptic release of neurotransmitters. The intrinsic and synaptic activation of motoneurons are difficult to dissociate in the human because unlike intracellular studies, it is difficult to control and quantify the synaptic input to the motoneuron in order to assess how intrinsic conductances then further shape its activation and firing behaviour. One approach used in humans to estimate the synaptic input to motoneurons is to use the firing rate profile(s) of low threshold motor units given their linear relationship between effective synaptic current, motoneuron depolarization and firing rate (Binder *et al.*, 2020). This representation of synaptic input to the motoneuron has been used to estimate the contribution of the intrinsic Na$^+$ and Ca^{++}-mediated PIC to self-sustained firing of the motoneuron during a slowly increasing, and then decreasing, triangular synaptic input profile. The lower synaptic input [i.e., firing rate of a low threshold motor unit(s) at de-recruitment of the motoneuron (motor unit) compared to at recruitment (ΔF)], is used as a measure of the reduction in synaptic input needed to counteract the added depolarization from the PIC (Gorassini *et al.*, 2002b). Complimentary studies in animals and computer modelling have shown that ΔF provides a reasonable estimate of the contribution of intrinsic conductances, such as the PIC, to the self-sustained activation of the motoneuron (Powers *et al.*, 2008; Powers & Heckman, 2015). However, recent studies in juvenile mice have shown that other intrinsic conductances, such as Ca^{++}-activated Na$^+$ currents (I$_{CaN}$) that are mediated by transient receptor potential channels from the melastatin subfamily (Trpm5) located on the initial

8

segment of the motor axon, may also contribute to the plateau potential and self-sustained firing of the motoneuron (Bos *et al.*, 2021).

Initial acceleration in secondary firing range

In addition to producing self-sustained firing as quantified by the ΔF, activation of the PIC before (subthreshold) or at the time of recruitment also helps to secure motoneuron activation and produces a steep slope in firing during a slowly increasing input, termed the secondary range (Hounsgaard *et al.*, 1988; Bennett *et al.*, 1998b; Powers & Binder, 2001; Heckman *et al.*, 2008b; Fuglevand *et al.*, 2015; Afsharipour *et al.*, 2020). The threshold at which the PICs are activated plays a crucial role in determining the steepness and duration of the secondary slope. A low, subthreshold activation of the PIC results in a steeper and shorter duration secondary range because the motoneuron starts to fire during the steep acceleration of the membrane potential near the mid-way point of PIC activation. This is in contrast to higher activation thresholds of the PIC where the motoneuron starts to fire during the more gradual increase in membrane potential at the onset of PIC activation (Bennett *et al.*, 1998b; Afsharipour *et al.*, 2020). Thus, it is easier to evoke a more subthreshold activation of the PIC and steep secondary range when the motoneuron is activated with synaptic inputs compared to current injected into the soma (Bennett *et al.*, 1998b) given the predominant dendritic location of the ion channels that mediate the PIC (Schwindt & Crill, 1982). Moreover, the threshold of the PIC may be lower in small compared to large motoneurons because of the higher input resistance in the former (Bennett *et al.*, 2001b).

Reduced firing gain in tertiary range

After the PIC is fully activated, the firing rate of the motoneuron increases linearly

with increases in current injected into the soma; however, the F-I slope is lower compared to the secondary range. The reduced F-I gain of the tertiary range is likely due to an increased shunting of synaptic current by both ligand-gated channels and the open Na^+ and Ca^{++} channels that mediate the PIC (Lee & Heckman, 1998; Hultborn *et al.*, 2003; Afsharipour *et al.*, 2020). In support of this, the tertiary F-I slope is lower in motoneurons of rodents with a chronic spinal cord injury where PICs are larger compared to after acute injury where the F/I slope is steeper and PICs are small or absent (Bennett *et al.*, 2001b).

Spike frequency adaptation and rate saturation

There can also be a slowing of the firing rate after the motoneuron discharges for several seconds during an increasing current injection or synaptic input that may be related to spike frequency adaptation (SFA) described above (Takazawa *et al.*, 2012; Binder *et al.*, 2020). The mechanism mediating SFA is not known but potential candidates include a small conductance K^+ channel that is activated by calcium from the PIC [SK_L: (Hallworth *et al.*, 2003; Li & Bennett, 2007)], inactivation of the CaPIC (Powers & Heckman, 2017), NaPIC (Brownstone, 2006; Button *et al.*, 2007) or fast Na^+ channels (Perrier & Cotel, 2008), or from a net hyperpolarization produced by the Na^+- K^+ pump (Sawczuk *et al.*, 1997) to name a few. Interestingly, there is a negative correlation between SFA and PIC amplitude, which suggests that the added depolarization from the PIC helps to counteract SFA (Button *et al.,* 2007).

In addition to SFA, rate saturation also occurs in motoneurons (Revill & Fuglevand, 2011; Fuglevand *et al.*, 2015), whereby the firing rate of the motoneuron reaches a maximum level and does not increase any further, despite increasing the somatic current injection or synaptic input to the motoneuron. Rate saturation can arise due to a progressive reduction in the driving potential at excitatory synapses as the dendritic membrane depolarizes. This occurs because motoneurons have a limited number of available sodium channels, which may

become inactive and limit their ability to respond to synaptic input (Barrett & Crill, 1974; Cushing *et al.*, 2005; Fuglevand *et al.*, 2015). Another intrinsic property that can contribute to rate saturation is the increase in open transmitter-gated and other types of channels (Burke, 1967), which reduces the neuron's input resistance and makes it less likely for a given increment in synaptic current to cause a significant change in membrane potential (Fuglevand *et al.*, 2015). The exact mechanism behind rate saturation in motoneurons is complex and involves many factors, including the number and type of ion channels, the properties of the neuronal membrane, and the activity of synaptic inputs (Barrett & Crill, 1974; Cushing *et al.*, 2005; Vandenberk & Kalmar, 2014). However, it is generally understood that rate saturation is an intrinsic property of motoneurons.

Non-linearities in motoneuron firing produced by intrinsic conductances

As described above, the PIC and other intrinsic conductances can produce nonlinearities in the firing behaviour of motoneurons during a linearly increasing synaptic input, including the initial fast acceleration in firing during PIC activation (secondary range), a lower gain but linear firing after full PIC activation (tertiary range) and the decrease in firing rate after the motoneuron has been discharging for several seconds during SFA (tertiary sag range) (Binder *et al.*, 2020). These three non-linearities in firing are also observed in the firing rate profiles of human motor units activated during an ascending isometric dorsiflexion where we assume the synaptic input to the motoneuron linearly increases with the measured torque (Afsharipour *et al.*, 2020). Thus, in this thesis we fit three continuous straight lines to the ascending portion of the firing rate profile as an additional method to examine the influence of potential intrinsic conductances on the secondary (slope 1) and tertiary (slope 2) ranges where slope 1 > 2, and to characterize the decrease in firing rates before peak torque during the tertiary sag range (slope 3) where slope 3 < 0 Hz/s.

11

Effects of neuromodulators serotonin and noradrenaline on motoneuron firing

Neuromodulators exert significant effects on motoneuron PICs to regulate their excitability and firing behaviour (Murray *et al.*, 2011; Rank *et al.*, 2011). One such neuromodulator is serotonin, which increases the amplitude and lowers the threshold of motoneuron PICs in the spinal cord (Li *et al.*, 2007; D'Amico *et al.*, 2013; Cheng *et al.*, 2021). This effect is mediated through the activation of $5\text{-}HT_2$ receptors activating signaling pathways involving Gq-proteins and second messengers like calmodulin and IP3, which leads to an increase in the conductance of the Ca^{++} channels mediating the PIC (Perrier *et al.*, 2002; Li *et al.*, 2007; Di Matteo *et al.*, 2008). Another neuromodulator that affects PICs in motoneurons is norepinephrine. Norepinephrine enhances PIC amplitude by activating α_1 adrenergic receptors on motoneurons which also activate facilitatory Gq-protein-coupled pathways (Heckman *et al.*, 2003; Harvey *et al.*, 2006b). Beyond serotonin and norepinephrine, acetylcholine is another neuromodulator that has been found to modulate the excitability of motoneurons. Specifically, acetylcholine binds to m_2-type muscarinic receptors on motoneurons and reduces the action potential afterhyperpolarization (AHP), thereby increasing motoneuron excitability and the ability to fire faster (Miles *et al.*, 2007). Overall, the regulation of PICs in motoneurons is an essential aspect of motor control, and neuromodulatory effects on these currents play a crucial role in shaping the firing behaviour of motoneurons.

Selective serotonin reuptake inhibitors (SSRI), like citalopram (D'Amico *et al.*, 2013) and escitalopram (Wei *et al.*, 2014), may increase the basal level of spinal serotonin as evidenced by an increase in estimated motoneuron PIC amplitude (ΔF) and long-lasting reflexes in humans, demonstrating increases in self-sustained activation of motoneurons.

Serotonin reduces the inactivation of voltage-gated Na^+ channels, allowing the motoneuron to fire action potentials for longer durations (Harvey *et al.*, 2006b). Increased excitability of motoneurons from enhanced levels of spinal serotonin may lead to alterations in their firing patterns, affecting the start, maximum, and end rates by shortening the afterhyperpolarization (AHP) and causing faster firing rates (Perrier *et al.*, 2013). In contrast, motoneuron excitability may also be reduced by prolonged activation of serotonin (5-HT) pathways from the raphe nucleus that results in 5-HT spillover [reviewed in (Perrier *et al.*, 2013)]. This diffuse 5-HT is thought to activate $5HT1_A$ receptors on the axon initial segment to inhibit Na^+ channels and slow repetitive firing that is akin to spike frequency adaptation.

Summary of experiments

In this thesis, we measured the developmental changes in the firing behaviour of motoneurons during a moderate, 30% MVC in 50 neurologically intact participants ranging in age from 7 to 53 years. Given the effects of serotonin on motoneuron excitability described above, we considered participants taking oral SSRIs as a separate group. To non-invasively isolate the activity of single motor units in the TA, we used HDsEMG with 64 electrode sites and blind source decomposition algorithms which have been extensively validated for this muscle (Negro *et al.*, 2016; Kim *et al.*, 2020). In *Chapter 2* of this thesis, we estimated the contribution of the PIC (and potentially I_{CaN}) to self-sustained firing of the motoneuron by using the ΔF technique, in addition to measuring the slope and duration of the secondary and tertiary ranges from joined straight lines fit to the ascending firing rate profile. These parameters were compared across age and with respect to the recruitment threshold of the motor units. In *Chapter 3*, we further analyzed the same dataset to measure the start, maximum, and end firing rates in all participants across age, and evaluated how the

maximum firing rates changed with recruitment threshold of the motor units. Additionally, we investigated the presence, slope and duration of the tertiary sag range and performed preliminary analysis to determine if it is produced by conductances intrinsic to the motoneuron or if it is produced by a decrease in common synaptic drive to the TA motoneuron pool. Together, these findings provide insights into the complex relationship between motoneuron firing properties, age, and neuromodulators, and shed light on the possible mechanisms underlying the modulation of motoneuron firing behaviour by intrinsic conductances.

References for Chapter 1

Afsharipour B, Manzur N, Duchcherer J, Fenrich KF, Thompson CK, Negro F, Quinlan KA, Bennett DJ & Gorassini MA. (2020). Estimation of self-sustained activity produced by persistent inward currents using firing rate profiles of multiple motor units in humans. *J Neurophysiol* **124,** 63-85.

Barrett JN & Crill WE. (1974). Influence of dendritic location and membrane properties on the effectiveness of synapses on cat motoneurones. *J Physiol* **239,** 325-345.

Belanger AY & McComas AJ. (1989). Contractile properties of human skeletal muscle in childhood and adolescence. *Eur J Appl Physiol Occup Physiol* **58,** 563-567.

Bennett DJ, Hultborn H, Fedirchuk B & Gorassini M. (1998). Synaptic activation of plateaus in hindlimb motoneurons of decerebrate cats. *J Neurophysiol* **80,** 2023-2037.

Bennett DJ, Li Y & Siu M. (2001). Plateau potentials in sacrocaudal motoneurons of chronic spinal rats, recorded in vitro. *J Neurophysiol* **86,** 1955-1971.

Binder MD, Powers RK & Heckman CJ. (2020). Nonlinear Input-Output Functions of Motoneurons. *Physiology (Bethesda)* **35,** 31-39.

Bos R, Drouillas B, Bouhadfane M, Pecchi E, Trouplin V, Korogod SM & Brocard F. (2021). Trpm5 channels encode bistability of spinal motoneurons and ensure motor control of hindlimbs in mice. *Nat Commun* **12,** 6815.

Bouchant A, Martin V, Maffiuletti NA & Ratel S. (2011). Can muscle size fully account for strength differences between children and adults? *J Appl Physiol (1985)* **110,** 1748-1749.

Brown MC, Jansen JK & Van Essen D. (1976). Polyneuronal innervation of skeletal muscle in new-born rats and its elimination during maturation. *J Physiol* **261,** 387-422.

Brownstone RM. (2006). Beginning at the end: repetitive firing properties in the final common pathway. *Prog Neurobiol* **78,** 156-172.

Buller AJ, Eccles JC & Eccles RM. (1960). Differentiation of fast and slow muscles in the cat hind limb. *J Physiol* **150,** 399-416.

Burke RE. (1967). Composite nature of the monosynaptic excitatory postsynaptic potential. *J Neurophysiol* **30,** 1114-1137.

Button DC, Gardiner K, Marqueste T & Gardiner PF. (2006). Frequency-current relationships of rat hindlimb alpha-motoneurones. *J Physiol* **573,** 663-677.

Button DC, Kalmar JM, Gardiner K, Cahill F & Gardiner PF. (2007). Spike frequency adaptation of rat hindlimb motoneurons. *J Appl Physiol (1985)* **102,** 1041-1050.

Chalchat E, Piponnier E, Bontemps B, Julian V, Bocock O, Duclos M, Ratel S & Martin V. (2019). Characteristics of motor unit recruitment in boys and men at maximal and submaximal force levels. *Exp Brain Res* **237,** 1289-1302.

Cheng Y, Song N, Ge R & Dai Y. (2021). Serotonergic Modulation of Persistent Inward Currents in Serotonergic Neurons of Medulla in ePet-EYFP Mice. *Front Neural Circuits* **15,** 657445.

Cushing S, Bui T & Rose PK. (2005). Effect of nonlinear summation of synaptic currents on the input-output properties of spinal motoneurons. *J Neurophysiol* **94,** 3465-3478.

D'Amico JM, Murray KC, Li Y, Chan KM, Finlay MG, Bennett DJ & Gorassini MA. (2013). Constitutively active 5-HT2/α1 receptors facilitate muscle spasms after human spinal cord injury. *J Neurophysiol* **109,** 1473-1484.

Del Vecchio A, Holobar A, Falla D, Felici F, Enoka RM & Farina D. (2020a). Tutorial: Analysis of motor unit discharge characteristics from high-density surface EMG signals. *J Electromyogr Kinesiol* **53,** 102426.

Del Vecchio A, Sylos-Labini F, Mondì V, Paolillo P, Ivanenko Y, Lacquaniti F & Farina D. (2020b). Spinal motoneurons of the human newborn are highly synchronized during leg movements. *Sci Adv* **6**.

Di Matteo V, Pierucci M, Esposito E, Crescimanno G, Benigno A & Di Giovanni G. (2008). Serotonin modulation of the basal ganglia circuitry: therapeutic implication for Parkinson's disease and other motor disorders. *Prog Brain Res* **172,** 423-463.

Dotan R, Mitchell C, Cohen R, Klentrou P, Gabriel D & Falk B. (2012). Child-adult differences in muscle activation--a review. *Pediatr Exerc Sci* **24,** 2-21.

Falk B, Usselman C, Dotan R, Brunton L, Klentrou P, Shaw J & Gabriel D. (2009). Child-adult differences in muscle strength and activation pattern during isometric elbow flexion and extension. *Appl Physiol Nutr Metab* **34,** 609-615.

Farina D & Enoka RM. (2011). Surface EMG decomposition requires an appropriate validation. *J Neurophysiol* **105,** 981-982; author reply 983-984.

Fuglevand AJ, Lester RA & Johns RK. (2015). Distinguishing intrinsic from extrinsic factors underlying firing rate saturation in human motor units. *J Neurophysiol* **113,** 1310-1322.

Gao BX & Ziskind-Conhaim L. (1998). Development of ionic currents underlying changes in action potential waveforms in rat spinal motoneurons. *J Neurophysiol* **80,** 3047-3061.

Gorassini M, Yang JF, Siu M & Bennett DJ. (2002). Intrinsic activation of human motoneurons: reduction of motor unit recruitment thresholds by repeated contractions. *J Neurophysiol* **87,** 1859-1866.

Gregory CM & Bickel CS. (2005). Recruitment patterns in human skeletal muscle during electrical stimulation. *Phys Ther* **85,** 358-364.

Grosset JF, Mora I, Lambertz D & Pérot C. (2008). Voluntary activation of the triceps surae in prepubertal children. *J Electromyogr Kinesiol* **18,** 455-465.

Hallworth NE, Wilson CJ & Bevan MD. (2003). Apamin-sensitive small conductance calcium-activated potassium channels, through their selective coupling to voltage-gated calcium channels, are critical determinants of the precision, pace, and pattern of action potential generation in rat subthalamic nucleus neurons in vitro. *J Neurosci* **23,** 7525-7542.

Harvey PJ, Li X, Li Y & Bennett DJ. (2006). Endogenous monoamine receptor activation is essential for enabling persistent sodium currents and repetitive firing in rat spinal motoneurons. *J Neurophysiol* **96,** 1171-1186.

Heckman CJ, Johnson M, Mottram C & Schuster J. (2008). Persistent inward currents in spinal motoneurons and their influence on human motoneuron firing patterns. *Neuroscientist* **14,** 264-275.

Heckman CJ, Lee RH & Brownstone RM. (2003). Hyperexcitable dendrites in motoneurons and their neuromodulatory control during motor behavior. *Trends Neurosci* **26,** 688-695.

Hounsgaard J, Hultborn H, Jespersen B & Kiehn O. (1988). Bistability of alpha-motoneurones in the decerebrate cat and in the acute spinal cat after intravenous 5-hydroxytryptophan. *J Physiol* **405,** 345-367.

Hultborn H, Denton ME, Wienecke J & Nielsen JB. (2003). Variable amplification of synaptic input to cat spinal motoneurones by dendritic persistent inward current. *J Physiol* **552,** 945-952.

Jean-Xavier C, Sharples SA, Mayr KA, Lognon AP & Whelan PJ. (2018). Retracing your footsteps: developmental insights to spinal network plasticity following injury. *J Neurophysiol* **119,** 521-536.

Kanehisa H, Ikegawa S, Tsunoda N & Fukunaga T. (1994). Strength and cross-sectional area of knee extensor muscles in children. *Eur J Appl Physiol Occup Physiol* **68,** 402-405.

Kim EH, Wilson JM, Thompson CK & Heckman CJ. (2020). Differences in estimated persistent inward currents between ankle flexors and extensors in humans. *J Neurophysiol* **124,** 525-535.

Kluka V, Martin V, Vicencio SG, Jegu AG, Cardenoux C, Morio C, Coudeyre E & Ratel S. (2015). Effect of muscle length on voluntary activation level in children and adults. *Med Sci Sports Exerc* **47,** 718-724.

Larsson L, Grimby G & Karlsson J. (1979). Muscle strength and speed of movement in relation to age and muscle morphology. *J Appl Physiol Respir Environ Exerc Physiol* **46,** 451-456.

Lee RH & Heckman CJ. (1998). Bistability in spinal motoneurons in vivo: systematic variations in persistent inward currents. *J Neurophysiol* **80,** 583-593.

Li X & Bennett DJ. (2007). Apamin-sensitive calcium-activated potassium currents (SK) are activated by persistent calcium currents in rat motoneurons. *J Neurophysiol* **97,** 3314-3330.

Li X, Murray K, Harvey PJ, Ballou EW & Bennett DJ. (2007). Serotonin facilitates a persistent calcium current in motoneurons of rats with and without chronic spinal cord injury. *J Neurophysiol* **97,** 1236-1246.

Lloyd RS, Faigenbaum AD, Stone MH, Oliver JL, Jeffreys I, Moody JA, Brewer C, Pierce KC, McCambridge TM, Howard R, Herrington L, Hainline B, Micheli LJ, Jaques R, Kraemer WJ, McBride MG, Best TM, Chu DA, Alvar BA & Myer GD. (2014). Position statement on youth resistance training: the 2014 International Consensus. *Br J Sports Med* **48,** 498-505.

Maffiuletti NA, Aagaard P, Blazevich AJ, Folland J, Tillin N & Duchateau J. (2016). Rate of force development: physiological and methodological considerations. *Eur J Appl Physiol* **116,** 1091-1116.

Martin V, Kluka V, Garcia Vicencio S, Maso F & Ratel S. (2015). Children have a reduced maximal voluntary activation level of the adductor pollicis muscle compared to adults. *Eur J Appl Physiol* **115,** 1485-1491.

Meehan CF, Sukiasyan N, Zhang M, Nielsen JB & Hultborn H. (2010). Intrinsic properties of mouse lumbar motoneurons revealed by intracellular recording in vivo. *J Neurophysiol* **103,** 2599-2610.

Merton PA. (1954). Voluntary strength and fatigue. *J Physiol* **123,** 553-564.

Miles GB, Hartley R, Todd AJ & Brownstone RM. (2007). Spinal cholinergic interneurons regulate the excitability of motoneurons during locomotion. *Proc Natl Acad Sci U S A* **104,** 2448-2453.

Miller JD, Sterczala AJ, Trevino MA, Wray ME, Dimmick HL & Herda TJ. (2019). Motor unit action potential amplitudes and firing rates during repetitive muscle actions of the first dorsal interosseous in children and adults. *Eur J Appl Physiol* **119,** 1007-1018.

Murray KC, Stephens MJ, Ballou EW, Heckman CJ & Bennett DJ. (2011). Motoneuron excitability and muscle spasms are regulated by 5-HT2B and 5-HT2C receptor activity. *J Neurophysiol* **105,** 731-748.

Nakanishi ST & Whelan PJ. (2010). Diversification of intrinsic motoneuron electrical properties during normal development and botulinum toxin-induced muscle paralysis in early postnatal mice. *J Neurophysiol* **103,** 2833-2845.

Negro F, Muceli S, Castronovo AM, Holobar A & Farina D. (2016). Multi-channel intramuscular and surface EMG decomposition by convolutive blind source separation. *J Neural Eng* **13,** 026027.

O'Brien TD, Reeves ND, Baltzopoulos V, Jones DA & Maganaris CN. (2010). In vivo measurements of muscle specific tension in adults and children. *Exp Physiol* **95,** 202-210.

O'Brien TD, Reeves ND, Baltzopoulos V, Jones DA & Maganaris CN. (2012). Commentary on child-adult differences in muscle activation--a review. *Pediatr Exerc Sci* **24,** 22-25.

Parmiggiani F & Stein RB. (1981). Nonlinear summation of contractions in cat muscles. II. Later facilitation and stiffness changes. *J Gen Physiol* **78,** 295-311.

Parra ME, Miller JD, Sterczala AJ, Trevino MA, Dimmick HL & Herda TJ. (2020). Differences in the firing rate versus recruitment threshold relationships of the vastus lateralis in children ages 7-10 years and adults. *Hum Mov Sci* **72,** 102650.

Perrier JF, Alaburda A & Hounsgaard J. (2002). Spinal plasticity mediated by postsynaptic L-type Ca2+ channels. *Brain Res Brain Res Rev* **40,** 223-229.

Perrier JF & Cotel F. (2008). Serotonin differentially modulates the intrinsic properties of spinal motoneurons from the adult turtle. *J Physiol* **586,** 1233-1238.

Perrier JF, Rasmussen HB, Christensen RK & Petersen AV. (2013). Modulation of the intrinsic properties of motoneurons by serotonin. *Curr Pharm Des* **19,** 4371-4384.

Powers RK & Binder MD. (2001). Input-output functions of mammalian motoneurons. *Rev Physiol Biochem Pharmacol* **143,** 137-263.

Powers RK & Heckman CJ. (2015). Contribution of intrinsic motoneuron properties to discharge hysteresis and its estimation based on paired motor unit recordings: a simulation study. *J Neurophysiol* **114,** 184-198.

Powers RK & Heckman CJ. (2017). Synaptic control of the shape of the motoneuron pool input-output function. *J Neurophysiol* **117,** 1171-1184.

Powers RK, Nardelli P & Cope TC. (2008). Estimation of the contribution of intrinsic currents to motoneuron firing based on paired motoneuron discharge records in the decerebrate cat. *J Neurophysiol* **100,** 292-303.

Quinlan KA, Schuster JE, Fu R, Siddique T & Heckman CJ. (2011). Altered postnatal maturation of electrical properties in spinal motoneurons in a mouse model of amyotrophic lateral sclerosis. *J Physiol* **589,** 2245-2260.

Rank MM, Murray KC, Stephens MJ, D'Amico J, Gorassini MA & Bennett DJ. (2011). Adrenergic receptors modulate motoneuron excitability, sensory synaptic transmission and muscle spasms after chronic spinal cord injury. *J Neurophysiol* **105,** 410-422.

Revill AL & Fuglevand AJ. (2011). Effects of persistent inward currents, accommodation, and adaptation on motor unit behavior: a simulation study. *J Neurophysiol* **106,** 1467-1479.

Rose PK & Neuber-Hess M. (1991). Morphology and frequency of axon terminals on the somata, proximal dendrites, and distal dendrites of dorsal neck motoneurons in the cat. *J Comp Neurol* **307,** 259-280.

Sawczuk A, Powers RK & Binder MD. (1997). Contribution of outward currents to spike-frequency adaptation in hypoglossal motoneurons of the rat. *J Neurophysiol* **78,** 2246-2253.

Schwindt PC & Crill WE. (1982). Factors influencing motoneuron rhythmic firing: results from a voltage-clamp study. *J Neurophysiol* **48,** 875-890.

Scott W, Stevens J & Binder-Macleod SA. (2001). Human skeletal muscle fiber type classifications. *Phys Ther* **81,** 1810-1816.

Sharples SA & Miles GB. (2021). Maturation of persistent and hyperpolarization-activated inward currents shapes the differential activation of motoneuron subtypes during postnatal development. *Elife* **10**.

Shield A & Zhou S. (2004). Assessing voluntary muscle activation with the twitch interpolation technique. *Sports Med* **34,** 253-267.

Smith CC & Brownstone RM. (2020). Spinal motoneuron firing properties mature from rostral to caudal during postnatal development of the mouse. *J Physiol* **598,** 5467-5485.

Takazawa T, Croft GF, Amoroso MW, Studer L, Wichterle H & Macdermott AB. (2012). Maturation of spinal motor neurons derived from human embryonic stem cells. *PLoS One* **7,** e40154.

Thorstensson A, Grimby G & Karlsson J. (1976). Force-velocity relations and fiber composition in human knee extensor muscles. *J Appl Physiol* **40,** 12-16.

Ulfhake B & Cullheim S. (1988). Postnatal development of cat hind limb motoneurons. III: Changes in size of motoneurons supplying the triceps surae muscle. *J Comp Neurol* **278,** 103-120.

Ulfhake B, Cullheim S & Franson P. (1988). Postnatal development of cat hind limb motoneurons. I: Changes in length, branching structure, and spatial distribution of dendrites of cat triceps surae motoneurons. *J Comp Neurol* **278,** 69-87.

Vandenberk MS & Kalmar JM. (2014). An evaluation of paired motor unit estimates of persistent inward current in human motoneurons. *J Neurophysiol* **111,** 1877-1884.

Vinay L, Brocard F & Clarac F. (2000). Differential maturation of motoneurons innervating ankle flexor and extensor muscles in the neonatal rat. *Eur J Neurosci* **12,** 4562-4566.

Wei K, Glaser JI, Deng L, Thompson CK, Stevenson IH, Wang Q, Hornby TG, Heckman CJ & Kording KP. (2014). Serotonin affects movement gain control in the spinal cord. *J Neurosci* **34,** 12690-12700.

Chapter 2

Introduction

Spinal motoneurons in rodents undergo marked changes in their intrinsic electrical properties during the first three weeks of postnatal development. These changes help to facilitate motoneuron recruitment and repetitive firing that are needed for sustained motor behaviours such as posture and weight bearing locomotion [reviewed in (Carrascal *et al.*, 2005; Jean-Xavier *et al.*, 2018)]. One such marked change is the decrease in threshold and increase in amplitude of persistent inward currents (PICs) in the first three weeks after birth (Quinlan *et al.*, 2011; Revill *et al.*, 2019; Sharples & Miles, 2021). PICs are mediated by voltage-activated sodium ($Na_{V1.2/1.6}$) and calcium ($Ca_{V1.2/1.3}$) channels and by a calcium-activated sodium conductance (I_{CaN}) (Bos *et al.*, 2021). Because PICs are activated near the recruitment threshold of the motoneuron, they provide an additional depolarization to amplify synaptic inputs and accelerate the initial firing rate of the motoneuron to help secure its recruitment (Hounsgaard *et al.*, 1988; Kiehn & Eken, 1997; Bennett *et al.*, 1998b; Lee & Heckman, 2000; Bennett *et al.*, 2001b; Lee *et al.*, 2003; Li *et al.*, 2004). Thus, the initial period of firing rate acceleration during a slowly increasing input, termed secondary range (Kernell, 1965; Li *et al.*, 2004), is in part a reflection of the onset activation of the intrinsic PIC in motoneurons.

Following the secondary range, the PIC further shapes the firing behaviour of motoneurons. After the PIC is fully activated and produces a sustained plateau potential, the firing rate of the motoneuron increases linearly in response to an increasing intracellular current injection, but with a much shallower slope (Bennett *et al.*, 1998a; Lee *et al.*, 2003). This lower-gain response, termed tertiary range, results in part from an increase in membrane conductance produced by the sustained opening of the Na^+ and Ca^{++} channels mediating the

PIC (Binder *et al.*, 2020). In adult animals, the tertiary range also exhibits a pronounced hysteresis whereby the sustained plateau potential mediated by the PIC allows the motoneuron to fire at inputs well below that needed to initially recruit the motoneuron. This hysteresis in firing reflects how much the PIC contributes to the self-sustained firing of the motoneuron and can be measured by the reduction in current injected into the soma at the offset of motoneuron firing (de-recruitment) compared to the higher current required to initiate firing at recruitment (Bennett *et al.*, 2001a; Gorassini *et al.*, 2004; Li *et al.*, 2004; Powers *et al.*, 2008). Although present at postnatal week three, PICs produce smaller amounts of self-sustained firing compared to adult motoneurons (Quinlan *et al.*, 2011; Leroy *et al.*, 2015; Revill *et al.*, 2019; Sharples & Miles, 2021), suggesting that PICs continue to increase in amplitude or become more persistent beyond the weaning and preadolescent stage of rodent development.

During human development, it is not known if motoneuron PICs also increase in amplitude and decrease in recruitment threshold in the first few weeks and months following birth or if there are continual changes from preadolescence to adulthood as observed in rodents (Carlin *et al.*, 2000; Quinlan *et al.*, 2011). To address the latter question, we used the simultaneous firing behaviour of multiple motor units to indirectly examine the contribution of motoneuron PICs to self-sustained firing in participants between the ages of 7 to 17 years in the preadolescent and adolescent stages (Brix *et al.,* 2019; Wood *et al.,* 2019) and during young adulthood (18 to 28 years of age). These two groups were also compared to an older adult group (32 to 53 years) before appreciable motor unit loss (McNeil *et al.*, 2005) or decreases in estimated motoneuron PICs (Hassan *et al.*, 2021; Orssatto *et al.*, 2021) occur. The firing rate profile of low threshold (control) tibialis anterior (TA) motor units activated during a triangular isometric dorsiflexion were used to estimate the synaptic input to higher threshold (test) motor units (Gorassini *et al.*, 2002a; Afsharipour *et al.*, 2020). Similar to the

hysteresis measurements described above, we calculated the difference in the estimated synaptic input needed to terminate firing of the test unit (control unit firing rate, F_T), compared with the synaptic input needed to recruit firing (control unit firing rate, F_R). Thus, the resulting variable, $\Delta F = F_R - F_T$, was employed as a measure of the self-sustained firing produced by the PIC.

Interestingly, the firing rate profiles of human motor units activated during a slow increase in voluntary effort, and presumably synaptic drive, also display an initial acceleration followed by a shallower increase in firing rate (Afsharipour *et al.*, 2020; Binder *et al.*, 2020; Beauchamp *et al.*, 2023), similar to the secondary and tertiary ranges observed in animal motoneurons in response to a slowly increasing somatic current injection. Thus, we iteratively fit two straight lines to the ascending portion of the TA motor unit firing profile to delineate the initial firing rate acceleration during the presumed activation of the PIC (secondary range) and the more gradual increase in firing rate following full PIC activation during the tertiary range. We hypothesized that a steep and brief secondary range is produced by a subthreshold activation of a PIC that is accelerating rapidly at the time of motoneuron recruitment compared to a more shallow and longer secondary range mediated by a more suprathreshold PIC that is activating more gradually during motoneuron recruitment [see Fig. 11 in (Afsharipour *et al.*, 2020)]. Thus, we measured both the slope and duration of the secondary range to estimate if there are any differences in the activation threshold of the PIC during development. The slope and duration of the tertiary range was also compared between age groups to estimate if there were any changes in the firing gain of the motoneuron. In some cases, firing rates also decreased during the later portion of the tertiary range just before peak torque, termed the tertiary sag range, and we present this data in *Chapter 3*.

The increased amplitude and persistence of motoneuron PICs during development may be mediated by a maturation of descending neuromodulatory inputs, like serotonin or

noradrenaline, to the ventral spinal cord (Bregman, 1987; Hounsgaard *et al.*, 1988; Perrier *et al.*, 2013; Xia *et al.*, 2017). Both these neuromodulators work through Gq-protein coupled receptors, such as 5-$HT_{2B/C}$ and $\alpha 1$ (Murray *et al.*, 2010; Murray *et al.*, 2011), that activate protein kinase C to subsequently phosphorylate and facilitate the Na_V and Ca_V channels that mediate the PIC (Mizuno & Itoh, 2009) [(reviewed in (Perrier *et al.*, 2013; D'Amico *et al.*, 2014)]. In adult humans, oral administration of selective serotonin reuptake inhibitors (SSRIs), such as citalopram or escitalopram, likely increase serotonin in the spinal cord and are associated with increases in indirect measures of PIC-mediated self-sustained firing in spinal motoneurons (Murray *et al.*, 2010; D'Amico *et al.*, 2013; Thompson & Hornby, 2013; Wei *et al.*, 2014). Because some participants in the young development and young adult groups were taking SSRIs to treat various affective and anxiety disorders (Dwyer & Bloch, 2019), we treated these participants as a separate group given the potential effect increased spinal levels of serotonin may have on the threshold and amplitude of the PIC (Harvey *et al.*, 2006a; Li *et al.*, 2007).

Across the age span of 7 to 53 years, we hypothesized that younger participants (< 18 years) would have greater amounts of self-sustained firing (ΔF) from larger motoneuron PICs compared to older participants (> 18 years), potentially due in part to lower levels of spinal inhibition (Willerslev-Olsen *et al.*, 2014; Geertsen *et al.*, 2017), which reduces the amplitude and persistence of PICs (Bennett *et al.*, 1998b; Hyngstrom *et al.*, 2007). Likewise, we hypothesized that participants taking oral SSRIs would have both steeper secondary range slopes and larger amounts of self-sustained firing given that serotonin reduces the threshold and increases the amplitude of the PIC, respectively (Harvey *et al.*, 2006a; Li *et al.*, 2007). Finally, we estimated the skill in producing a targeted triangular dorsiflexion by quantifying the amount of force steadiness [coefficient of variation of the detrended torque trace, (Skinner

et al., 2019)] and examined if it followed a similar profile to the estimates of PIC activation,

namely ΔF and the secondary range slope, across development.

Methods

Ethics and participants

Experiments were approved by the Health Research Ethics Board of the University of Alberta (Protocol 00076790) and conformed to the Declaration of Helsinki. All 50 participants provided written informed consent prior to the experiment. The young development group had an average age of 12.18 ± 2.69 years (mean $\pm$ standard deviation) with 12 males and 8 females (n = 20), the young adult group had an average age of 22.61 ± 3.60 years with 6 males and 7 females (n = 13) and the older adult group had an average age of 42.38 ± 7.92 years with 3 males and 5 females (n = 8). A separate group of participants between the ages of 11 and 28 years (17.02 ± 5.02 years), with 4 females and 5 males (n = 9), were on selective serotonin reuptake inhibitors (SSRI). This SSRI group was compared to their peers also aged between 11 to 28 years who were not taking SSRIs (18.17 ± 5.32 years, p = 0.584 Mann-Whitney Rank Sum test) and comprised of 12 females and 14 males (n = 26) from the young development and young adult group. All participants were excluded for any history of central or peripheral nerve injury or disease. Puberty, menstrual or menopausal status were not recorded. In six of the adult participants, parts of the data were taken from a previous study (Afsharipour *et al.*, 2020).

EMG Recordings

To identify single motor units, flexible high-density surface EMG (HDsEMG) electrodes with 64 recording sites (GR08MM1305; OT Bioelecttronica Inc., Turin, Italy) were placed over the tibialis anterior (TA) muscle. The recordings sites, arranged in a 5 (wide) by 13 (long) grid with 8 mm spacing, were placed lengthwise approximately 1 cm lateral to the tibia and 4-5 cm below the lower edge of the patella over the belly of the TA

muscle. Recordings were made in a monopolar configuration with the reference and ground electrode straps (WS2; OT Bioelecttronica Inc.) wrapped around the lower leg just above the ankle, with the ground strap most distal. To reduce impedance, the skin over the TA was first rubbed with an abrasive paste (Nuprep, Weaver and Company, CO) and any excess was removed with a saline or alcohol-soaked gauze. HDsEMG signals were amplified (150 times) and filtered with a 10 Hz high pass and 900 Hz low pass filter using a Quattrocento amplifier (OT Bioelecttronica, 16 bit, Inc., Turin. Italy). A pair of Ag-AgCl surface EMG electrodes (Kendall; Chicopee, MA, USA, 3.2 cm by 2.2 cm) were placed in a bipolar configuration over the soleus to measure antagonist muscle activity during the isometric contractions. All signals were digitized with the Quatrocentro A/D and sampled at a frequency that was set to 2048 Hz.

Experimental protocol

Participants sat in a chair with their knee extended to ~120° and their dominant foot tightly sandwiched between two plates of an adjustable 3D printed foot holder, with the heel on the floor and ankle at ~90°. Dorsiflexion torque was measured by an S-shaped strain gauge (150-lb SSM, Interface Force Measurement Solutions, AZ) attached to the bottom of the foot holder directly underneath the metatarsophalangeal joint. The maximum dorsiflexion torque was measured from the largest of two maximum voluntary contractions (MVCs) separated by at least 30 seconds. Participants were then tasked to perform an isometric triangular dorsiflexion at either 10, 20 or 30% of their MVC torque, and match their torque output to a target triangle presented over a computer screen with the exerted torque being displayed from left to right. Each triangular contraction consisted of a 10-second ascending phase and a 10-second descending phase, with 20 seconds between each contraction to avoid frequency-dependent facilitation of motor units (Gorassini *et al.*, 2002b). At least 8 to 10

contractions were performed at each level of MVC torque in 2 trial runs, and the 4 best trials were selected post-hoc for analysis. Participants started with a 20 or 30% MVC contraction because these were easier to perform. Only the 30% MVC data were used for this protocol for clarity of presentation with the 10% and 20% MVC data presented in a separate paper.

Data Analysis

Decomposition of single motor units: The HDsEMG signals were first converted into a MATLAB file format (MATLAB version R2021b/R2022a) with custom-built functions, and then digitally filtered (4th-order, zero lag Butterworth filter with a bandpass of 10 - 500 Hz and an additional 60-Hz notch). HDsEMG signals with poor signal-to-noise were removed (typically 2-3 of the 64 recorded signals). Blind source separation (Negro *et al.*, 2016) was used to decompose the HDsEMG signals into the contributing single motor units. Only motor unit action potentials with a Silhouette (SIL) value of 0.85 or higher were used (Negro *et al.*, 2016). The trains of motor unit action potentials (or pulses) were manually edited to remove or add extra pulses to correct too high or too low firing rates, respectively. Only 10% or less of the pulses were modified in a single firing rate profile. A fifth-order polynomial curve was fit to the firing rate profile of each motor unit for subsequent analysis as described below.

Average number of motor units per contraction: In each participant, the number of decomposed motor units in each contraction that met the criteria for selection (see above), were averaged across the four contractions and plotted against the age of the participant.

Distribution of motor unit recruitment thresholds: The recruitment threshold of the motor units was measured as the torque level when the motor unit began firing, expressed as a percentage of the torque at MVC (% MVC). To examine the distribution of motor units with different recruitment thresholds for each group, the total number of motor units (count)

within a range of recruitment thresholds (e.g., bins of 0-5% MVC, 5-10% MVC, etc) for all 4 contractions in each participant was pooled within each group. Each bin count was then divided by the number of participants in each group and plotted as a histogram.

ΔF: The contribution of the PIC to self-sustained firing of motoneurons was estimated as per (Afsharipour *et al.*, 2020). First, to estimate the synaptic input to the TA motoneuron pool, the firing profiles of the lowest threshold motor units (typically 2-5 units with recruitment thresholds < 3% MVC), were superimposed to produce a composite profile as an average measure of the synaptic drive to the TA motoneuron pool. Abrupt accelerations in firing rate at the onset of the composite firing rate profile (i.e., secondary range) were manually removed so only the tertiary range remained, which we propose provides a more linear estimate of the synaptic drive to the TA motoneurons. A fifth-order polynomial line was then fit to the composite profile. In the remaining higher-threshold (test) motor units that were activated for at least 1 second before peak torque, the firing rate of the composite profile (measured from the polynomial line) when the test unit was de-recruited (F_T) was subtracted from the firing rate when the test unit was initially recruited (F_R) to produce a ΔF value (ΔF = F_R – F_T). Thus, ΔF is an estimate of the reduction in synaptic input needed to stop motor unit firing in order to counteract the added depolarization provided by the motoneuron PIC. An average ΔF across all units was obtained from the 4 contractions in each participant and then averaged across participants within each respective group (e.g., young development, young adult, older adult and SSRI).

Self-sustained firing duration (SSD): The Self-Sustained firing Duration (SSD) may provide another measure of how much the PIC produces self-sustained firing of the motoneuron. SSD is the percentage of time a motor unit fires on the descending phase of the contraction that is below the level of torque needed on the ascending phase to initially recruit the motor unit. In this case, the torque profile is used as a rough measure of synaptic input to

the motoneuron. To calculate SSD, the formula below is used where a = the duration of time the test unit was active on the ascending phase and d = the duration of time the test unit was active on the descending phase):

$$\text{SSD}= \frac{(duration\ of\ descending\ phase - duration\ of\ ascending\ phase)}{(duration\ of\ descending\ phase + duration\ of\ ascending\ phase)} \times 100\%$$

Thus, a motor unit that fired for 10 seconds on the descending phase of the contraction, but for only 5 seconds on the ascending phase (i.e., 5 seconds longer than expected if the motor unit was de-recruited at the same input as during recruitment), would have a SSD of 33%.

Composite Modulation Depth (CMod): To measure the excursion (modulation depth) in the firing rate of the composite profile that was used to measure the ΔF, the minimum value of the fit polynomial line on the descending phase of the contraction was subtracted from the maximum value (CMod). This was done to ensure that any differences in ΔF between groups were not due to a small CMod constraining the ΔF values.

Piecewise linear fit to the ascending firing rate profile (3-slope analysis): The firing rate profiles during the ascending portion of the contraction exhibit a non-linear shape with roughly three distinct ranges (slopes) that arise from the activation of motoneuron intrinsic conductances. We approximated this non-linear response by three connected straight lines of different slopes (piecewise linear fit). The first range is a rapid increase in motor unit firing at the onset of the contraction (termed secondary range), likely due to the activation of the motoneuron PIC at recruitment (Afsharipour *et al.*, 2020; Binder *et al.*, 2020), and we approximated this with a straight line given the linear increase in firing rate during this period. After full PIC activation, the firing rate of the motor unit increases more slowly (termed the tertiary range) that we model with a second joined line of lower slope. During the tertiary range, where we presume synaptic drive is still increasing, motor unit firing can decrease before peak torque is reached. We refer to this as the tertiary sag range; this data will be presented in *Chapter 3*. To fit a piecewise linear model to the secondary, tertiary and

tertiary sag ranges we employed a non-linear search for parameters $m_1 - m_3$ (slopes) and $b_1 - b_3$ (offsets) of three linear equations:

$$F(t) = m_1 t + b_1 \quad \text{if} \quad t < t_{BP1} \qquad \text{(Secondary range)}$$

$$F(t) = m_2 t + b_2 \quad \text{if } t_{BP1} < t < t_{BP2} \qquad \text{(Tertiary range)}$$

$$F(t) = m_3 t + b_3 \quad \text{if } t > t_{BP2} \qquad \text{(Tertiary sag range)}$$

where F(t) is the model firing rate and t is time. These lines are constrained to be joined at two breakpoints in time, t_{BP1} and t_{BP2}, since we do not see discontinuities in firing at the transitions between ranges. Thus, $F(t_{BP1}) = m_1 t_{BP1} + b_1 = m_2 t_{BP1} + b_2$ and thus, by rearranging we compute:

$$t_{BP1} = (b_1 - b_2) / (m_1 - m_2) \quad \text{and likewise for the second breakpoint}$$

$$t_{BP2} = (b_2 - b_3) / (m_2 - m_3)$$

The 6 unknown parameters (m_1, m_2, m_3, b_1, b_2, b_3) in this function F(t) were determined iteratively by minimizing the least squared error between the model and actual firing rates, starting with initial guesses (values) for the breakpoints, and using the unconstrained Matlab simplex search method called fminsearch. Initial guesses for the m and b parameters were obtained by separate linear regressions on the segments of data between the breakpoint values. Because of the non-linear nature of this model (with variable breakpoints), there are multiple possible solutions (at minima in criteria) depending on the starting initial values given to the breakpoints. We systematically searched the solution space by testing all possible initial values for t_{BP1} and t_{BP2} pairings at each frequency point. Many nearby initial values converged onto a single solution with a common minimum error, and we manually chose the final solution with both the near minimum error and the largest number of initial value pairs that led to that error. Sometimes two or more such solutions arose, and we chose the one that best fit the bin averaged (10 ms bins) firing rate profile, as determined visually. Final solutions were also constrained to have a positive secondary range slope that was at least

twice as steep as the tertiary range slope and a tertiary sag range with a slope < 0 Hz/s. If there was no secondary range (i.e., $b_1 < 2xb_2$), the firing rate profile was fit with just one or two straight lines to delineate the tertiary range only or the tertiary and tertiary sag range, respectively. In many of the higher threshold units when there was no period of low slope firing that was similar to the tertiary range observed in the lower threshold units, we also fit one or two lines to the firing rate profile to delineate the secondary range only or the secondary and tertiary sag ranges, respectively. Finally, in cases where there was no tertiary sag range, the straight line through the tertiary range was extended to the peak torque to measure its slope and duration. The proportion of motor units exhibiting a secondary and/or tertiary range was calculated in each participant by first binning the motor units according to their recruitment threshold (see below) and pooling all of the motor units from the four contractions together. The percentage of total units in each bin with a secondary or tertiary range was then calculated (e.g., number of units with a secondary or tertiary range/number of total units within the bin x 100%), and this percentage was then averaged across participants within each group for each bin. The slope and duration of the secondary and tertiary ranges were also analyzed similar to ΔF with respect to group and age described above and with respect to the recruitment threshold of the motor units described below.

Analysis according to recruitment threshold of the motor units: To examine if the ΔF, secondary and tertiary range values varied according to the recruitment threshold of the motor units, values from motor units having a recruitment threshold within a given range (e.g., bins of 0-3%, 3-5%, 5-7% … 25-27% MVC) from the 4 contractions were averaged together in each participant using a custom Matlab program. These binned averages were then averaged across participants within each group.

Torque steadiness: Torque steadiness was quantified by measuring the coefficient of variation (CoV) of the detrended torque trace. In each participant, the 4 triangular torque

ramps were subjectively split into ascending and descending components, determined visually as the point where the torque transitioned from an ascending to a descending profile near its peak. The Matlab detrend function was applied to the separated ascending and descending components where the best straight-line fit to the data was removed. The standard deviation (SD) of the detrended torque was calculated across the entire ascending or descending phase. The SD of the ascending or descending detrended torque was then divided by the mean of the non-detrended torque to produce the CoV (SD/mean) (Skinner *et al.*, 2019). Note that the homoscedasticity of the standard deviation across the ascending or descending phase was not measured.

Statistics

Sigma Plot 11.0 software was used for all statistics. Because ΔF and mean firing rates did not differ between males and females during the 30% MVC contractions, as will be detailed in another paper, data from the two sexes were collapsed within each group. A Shapiro-Wilk test was used to assess the normality of the data. Group comparisons consisted of young development vs young adult, young development vs older adult, young adult vs older adult and SSRI vs SSRI controls. Unpaired, between-group comparisons for normally distributed data were assessed with Student's t-test and non-parametric data were assessed with the Mann-Whitney-rank-sum test. The relationship between variables (i.e., ΔF, CMod, slopes, torque steadiness) and participant age were evaluated with a Pearson product correlation moment (r). Within each group, a one-way ANOVA was performed on normally distributed data and a one-way ANOVA on Ranks was used on non-normally distributed data to compare the effect of motor unit recruitment threshold on the ΔF or secondary and tertiary range variables (e.g., slope and duration). A two-way ANOVA was performed to analyze the effect of group and recruitment threshold on the ΔF and the secondary and tertiary range

variables. Statistical significance for all analyses was defined as p ≤ 0.05. Data are presented in text and tables as the mean ± SD or in some cases, median (range).

Results

Number and firing rate profiles of decomposed motor units

Using the blind-source separation algorithm (Negro *et al.*, 2016), a total of 2164 single motor units were decomposed from the TA HDsEMG activated during the 30% MVC dorsiflexion, with 575 units decomposed in the young developmental group (aged 7- 17 years, n = 20), 669 units in the young adult group (aged 18 - 28 years, n = 13), 384 units in the SSRI group (aged 11-28 years, n = 9) and 536 units in the adult group (32-53 years, n = 8). In all groups the average silhouette (SIL) value, was greater than the cutoff of 0.85 (young development = 0.89 ± 0.023; young adult = 0.90 ± 0.030, SSRI = 0.900 ± 0.018 and older adult group =0.94 ± 0.025). Example motor unit firing profiles and dorsiflexion torque traces from a single 30% MVC contraction are shown in Figure 2.1 for an 11-year old in the young development group, a 19-year-old participant in the young adult group and from a 16-year-old participant taking an SSRI. All ten decomposed motor units are displayed for the 11-year-old and are plotted in order of recruitment threshold, whereas ten representative motor units having similar increments in recruitment threshold are displayed for the other two participants. The motor unit firing rate profiles of the 11-year old participant were similar to the participant taking SSRIs and different from the older 19-year old participant. For example, the maximum firing rates of several units in the young development and SSRI participants (e.g., units 3 to 7) were higher compared to units of similar threshold in the young adult participant. Moreover, firing rates of motor units recruited at higher torques (e.g., units 6 to 10) decreased more slowly in the young development and SSRI participants and/or continued to fire for longer while the torque was reduced towards zero at the end of the

contraction (marked by the vertical dotted line) compared to the young adult participant,

suggesting a greater amount of prolonged, self-sustained firing in the former two groups.
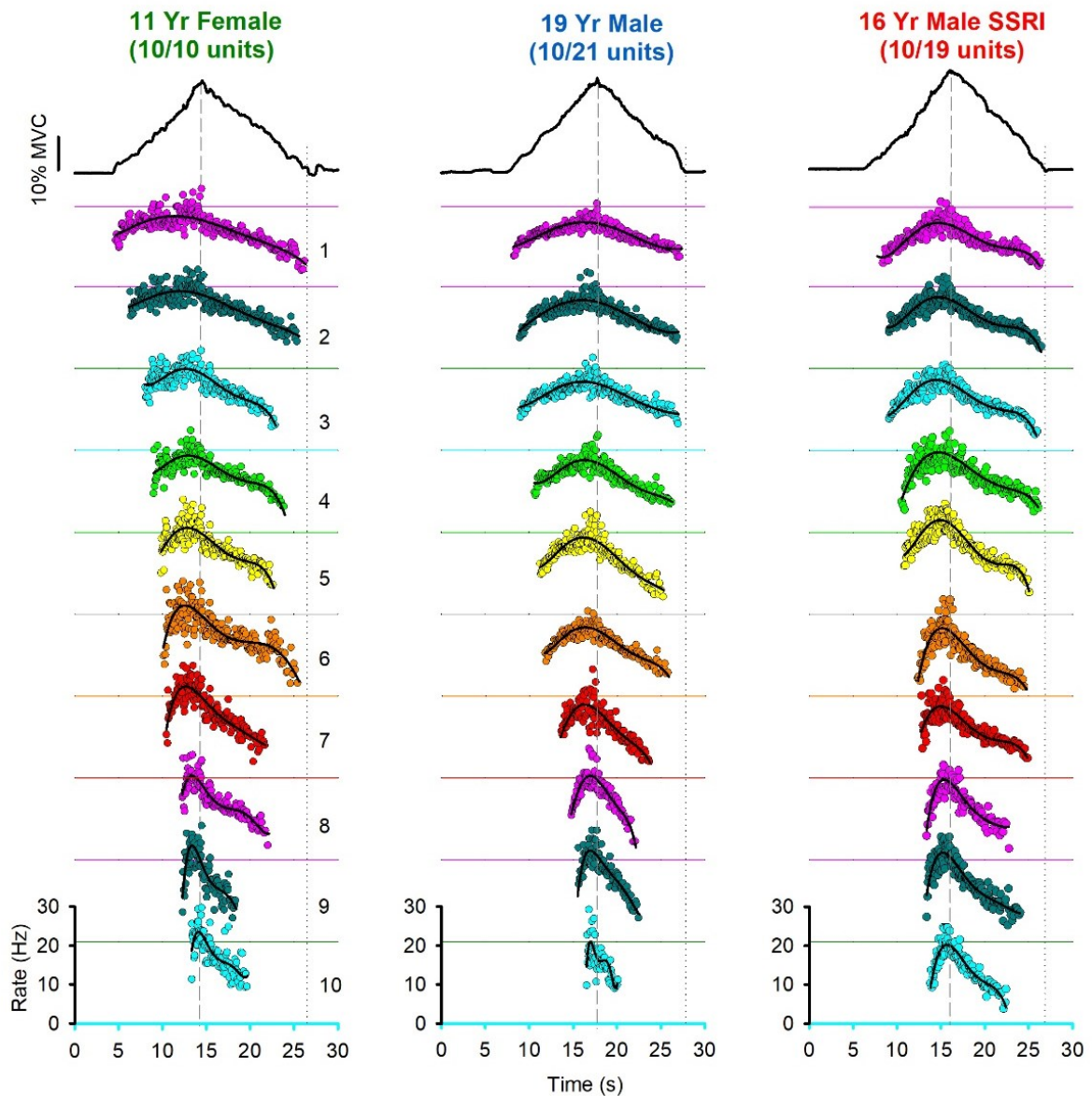
Figure 2.1. Dorsiflexion torque (top trace) and firing rate profiles of 10 decomposed TA motor units during a triangular 30% maximum voluntary contraction (MVC) plotted from top to bottom in order of recruitment threshold. Left: 11-year-old female (10 out of 10 units decomposed); Middle: 19-year-old male (10 out of 21 units); Right: 16-year-old male taking an SSRI (10 out of 19 units). The vertical long dashed line marks the time of peak torque and the short, dashed line marks the time of zero torque at the end of the contraction. The black lines show the fifth-order polynomial fit to the firing rate profiles. The 0 Hz baseline (x-axis) is displayed in the corresponding colour for each unit except for the yellow units where grey is used.

When first comparing across all participants, the average number of motor units decomposed per contraction increased more steeply with age up until ~30.25 years as measured by fitting two straight lines to the data (Fig. 2.2A, SSRI participants in red). On average, there were more units decomposed per contraction in the young adult (12.86 ± 7.65) and older adult (16.75 ± 6.40) groups compared to the young development group (7.03 ± 3.67, $p = 0.041$ and 0.021, respectively, Mann-Whitney Rank Sum), with no difference compared to the SSRI group (10.66 ± 5.96, $p = 0.479$ Student's t-test and $p = 0.295$ Mann-Whitney Rank Sum, respectively). Moreover, the young adult and older adult participants had a greater proportion of lower-threshold units (i.e., peak of gaussian curve at 2.5% MVC, Fig. 2.2B middle graphs) compared to the younger development group (peak at 7.5% MVC, top left) and the participants taking SSRIs (peak at 12.5% MVC, bottom right). Because the distribution of motor unit recruitment thresholds was different across groups, in addition to age, we also plotted ΔF and other measures across the recruitment threshold of the motor units to determine if it was a contributing factor.
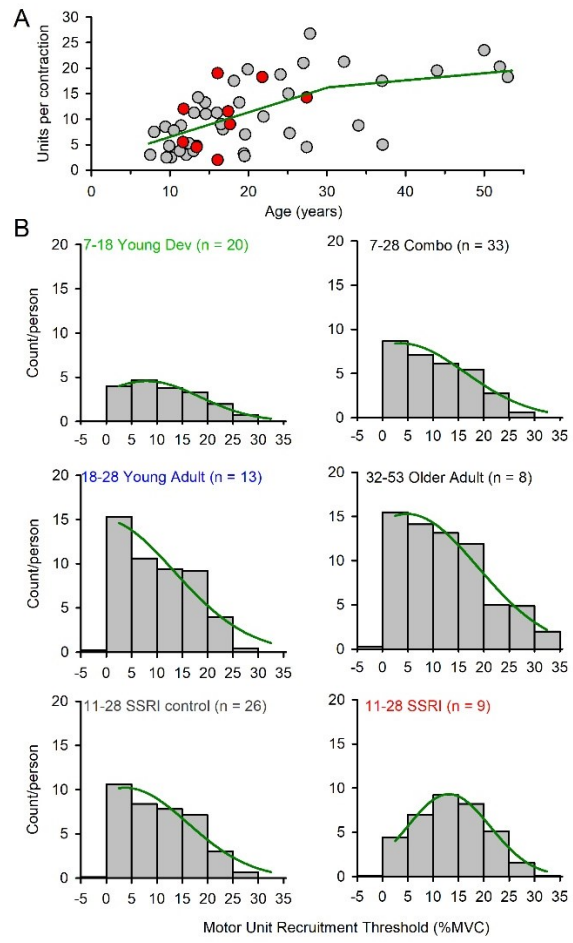
Figure 2.2. A) Number of TA motor units per contraction plotted against the age of the participant. Participants taking SSRIs are marked with red circles. **B)** Histogram distribution of number of motor units binned according to the recruitment threshold of the motor unit (in increments of 5% MVC) and divided by the number of participants in each group. The combined young development and young adult group (Combo: 7-28 years) is also displayed. N = number of participants in each group.

Estimation of PIC amplitude

ΔF was measured to examine if there were changes in the estimated contribution of the PIC to self-sustained firing of the motoneuron across development and if it was larger in participants taking SSRIs. To measure ΔF, the profile of the synaptic input to the TA motoneurons was estimated by averaging the mean firing rate profile of the 2-3 lowest-threshold control units (e.g., bottom profiles in Fig. 2.3A with grey, light blue and green dots) to produce a composite control motor unit profile as per (Afsharipour *et al.*, 2020). This estimated synaptic input was typically lower when the test motor units (orange dots, top profiles) were de-recruited compared to when they were first recruited (ΔF marked by length of downward arrows in Fig. 2.3A), potentially from the added depolarization of the PIC assisting self-sustained firing at low synaptic inputs. ΔF was larger in both the young development (7.1 Hz) and SSRI (9.3 Hz) participants compared to the young adult participant (4.6 Hz), consistent with the motoneuron PIC in the former two groups producing greater amounts of self-sustained firing.

To explore the relationship of age to ΔF further, we plotted the mean ΔF for each of the young development and adult participants across age and noted a negative correlation as marked by the black regression line ($r = -0.496$, $p = 0.006$, Table 2.1a), showing that ΔF decreases with age from 7 to 28 years (Fig. 2.3Bi). Correspondingly, the average ΔF in the young development group (5.83 ± 1.15 Hz), but not the young adult group (4.88 ± 0.80 Hz), was larger compared to the older adult group (4.78 ± 1.05 Hz, results of unpaired comparisons for ΔF are presented in top row of Table 2.1b with bolded numbers indicating significant differences). Moreover, the average ΔF was higher in the SSRI group (6.45 ± 0.56 Hz, marked by the solid red circles in Fig. 2.3Bi) compared to the age-matched controls (5.27 ± 1.05 Hz).
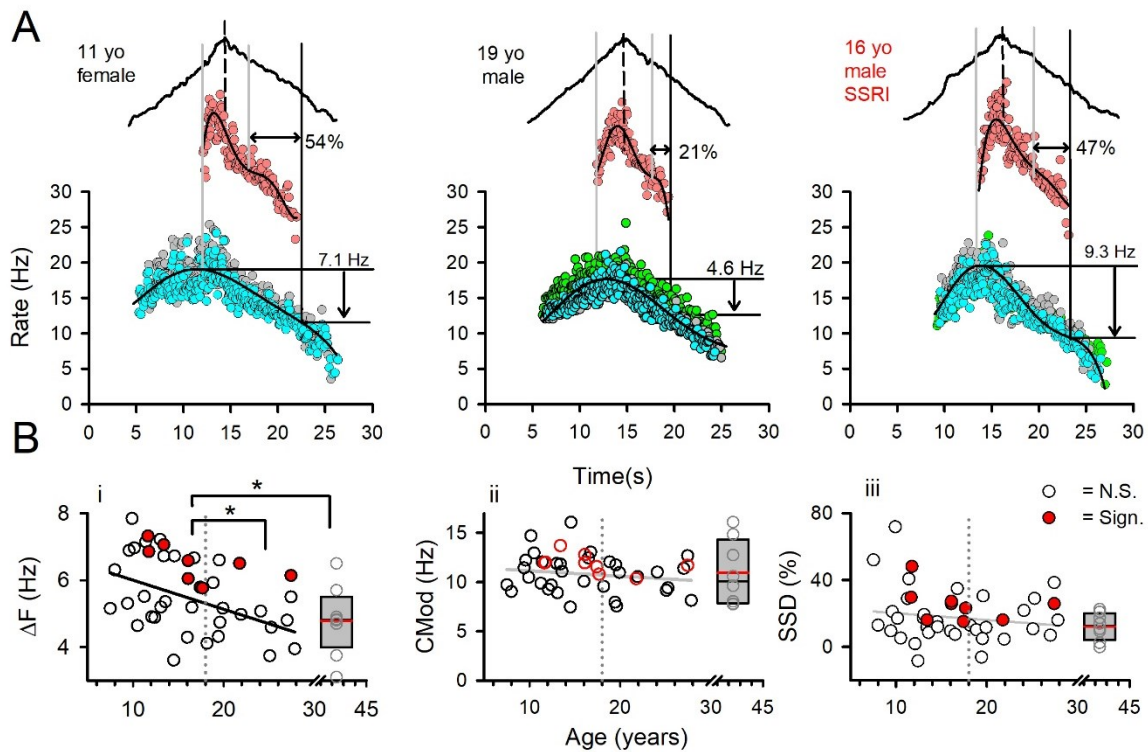
Figure 2.3. **A)** Representative firing rate profiles of composite control (bottom) and test (top) TA motor units used to measure ΔF, CMod and SSD in the same three participants from Fig. 2.1. **B)** ΔF, CMod and SSD plotted against age for the young development and young adult groups (open circles), the SSRI group (red circles). Adult values in box plot with individual participant data in grey circles, mean red line, median black line, box bounds 25% and 75% percentiles plotted at the average age of 42.4 years. Black regression lines indicate there is a significant correlation with age, grey regression lines indicate no correlation (see Table 2.1a for r and p values). Filled red circles indicate significant difference between the SSRI group and the age-matched controls. The dashed vertical line separates the young development and young adult participants. * indicates difference between groups with p < 0.05, results of unpaired comparisons in Table 2.1b.

Table 2.1	(a) Combo (7-28 years)	(b) Young Dev vs Young Adult	Young Dev vs Older Adult	Young Adult vs Older Adult	SSRI vs Age-matched Control
ΔF	**r= -0.469, p=0.006**	**p= 0.015 (S) t= 2.574**	**p= 0.035 (S) t= 2.218**	p= 0.811 (S) t= 0.243	**p= 0.003 (S) t= 3.229**
CMod	r= -0.166, p=0.357	p= 0.139 (S) t= 1.519	p= 0.787 (S) t= -0.273	p= 0.485 (S) t= -0.711	p= 0.076 (S) t=1.833
SSD	r= -0.149, p= 0.407	p= 0.543 (MW) T= 204.000	p= 0.525 (MW) T=103.000	p= 0.606 (S) t= -0.525	**p= 0.035 (S) t= 2.205**

Table. 2.1. a) Pearson's Product (r) and p-values for correlation between ΔF, CMod and SSD against age across the young developmental and young adult groups (Combo). **b)** P and t-values of Student's t-tests and Mann-Whitney Rank sum tests for the values listed in the left column between the various groups listed in the top row. Significant values where p < 0.05 are marked in bold. S = Unpaired Student's t-tests. MW = Mann-Whitney Rank sum test.

The larger ΔF in the young development and SSRI groups could have been mediated by a greater excursion in firing rate modulation of the composite control motor units (CMod, lower profiles in Fig. 2.3A). However, unlike ΔF, there were no differences in CMod (Fig. 2.3Bii) between the young development (11.22 ± 2.09 Hz), young adult (10.17 ± 1.66 Hz) or older adult groups (10.94 ± 3.28 Hz), nor were there differences between the SSRI group (11.88 ± 0.99 Hz) and the age-matched controls (10.62 ± 1.97 Hz, middle row Table 2.1b), with CMod being nearly twice that of the ΔF values. Moreover, there was no relationship between CMod and age across the young development and young adult groups as marked by the grey regression line in Figure. 2.3Bii (r = -0.166, p = 0.357, Table 2.1a). A similar CMod across groups suggests that the lower ΔF in the young adult and older adult groups were not constrained by a lower CMod. The smaller number of decomposed TA motor units in the young development group (Fig. 2.2) also could have biased sampling to produce a higher ΔF. However, when comparing ΔF to a group of young and older adults (n = 10) with a similar number of decomposed motor units per contraction (median number of units = 7.13) compared to the young development group (median: 7.50, P = 0.704 Mann-Whitney), ΔF was still larger in the young development group (5.83 ± 1.15 Hz) compared to this young and older adult group (4.95 ± 0.99 Hz, p = 0.035, Student's t-test).

The differences in estimated PIC activation between the three participants from Figure 2.3 were also reflected in the measure of Self-sustained Firing Duration (SSD), which is the percentage of time a motor unit fires below the torque needed to initially recruit the motor unit (horizontal double arrow, Fig. 2.3A). The SSD was 54% in the 11-year-old participant, 21% in the 19-year-old participant and 47% in the 16- year-old participant taking an SSRI. However, in the group data (Fig. 2.3Biii), SSD in the young development group (19.44 ± 18.51%) was not larger compared to the young adult (14.74 ± 12.29 %) or the older adult group (10.52 ± 7.71%, Table 2.1b) nor was there a correlation between SSD and age

across the young development and young adult groups (grey regression line, Table 2.1a). In contrast, SSD in the participants taking SSRIs (25.27 ± 10.12%) was larger compared to the age-matched controls (15.02 ± 12.57%, bottom row in Table 2.1b), similar to ΔF (Fig. 2.3Bi).

We also examined ΔF as a function of recruitment threshold of the test motor units (Fig. 2.4) given the potential for it to affect ΔF and the different distribution of motor unit recruitment thresholds between the groups (Fig. 2.2). When tested with a one-way ANOVA, there was no main effect of recruitment threshold on ΔF within any of the groups (see one way ANOVA results in Table 2.2a), in agreement with Ashfaripour *et al.,* 2020. Although the two-way ANOVA showed a main effect of age or SSRI intake (i.e., group) on ΔF as expected, there was no main effect with recruitment threshold or in their interaction with age or SSRI intake (Table 2.2b).
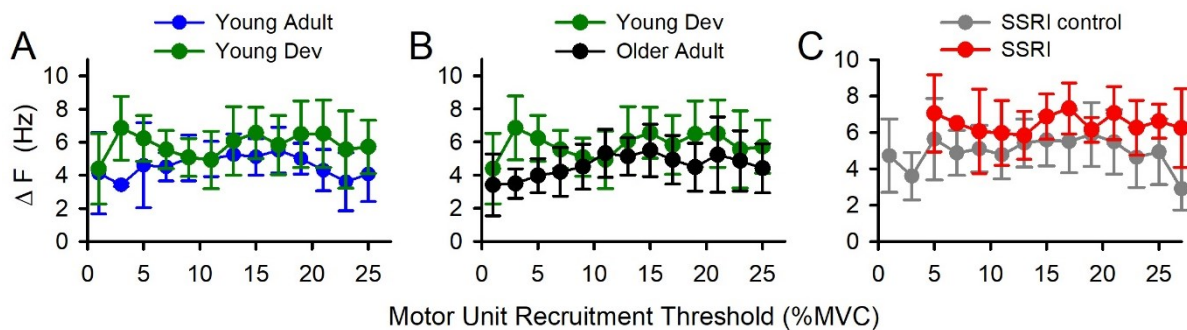
Figure. 2.4. ΔF plotted against recruitment threshold of the test motor units (binned every 2% MVC) for: **A)** young development (n=20, green) and young adult (n=13, blue); **B)** young development and older adult (n=8, black) and **C)** SSRI (n=9, red) and their aged-match controls (n=26, grey). Solid symbols denote a significant group effect from the two-way ANOVA analysis. Error bars are ± SD.

Table 2.2 (ΔF)	Young Dev	Young Adult	Older Adult	SSRI
a. One-way ANOVA	H (12) =11.67 P = 0.472	H (12)=16.623 P = 0.164	F(1,12) = 0.993 P = 0.465	F(1,10) = 0.688 P = 0.731
b. Two-way ANOVA	Young Dev vs Young Adult		Young Dev vs Older Adult	SSRI vs Age-matched Control
Group x RT	F(1,12) = 1.285 P = 0.228		F(1,12) = 0.788 P = 0.662	F(1,11)=0.537 P = 0.877
Group	**F(1) = 24.781 P < 0.001**		**F(1) = 21.690 P < 0.001**	**F(1) = 24.558 P < 0.001**
RT	F(12) = 1.343 P = 0.195		F(12) = 1.074 P = 0.384	F(11) = 1.115 P = 0.350

Table 2.2. a) Results from a one-way ANOVA examining the effect of motor unit recruitment threshold (RT) on ΔF within each group in Figure 2.4. H values are given for one-way ANOVA on Ranks. **b)** Results from a 2-way ANOVA for ΔF with Group and Recruitment Threshold (RT) as factors.

Proportion of motor units having a secondary and/or tertiary range.

Three joined, straight lines of different slopes were fit to the ascending portion of the firing rate profiles to quantify the non-linearities in motor unit firing in response to the presumed linear increase in synaptic drive to the TA motoneurons. The first slope, termed the secondary range (light blue, Fig. 2.5A), is thought to reflect the acceleration in firing rate when the PIC is activated during recruitment of the motoneuron and thus, may potentially provide an estimate of the upswing in membrane potential during PIC activation. As shown for the top firing rate profiles in Figure 2.5A, ~ 85-90% of motor units activated between 0 and 15% MVC had a secondary range in all groups (Fig. 2.5B top graphs), with the remaining units having firing rate profiles that jumped directly onto the tertiary range (e.g., unit 2 in 11-year-old, Fig. 2.1). As the recruitment threshold of the motor units increased above 18% MVC (e.g., bottom units in Fig. 2.5A), ~100% of motor units had a secondary range. The second slope, termed the tertiary range (green, Fig. 2.5A), is thought to reflect the lower gain firing of the motoneuron after the full activation of the PIC increases the conductance of the cell. All motor units between 0 and 5% MVC had a tertiary range in all groups (Fig. 2.5B bottom rows), and this proportion rapidly dropped off for motor units with recruitment thresholds >13% MVC when the secondary range started to dominate most of the ascending firing rate profile (e.g., Fig. 2.5A, bottom profiles). A two-way ANOVA did not show a main effect of age (group) or motor unit recruitment threshold on the proportion of motor units having a secondary or tertiary range or an interaction effect. However, there was a main effect of recruitment threshold on the proportion of units having a secondary range in between the SSRI and SSRI control groups and between all group pairings for the tertiary range (see bolded numbers in Table 2.3). Note that the third slope, where the firing rate decreases during the tertiary range even though the torque continues to increase (tertiary sag range, red, Fig. 2.5A), is presented in *Chapter 3*.
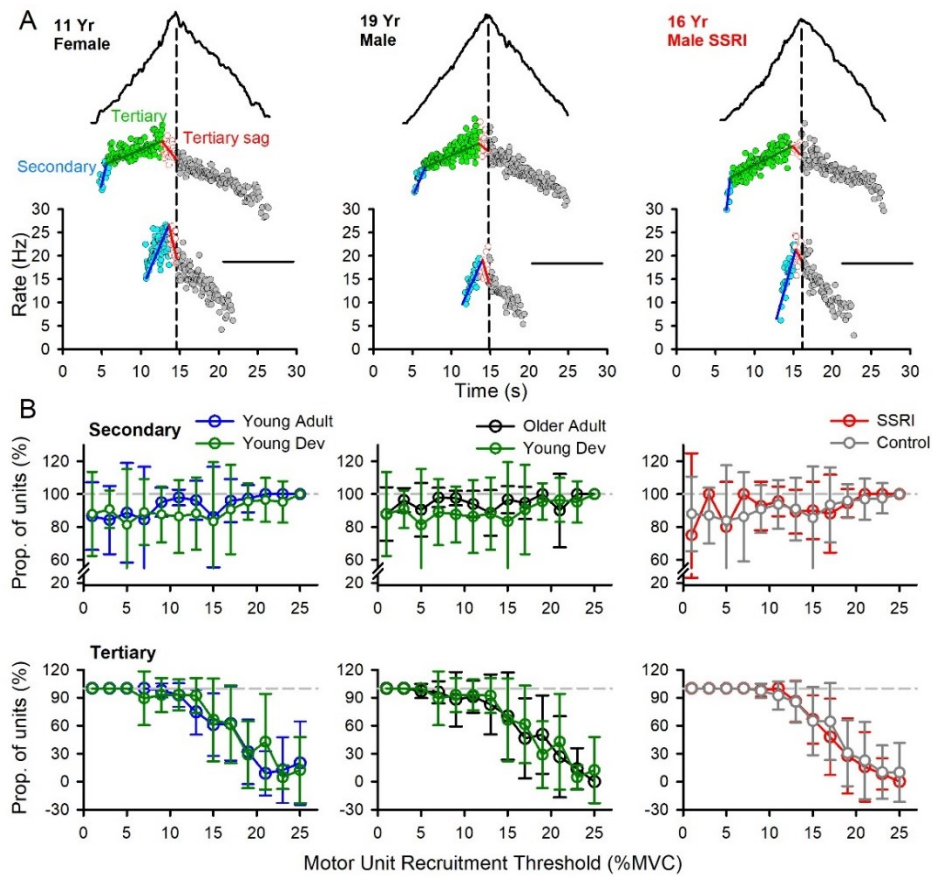
Figure 2.5. A) Examples of secondary (blue), tertiary (green) and tertiary sag (red) ranges fit to the ascending profile of both a lower threshold (middle plot) and higher threshold (bottom plot) motor unit in the same three participants as in Figure 2.1. The vertical dashed line marks peak torque and the black horizontal line represents 0 Hz for the top firing rate profiles. **B)** *Top row:* Proportion of units with secondary ranges plotted against motor unit recruitment threshold averaged in 2% MVC bins in young development (green) and young adult (blue) groups (left); young development and older adult (black) groups (middle); and SSRI (red) and age-matched controls (grey) (right). *Bottom row:* Same as *Top row* but for tertiary range. Error bars = SD.

Table 2.3: Prop. Secondary Range	Young Dev vs Young Adult	Young Dev vs Older Adult	SSRI vs Age-matched Control
Group x RT	F(1,12)=0.306 P=0.988	F(1,12)=0.372 P=0.972	F(1,12)=0.889 P=0.559
Group	F(1) = 1.544 P = 0.215	F(1) = 3.323 P = 0.070	F(1) = 0.002 P = 0.961
RT	F(12) = 1.097 P=0.363	F(12) = 0.581 P=0.856	**F(12) = 2.030 P=0.022**
Tertiary Range			
Group x RT	F(1,12)=0.746 P=0.705	F(1,12)=0.352 P=0.978	F(1,12)=0.975 P=0.363
Group	F(1,12)=1.216 P = 0.271	F(1,12)=0.363 P = 0.548	F(1,12)=0.079 P = 0.779
RT	**F(12) = 35.430 P < 0.001**	**F(12) = 21.337 P < 0.001**	**F(12) = 47.947 P < 0.001**

Table 2.3. Results from a two-way ANOVA examining the effect of age or SSRI intake (group) and motor unit recruitment threshold on the proportion of units having a secondary or tertiary range for the data plotted in Figure 2.5B.

Secondary and tertiary range slopes and durations

Similar to ΔF and SSD, we first plotted the slope and duration of the secondary and tertiary ranges across the age of the participants. Like ΔF, the *slope* of the secondary range decreased with age (Fig. 2.6A, see r and p values in Table 2.4b), with the young development group having a steeper secondary range slope (5.73 ± 1.93 Hz/s) compared to the young adult (4.34 ± 0.90 Hz/s) and older adult (4.35 ± 1.20 Hz/s) groups (mean ± SD values in Table 2.4a and results of unpaired comparisons in Table 2.4c). In contrast, the *duration* of the secondary range did not vary with age across the young development and young adult groups (Fig. 2.6B, Table 2.4b), nor were there differences between the young development, young adult and older adult groups (Table 2.4a,c). The secondary range slope was steeper in the SSRI group (7.20 ± 2.38 Hz/s, Fig. 2.6A solid red circles,) and with a shorter duration (1.39 ± 0.25 s, Fig. 2.6B) compared to the age-matched controls (slope: 4.96 ± 1.69 Hz/s, duration: 1.68 ± 0.32 s, Table 2.4a,c). Thus, the slope (and sometimes duration) of the secondary range, which may be related to the threshold and acceleration of the PIC at motoneuron recruitment, followed a trend across the groups that was similar to the ΔF estimate of the PIC as detailed below. In contrast, there were no associations in the slope or duration of the tertiary range with age where motoneuron firing is thought to occur during full PIC activation (grey regression lines
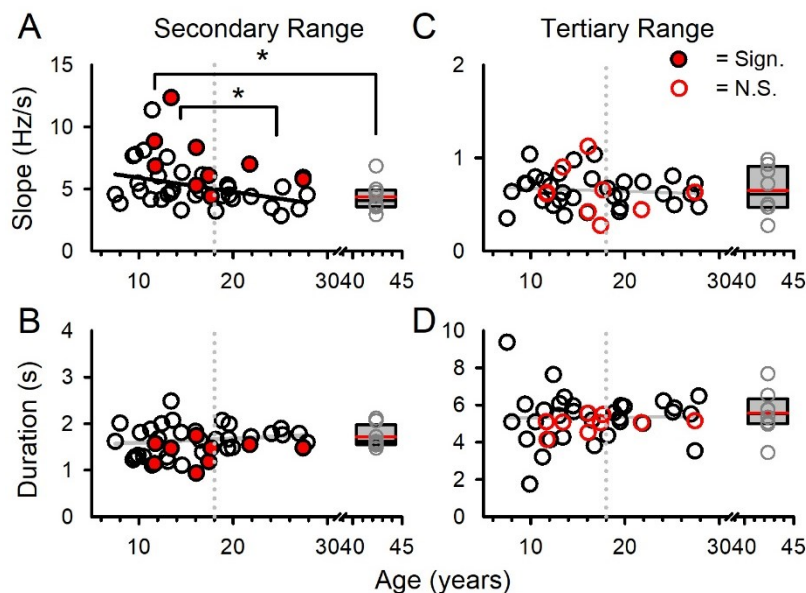
in Fig. 2.6C&D, Table 2.4b), nor were there any differences between age groups or between the SSRI group and the age-matched controls (Table 2.4a,c).

44

Figure 2.6. A) Mean slope and **B)** duration of the secondary range plotted against age of the participants in the young development and young adult groups (open circles, n = 33) and participants taking SSRIs (red, n = 9). Older adults (grey circles, n = 8) are plotted at the average age of the group (42.4 years). **C)** and **D)** Same values in A and B for the tertiary range. Black regression line indicates a correlation to age. * = difference between groups (see bolded numbers in Table 2.4c). Filled red circles indicate differences between the SSRI group and their age-matched controls (n = 26).

Table 2.4	Young Dev	Young Adult	Older Adult	SSRI	SSRI Control
(a) Secondary range slope	5.73 ± 1.88	4.34 ± 0.90	4.35 ± 1.20	7.20 ± 2.38	4.96 ± 1.69
Secondary range duration	1.57 ± 0.28	1.72 ± 0.18	1.75 ± 0.31	1.39 ± 0.25	1.69 ± 0.32
Tertiary range slope	0.67 ± 0.1	0.61 ± 0.12	0.64 ± 0.11	0.63 ± 0.13	0.64 ± 0.17
Tertiary range duration	5.27 ± 1.59	5.41 ± 0.79	5.01 ± 0.43	5.56 ± 1.23	5.36 ± 0.99
	(b) Combo (7-28 years)	**(c) Young Dev vs Young Adult**	Young Dev vs Older Adult	Young Adult vs Adult	SSRI vs Control
Secondary range slope	**r = -0.387, p = 0.026**	**P= 0.026(MW) T=160.000**	**P = 0.050(MW) T= 77.000**	p = 0.981 (S) t= -0.024	**P =0.004 (MW) T=238.000**
Secondary range duration	r = 0.167, p = 0.354	P = 0.347 (MW) T= 247.000	p = 0.448 (S) t= -0.770	p = 0.940 (S) t= 0.0768	**p = 0.019(S) t= 2.469**
Tertiary range slope	r = -0.104, p = 0.570	p = 0.297 (S) t= -1.062	p = 0.753 (S) t= -0.318	P = 0.800 (MW) T=92.000	p = 0.934 (S) t= -0.083
Tertiary range duration	r = 0.013, p = 0.945	P = 0.645 (MW) T= 227.000	p = 0.675 (S) t= 0.424	p = 0.742 (S) t= 0.334	p = 0.320 (S) t= -1.010

Table 2.4. a) Mean ± SD of secondary and tertiary range slopes and durations in the groups compared in Figure 2.6. **b)** Pearson's product correlation (r) and p-value of secondary and tertiary range slope and duration with age in the combined young development and young adult (Combo) group. **c):** Results of Student's t-test (S) and Mann-Whitney Rank Sum (MW) test results for unpaired comparisons of secondary and tertiary slopes and durations between age groups and between SSRI and age-matched participants. P < 0.05 in bold numbers.

We also examined if the slope and duration of the secondary and tertiary ranges varied across the recruitment threshold of the motor units within each group (Fig. 2.7). In general, the slope of the secondary range decreased and became longer in duration as the recruitment threshold of the motor units increased. A one-way ANOVA revealed that there was a statistically significant difference in secondary range slope between motor units of different recruitment thresholds in all groups except for the young adults (marked by *,*,* in top row of Fig. 2.7A for the young development, older adult and SSRI groups respectively, see bolded numbers in Table 2.5), consistent with the threshold of PIC increasing with the recruitment threshold of the motoneuron. Likewise, the duration of the secondary range

increased with recruitment threshold in most groups but then decreased in the very highest

threshold units given their shorter activation times before peak torque (Fig. 7A, bottom row).

As a result, only the SSRI group had a statistically significant difference in the duration of the

secondary range between motor units of different recruitment thresholds (* and bolded

numbers in Table 2.5). In contrast, a one-way ANOVA revealed that there was no

statistically significant difference in the slope of the tertiary range between motor units of

different recruitment thresholds but as expected, there was a difference in the tertiary range

duration because more of the firing rate profile in the higher threshold units was comprised of

the secondary range (*'s in bottom row of Fig. 2.7B, bolded numbers in Table 2.5), with

many of the motor units recruited at or above 23% MVC having no tertiary range and only a secondary range (Fig. 2.5B).
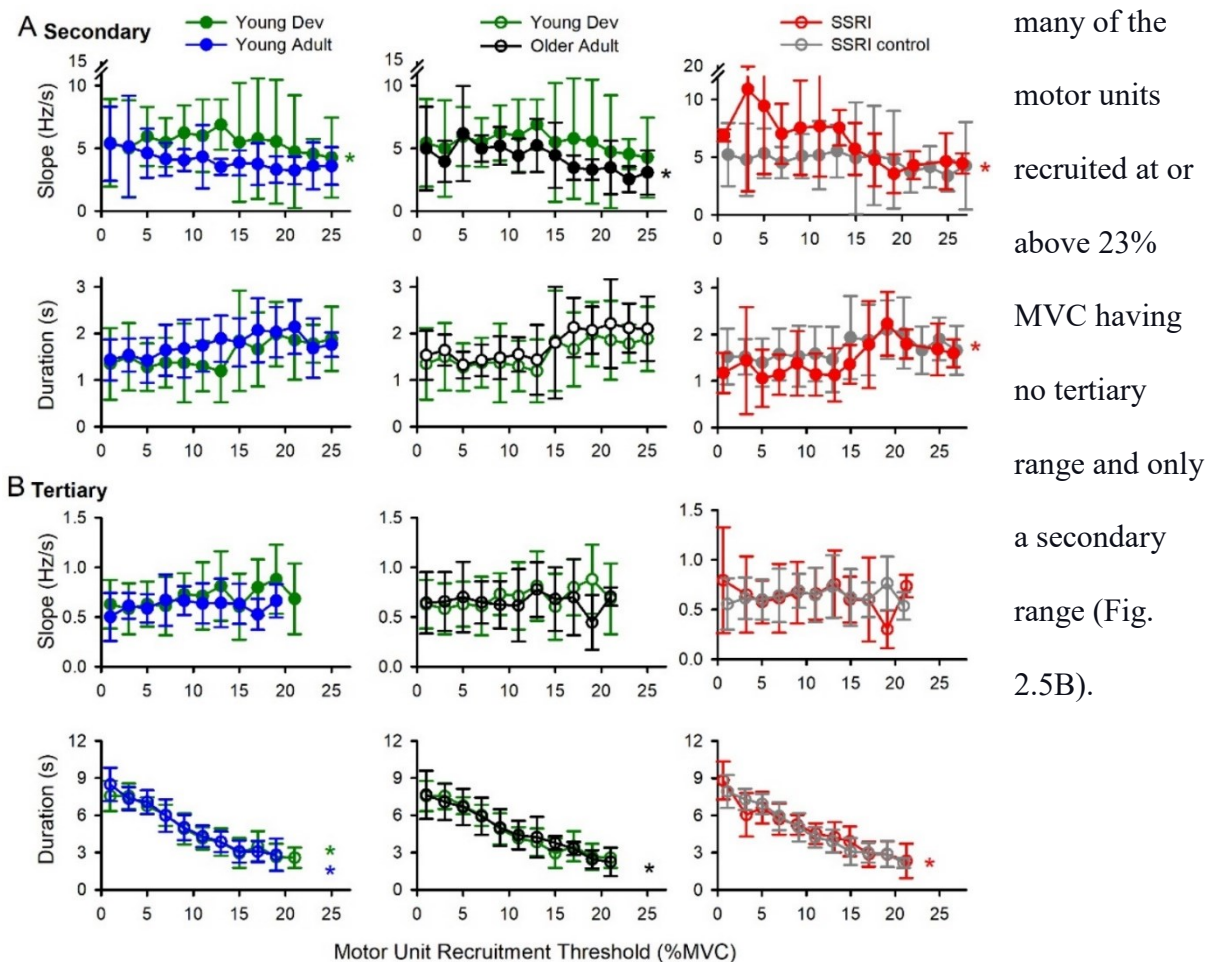
Figure 2.7. A) Slope (top) and duration (bottom) of the secondary range plotted against motor unit recruitment threshold (2% MVC bin widths): left: young development vs young adult; middle: young development vs older adult; right: SSRI vs SSRI controls. **B)** Same as in A but for tertiary range. * = significant effect of recruitment threshold on dependent variables (bolded numbers in Table 2.5). Solid circles = group effect from two-way ANOVA (bolded numbers in Table 2.6). Error bars ± SD.

Table 2.5 One-way ANOVA	Young Dev	Young Adult	Older Adult	SSRI
Secondary range slope	**H(12) = 22.496 P=0.032**	H(12) = 11.799 P=0.462	**H(12) = 25.177 P=0.014**	**H(12) = 23.261 P=0.039**
Secondary range duration	H(12) = 20.664 P=0.056	F(12) = 1.674 P=0.082	H(12)= 20.233 P=0.063	**H(13) = 22.576 P=0.047**
Tertiary range slope	F(10) = 1.60 P=0.326	F(9) = 0.782 P=0.633	H(10) = 3.891 P=0.952	H(10) = 7.518 P=0.676
Tertiary range duration	**F(10) = 34.450 P<0.001**	**F(9) = 34.865 P<0.001**	**H(10) = 41.817 P<0.001**	**F(10) = 8.005 P<0.001**

Table 2.5. Results from a one-way ANOVA examining the effect of motor unit recruitment threshold on the secondary and tertiary range slope and durations within each group plotted in Figure 2.7. H values are given for results of one-way ANOVA on Ranks.

When taking the recruitment threshold of the motor units into account, the slope of the secondary range remained higher in the young development compared to the young adult and older adult groups, and between the SSRI and age-matched control groups. Although the two-way ANOVAs examining group and recruitment threshold on the secondary or tertiary range slope and duration did not show an interaction effect with the three group pairings in Figure 2.7 (see non-bolded numbers in Table 2.6), there was a significant main "group" effect on the secondary range *slope* for all group pairs, and for the secondary range *duration* between the young development vs. young adult groups and SSRI vs. SSRI control groups (see bolded numbers in top 2 sections of Table 2.6). Likewise, there was a significant main effect of "group" on the tertiary range *slope* between the young development vs. young adult groups (third section Table 2.6). Lastly, the two-way ANOVA showed a main effect of motor unit "recruitment threshold" on the *duration* of both the secondary and tertiary ranges between all group pairs in Figure 7A and B (bottom rows) respectively (second and bottom sections respectively in Table 2.6).

Table 2.6 Secondary slope	Young Dev vs Young Adult	Young Dev vs Older Adult	SSRI vs Control
Group x RT	F(1,12)=0.865 P=0.571	F(1,12)=0.272 P=0.993	F(1,12)=1.486 P=0.129
Group	**F(1)= 15.679** **P < 0.001**	**F(1)= 8.553** **P = 0.002**	**F(1)= 23.281** **P < 0.001**
RT	F(12) = 0.503 P = 0.912	F(12) = 0.963 P = 0.486	**F(12) = 37.927** **P = 0.002**
Secondary duration			
Group x RT	F(1,12)=0.665 P=0.784	F(1,12)=0.204 P=0.998	F(1,12)=0.689 P=0.762
Group	**F(1)= 5.140** **P = 0.024**	F(1)= 3.788 P = 0.053	**F(1)= 10.152** **P = 0.002**
RT	**F(12) = 2.400** **P < 0.006**	**F(12) = 2.864** **P = 0.001**	**F(12) = 3.568** **P < 0.001**
Tertiary slope			
Group x RT	F(1,9)=0.966 P=0.469	F(1,10)=0.781 P=0.647	F(1,10)=0.950 P=0.488
Group	**F(1)= 5.194** **P = 0.024**	F(1)= 0.688 P = 0.408	F(1)= 0.017 P = 0.896
RT	F(9) = 1.141 P = 0.335	F(10) = 0.541 P = 0.859	F(10) = 0.767 P = 0.660
Tertiary duration			
Group x RT	F(1,9)=0.609 p=0.789	F(1,10)=0.358 p=0.963	F(1,10)=0.659 p=0.762
Group	F(1)= 0.481 P = 0.489	F(1)= 0.003 P = 0.953	F(1)= 0.277 P = 0.599
RT	**F(9) = 69.261** **P < 0.001**	**F(10) = 36.138** **P < 0.001**	**F(10) = 43.156** **P < 0.001**

Table 2.6. Results from a two-way ANOVA examining the effects of age or SSRI intake (group) and recruitment threshold of the motor units and their interaction on the secondary and tertiary range slope and duration between each group pairing in Figure 2.7. Significant main effects marked in bold.

Correlation between ΔF and slope of the secondary range

The slope of the secondary range exhibited similar trends across age and between the different groups as the ΔF. For example, both the ΔF and the slope of the secondary range decreased with age across the young development and young adult groups and both where greater in the young development group compared to the young adult and older adult groups and between the SSRI group and the age-matched controls (compare Figs. 2.3Bi and 2.6A). Thus, we plotted the average slope of the secondary range for each participant against their average ΔF to determine if they were indeed correlated (Fig. 2.8). Across the entire group,

there was a correlation between ΔF and the slope of the secondary range (r = 0.536, p < 0.001, n = 50), showing that these two estimates of motoneuron PIC activation co-vary with one another.
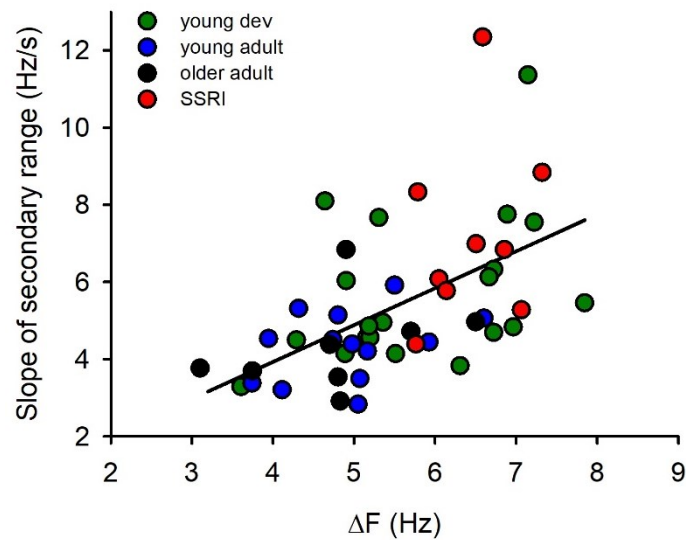
Figure 2.8. The average secondary range slope plotted against the corresponding average ΔF in each participant (n = 50): young development (green), young adult (blue), older adult (black) and SSRI (red). The black regression line was fit through all data points.

Torque steadiness

Lastly, we quantified the amount of torque steadiness as the participants tried to match the trajectory of their ankle torque to the target triangle displayed over the computer screen by measuring the coefficient of variation (CoV= SD/mean) of the detrended ascending and descending torque trace. Similar to ΔF and the slope of the secondary range, the CoV of the detrended torque, for both the ascending and descending phases of the contraction, decreased across age between 7 to 28 years (Combo, r and p values in Table 2.7b), with the ascending CoV in the young development group larger compared to the young adult and older adult groups and the descending CoV larger in the young development group compared to the young adult group only (mean ± SD values in Table 2.7a, results of unpaired comparisons in Table 2.7c). In contrast, torque steadiness in the participants taking SSRIs

(open red circles, Fig. 2.9) was not different compared to the age-matched controls (Table 2.7a,c).
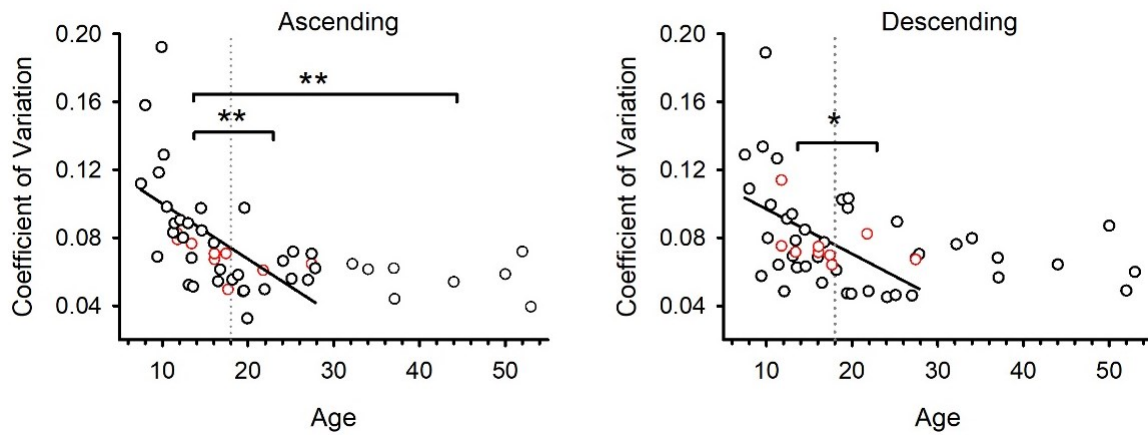
Figure 2.9. The average coefficient of variation (CoV) of the detrended torque from each participant for the ascending (left) and descending (right) phase of the contraction plotted against age of the participant. A straight line was fit through the data for the young development and young adult participants (7 to 28 years) with black line indicated a significant correlation (values in Table 2.7b). Participants taking SSRIs are marked by red circles. * ($P < 0.05$) and ** ($P < 0.01$) denote significant differences between groups (see bolded numbers in Table 2.7).

Table 2.7	Young Dev	Young Adult	Older Adult	SSRI	SSRI age-matched control
(a) CoV Ascending	0.093 ± 0.036	0.059 ± 0.016	0.057 ± 0.011	0.069 ± 0.010	0.067 ± 0.017
CoV Descending	0.089 ± 0.034	0.067 ± 0.023	0.068 ± 0.013	0.077 ± 0.015	0.071 ± 0.022
	(b) Combo (7-28 years)	**(c)** Young Dev vs Older Dev	Young Dev vs Adult	Older Dev vs Adult	SSRI vs age-matched control
CoV Ascending	**r= -0.587, p < 0.001**	** **P= 0.002 (MW) T = 137.000**	** **P= 0.004 (MW) T = 59.000**	p= 0.706 (S) t = -0.383	p= 0.770 (S) t = 0.294
CoV Descending	**r= -0.493, p= 0.004**	* **P= 0.041 (MW) T = 165.000**	P= 0.109 (MW) T = 84.000	P=0.587 (MW) T = 96.000	P= 0.282 (MW) T = 191.00

Table 2.7. a) Mean (±SD) of the CoV of the detrended torque for the ascending and descending phase of the contraction. **b)** *Column 1*: Pearson's product and p value for the correlation between CoV and age across the young development and young adult groups. **c)** *Columns 2-5:* Results of Student's t-test (S) or Mann-Whitney Rank Sum (MW) comparisons between the various groups. Significant values where P < 0.05 are marked in bold. ** = P < 0.01, * = P < 0.05.

Discussion

In rodents during the first three weeks after birth, motoneuron PICs decrease in threshold and increase in amplitude to help secure motoneuron recruitment and amplify synaptic inputs (Quinlan *et al.*, 2011; Sharples & Miles, 2021). However, at this developmental stage PICs produce little self-sustained activation of the motoneuron to prolong the effects of synaptic inputs. Using indirect methods, we show here in humans that by 7 years of age, motoneurons have appreciable self-sustained activity, with participants between the ages of 7 to 17 years having larger ΔFs compared to participants between the ages of 18 to 28 years or 32 to 53 years of age. We also directly quantified the slope and duration of the initial acceleration in motor unit firing during a slowly increasing synaptic drive as a measure of the acceleration in membrane potential produced by the PIC during its initial activation. Similar to ΔF, the slope of this secondary firing range was also steeper in the young development group compared to both adult groups, suggesting that in addition to producing more self-sustained firing, the threshold of motoneuron PICs is lower before and during adolescence compared to adulthood. Interestingly, in participants taking SSRIs both measures of PIC activation, ΔF and slope of the secondary range, were also larger and steeper respectively compared to their age-matched controls, consistent with serotonin increasing the amplitude and decreasing the threshold of motoneuron PICs (Li *et al.*, 2007). We propose that the immaturity of both the corticospinal tract (Nezu *et al.*, 1997; Yeo *et al.*, 2014) and inhibitory pathways in the spinal cord (Geertsen *et al.*, 2017) may contribute to the larger motoneuron PICs observed in participants aged between 7 to 17 years, with these factors combining to contribute to the lesser torque steadiness also observed in this group.

Slope and duration of the secondary range

The initial acceleration in firing rate at the onset of motor unit recruitment, as

quantified by the slope and duration of the secondary range, is thought to be produced by the low-voltage activation of the PIC near the onset of motoneuron recruitment (Bennett *et al.*, 1998b; Lee & Heckman, 1998; Afsharipour *et al.*, 2020; Binder *et al.*, 2020). In addition, a slow inactivation of Kv1.2 channels in the axon initial segment may also contribute to the firing rate acceleration during the secondary range (Bos *et al.*, 2018). This could occur if the Kv1.2 channels were activated quickly at the onset of firing to resist recruitment and then slowly inactivated over the next few seconds to facilitate the initial firing rate acceleration mediated by the increasing synaptic input and PIC. As we have previously predicted (Afsharipour *et al.,* 2020), motor units with low recruitment thresholds have a steeper and shorter secondary range slope compared to higher threshold units (Fig. 2.7). A steep and brief secondary range in low threshold units could be produced if a substantial portion of the PIC is activated subthreshold to firing, with initial motor unit firing occurring during the latter, steep rising portion of the PIC. In contrast, the shallower and longer secondary range slope in the higher threshold motor units could result from the PIC being activated closer to motoneuron recruitment where the initial acceleration of the PIC is much slower (Svirskis & Hounsgaard, 1997; Bennett *et al.*, 1998a; Binder *et al.*, 2020). The finding that the young development and SSRI participants had steeper and/or shorter duration secondary ranges would also suggest that the PICs in these two groups have a reduced threshold compared to the young adult and older adult groups (Fig. 2.4). In support of this, one of the major effects of serotonin is to reduce the threshold of the PIC (Li *et al.*, 2007) and this might contribute to more of the lower threshold units in the SSRI group starting directly on their tertiary ranges (Fig. 2.5). As discussed below, a steep secondary range produced by a subthreshold PIC may provide a more secure recruitment of motor units but may also make gradually increasing the torque at the onset of a contraction more difficult if several motor units are abruptly recruited together (Del Vecchio *et al.*, 2020b).

ΔF and Self-Sustained Discharge

Interestingly, participants with steep secondary range slopes also had longer self-sustained firing as estimated by the ΔF (Fig. 2.8), consistent with the presence of larger motoneuron PICs in the young development and SSRI groups compared to the adults and age-matched controls. The self-sustained firing duration (SSD), which uses the torque profile as an estimate of the synaptic input to the motoneurons, may also reflect the contribution of the PIC to self-sustained firing but could be less sensitive as larger SSD values were only seen for the SSRI group compared to the age-matched controls. The larger self-sustained firing (ΔF) in the young development group may result, in part, from having smaller motoneurons compared to the adults. In the cat, smaller motoneurons with lower input conductance have larger PIC hysteresis (and likely self-sustained firing) compared to larger motoneurons with higher input conductance (Heckman & Lee, 1999). In addition, excitatory reflexes such as the stretch reflex, show an age-related decline during childhood that reaches adult levels around 12-14 years, potentially from a maturation of inhibitory spinal circuitry (Willerslev-Olsen *et al.*, 2014; Geertsen *et al.*, 2017). Hormones, such as estradiol and testosterone, facilitate the maturation of inhibitory GABAergic signaling (Gilfarb & Leuner, 2022). As these hormones increase during the young development period (Barrientos *et al.*, 2019; Wood *et al.*, 2019), increases in the excitability of inhibitory circuitry may contribute to the age-related decrease in the estimated PIC we observed in this study given that inhibitory inputs reduce the PIC (Bennett *et al.*, 1998b; Hyngstrom *et al.*, 2007; Heckman *et al.*, 2008a). We did not measure if participants in the young development group were before, within or after puberty, to determine if motoneuron PICs changed in direct relation to predicted changes in sex hormones. There may also be a developmental decrease in the activation of the thermosensitive, transient receptor potential melastatin 5 (Trpm5) channel

which is the main sodium ion carrier for I_{CaN} that also contributes to the self-sustained firing of spinal motoneurons (Bos *et al.*, 2021). Finally, the larger self-sustained firing (ΔF) in the SSRI group may result from the direct facilitation of the Na_V and Ca_V channels that mediate the PIC via activation of serotonin (5-HT2$_{B/C}$) receptors on the motoneuron (Murray *et al.*, 2010; Murray *et al.*, 2011; D'Amico *et al.*, 2013; Wei *et al.*, 2014; Goodlich *et al.*, 2023) or microglia (El Oussini *et al.*, 2016).

Slope and duration of the tertiary firing range

Despite the potential differences in PIC amplitude, the slope of the tertiary range was not different between the various groups, although when taking the recruitment threshold of the motor units into account, the slope of the tertiary range was higher in the young development group compared to the young adults. This would suggest that the transduction of synaptic inputs into motoneuron firing following full PIC activation occurs at a higher gain in the young development group and agrees with the overall higher firing rates observed in this group (see *Chapter 3*), although differences in synaptic inputs between groups cannot be ruled out. The average slope of the tertiary firing range was around 0.6 Hz/s, which was around 10 times shallower than the average slope of the secondary firing range at around 6.0 Hz/s. These slope values are higher compared to the slopes measured by drawing a straight line from the discharge rate at motor unit recruitment to the peak firing rate at the end of the ascending phase of the contraction and measuring the location of the longest orthogonal line to determine the transition point between the secondary and tertiary ranges [secondary range slope: 2.44 Hz/s, tertiary range slope: 0.4 Hz/s in (Beauchamp *et al.*, 2023)]. The lower secondary range slope from this geometric method likely stems from including more of the tertiary range into the secondary range and the lower tertiary range slope likely stems from not including the tertiary sag range compared to when these slopes are directly fitted with

three joined straight lines from our linear piecewise method. Further experiments with more defined and controlled synaptic inputs, such as muscle stretch (Gorassini *et al.*, 1999; Powers *et al.*, 2008), are needed to examine the true input/output gain of the tertiary range and if it varies across development (Smith & Brownstone, 2020), after brain or spinal cord injury (Harvey *et al.*, 2006c) or from motoneuron disease such as amyotrophic lateral sclerosis (ALS) (Jensen *et al.*, 2020).

Confounds from different motor unit numbers and thresholds between groups

The young development group had lower numbers of decomposed motor units compared to the young and older adults given that the blind source separation technique works best on muscles with a larger cross-sectional area and less subcutaneous tissue (Del Vecchio *et al.*, 2020a; Oliveira *et al.*, 2022; Taylor *et al.*, 2022). The smaller number of decomposed motor units in the young development group may have biased sampling of test motor units with higher ΔF values. However, when participants in the young and older adult groups with a similar number of decomposed motor units were selected, the mean ΔF was still lower compared to the young development group. The young development and SSRI groups also had a smaller proportion of low threshold motor units that could potentially have lower ΔFs. For example, measuring ΔF in the lowest threshold test units could have a floor effect where the firing rate of the composite control motor units when the test motor units are de-recruited cannot reach rates that are lower than the rate when the test motor units are recruited early in the contraction. However, there were no main effects of motor unit recruitment threshold on the differences in ΔF in any of the group comparisons.

Functional consequences of lower threshold and larger PICs in young development group

A lower-threshold and potentially larger motoneuron PIC in the young development

group may help descending synaptic inputs recruit and prolong motoneuron firing during voluntary contractions. However, these facilitated PICs may produce a more abrupt and synchronous recruitment of motor units, contributing to the greater torque unsteadiness (i.e., higher CoV) observed during the ascending phase of the contraction in the young development group (Fig. 2.9). Likewise, greater self-sustained firing of motoneurons may contribute to the greater torque unsteadiness during the descending phase of the contraction, making the descending control of motoneuron de-recruitment more challenging. Although PICs are instrumental in amplifying synaptic inputs and facilitating repetitive discharge, the membrane potential of motoneurons can vary more while on a plateau potential (Bennett *et al.*, 1998b). Thus, the potentially lower threshold and larger PIC in the younger participants may make synaptic activation of motoneurons less controlled to increase the difficulty of matching the triangular torque profile. This may be especially problematic in participants less than 12-14 years of age when the corticospinal tract is still undergoing substantial anatomical and functional development (Nezu *et al.*, 1997; Petersen *et al.*, 2010; Yeo *et al.*, 2014). In contrast, participants taking SSRIs also had steeper and shorter secondary ranges and more self-sustained motoneuron firing but without a larger torque unsteadiness. Because this group was older (17.02 ± 5.02 years) compared to the young development group (12.18 ± 2.69 years), the SSRI group may have a corticospinal tract and inhibitory spinal circuitry that are more developed to help control the lower threshold and larger amplitude motoneuron PICs.

Relation to previous animal and human work and clinical implications

As mentioned in the Introduction, in rodents the amplitude of the PIC increases in the first 3 weeks after birth as the animal gains weight bearing locomotion, although PICs are not large enough to produce hysteretic or self-sustained firing present in adult animals (Quinlan *et al.*, 2011; Leroy *et al.*, 2015; Revill *et al.*, 2019; Sharples & Miles, 2021). We observed

evidence consistent with PIC activation and self-sustained firing in motoneurons of children as young as 7 years of age where the ΔF is larger between 7 to 17 years of age and then declines into adulthood where the influence of the PIC on self-sustained firing appears to remain stable until it starts to decline around 65-70 years of age (Hassan *et al.*, 2021; Orssatto *et al.*, 2021). Thus, it would be interesting to determine in newborns if motoneuron PICs, like in rodents, also start out small and non-hysteretic and become larger and more persistent to provide synaptic amplification and self-sustained firing as bipedal locomotion is achieved. None-the-less, data from this study can be used to compare to childhood neurological disorders such as cerebral palsy, Down's Syndrome and spinal muscular atrophy to determine if alterations in the threshold and persistence of PICs may contribute to the motor abnormalities, such as hyper and hypotonia, present in these conditions.

References for Chapter 2

Afsharipour B, Manzur N, Duchcherer J, Fenrich KF, Thompson CK, Negro F, Quinlan KA, Bennett DJ & Gorassini MA. (2020). Estimation of self-sustained activity produced by persistent inward currents using firing rate profiles of multiple motor units in humans. *J Neurophysiol* **124,** 63-85.

Barrientos RM, Brunton PJ, Lenz KM, Pyter L & Spencer SJ. (2019). Neuroimmunology of the female brain across the lifespan: Plasticity to psychopathology. *Brain Behav Immun* **79,** 39-55.

Beauchamp JA, Pearcey GEP, Khurram OU, Chardon M, Wang YC, Powers RK, Dewald JPA & Heckman CJ. (2023). A geometric approach to quantifying the neuromodulatory effects of persistent inward currents on individual motor unit discharge patterns. *J Neural Eng* **20**.

Bennett DJ, Hultborn H, Fedirchuk B & Gorassini M. (1998a). Short-term plasticity in hindlimb motoneurons of decerebrate cats. *J Neurophysiol* **80,** 2038-2045.

Bennett DJ, Hultborn H, Fedirchuk B & Gorassini M. (1998b). Synaptic activation of plateaus in hindlimb motoneurons of decerebrate cats. *J Neurophysiol* **80,** 2023-2037.

Bennett DJ, Li Y, Harvey PJ & Gorassini M. (2001a). Evidence for plateau potentials in tail motoneurons of awake chronic spinal rats with spasticity. *J Neurophysiol* **86,** 1972-1982.

Bennett DJ, Li Y & Siu M. (2001b). Plateau potentials in sacrocaudal motoneurons of chronic spinal rats, recorded in vitro. *J Neurophysiol* **86,** 1955-1971.

Binder MD, Powers RK & Heckman CJ. (2020). Nonlinear Input-Output Functions of Motoneurons. *Physiology (Bethesda)* **35,** 31-39.

Bos R, Drouillas B, Bouhadfane M, Pecchi E, Trouplin V, Korogod SM & Brocard F. (2021). Trpm5 channels encode bistability of spinal motoneurons and ensure motor control of hindlimbs in mice. *Nat Commun* **12,** 6815.

Bos R, Harris-Warrick RM, Brocard C, Demianenko LE, Manuel M, Zytnicki D, Korogod SM & Brocard F. (2018). Kv1.2 Channels Promote Nonlinear Spiking Motoneurons for Powering Up Locomotion. *Cell Rep* **22,** 3315-3327.

Bregman BS. (1987). Development of serotonin immunoreactivity in the rat spinal cord and its plasticity after neonatal spinal cord lesions. *Brain Res* **431,** 245-263.

Carlin KP, Jones KE, Jiang Z, Jordan LM & Brownstone RM. (2000). Dendritic L-type calcium currents in mouse spinal motoneurons: implications for bistability. *Eur J Neurosci* **12,** 1635-1646.

Carrascal L, Nieto-Gonzalez JL, Cameron WE, Torres B & Nunez-Abades PA. (2005). Changes during the postnatal development in physiological and anatomical characteristics of rat motoneurons studied in vitro. *Brain Res Brain Res Rev* **49,** 377-387.

D'Amico JM, Condliffe EG, Martins KJ, Bennett DJ & Gorassini MA. (2014). Recovery of neuronal and network excitability after spinal cord injury and implications for spasticity. *Front Integr Neurosci* **8,** 36.

D'Amico JM, Murray KC, Li Y, Chan KM, Finlay MG, Bennett DJ & Gorassini MA. (2013). Constitutively active 5-HT2/α1 receptors facilitate muscle spasms after human spinal cord injury. *J Neurophysiol* **109,** 1473-1484.

Del Vecchio A, Holobar A, Falla D, Felici F, Enoka RM & Farina D. (2020a). Tutorial: Analysis of motor unit discharge characteristics from high-density surface EMG signals. *J Electromyogr Kinesiol* **53,** 102426.

Del Vecchio A, Sylos-Labini F, Mondì V, Paolillo P, Ivanenko Y, Lacquaniti F & Farina D. (2020b). Spinal motoneurons of the human newborn are highly synchronized during leg movements. *Sci Adv* **6**.

Dwyer JB & Bloch MH. (2019). Antidepressants for Pediatric Patients. *Curr Psychiatr* **18,** 26-42F.

El Oussini H, Bayer H, Scekic-Zahirovic J, Vercruysse P, Sinniger J, Dirrig-Grosch S, Dieterle S, Echaniz-Laguna A, Larmet Y, Muller K, Weishaupt JH, Thal DR, van Rheenen W, van Eijk K, Lawson R, Monassier L, Maroteaux L, Roumier A, Wong PC, van den Berg LH, Ludolph AC, Veldink JH, Witting A & Dupuis L. (2016). Serotonin 2B receptor slows disease progression and prevents degeneration of spinal cord mononuclear phagocytes in amyotrophic lateral sclerosis. *Acta Neuropathol* **131,** 465-480.

Geertsen SS, Willerslev-Olsen M, Lorentzen J & Nielsen JB. (2017). Development and aging of human spinal cord circuitries. *J Neurophysiol* **118,** 1133-1140.

Gilfarb RA & Leuner B. (2022). GABA System Modifications During Periods of Hormonal Flux Across the Female Lifespan. *Front Behav Neurosci* **16,** 802530.

Goodlich BI, Del Vecchio A, Horan SA & Kavanagh JJ. (2023). Blockade of 5-HT(2) receptors suppress motor unit firing and estimates of persistent inward currents during voluntary muscle contraction in humans. *J Physiol*.

Gorassini M, Bennett DJ, Kiehn O, Eken T & Hultborn H. (1999). Activation patterns of hindlimb motor units in the awake rat and their relation to motoneuron intrinsic properties. *J Neurophysiol* **82,** 709-717.

Gorassini M, Yang JF, Siu M & Bennett DJ. (2002a). Intrinsic activation of human motoneurons: possible contribution to motor unit excitation. *J Neurophysiol* **87,** 1850-1858.

Gorassini M, Yang JF, Siu M & Bennett DJ. (2002b). Intrinsic activation of human motoneurons: reduction of motor unit recruitment thresholds by repeated contractions. *J Neurophysiol* **87,** 1859-1866.

Gorassini MA, Knash ME, Harvey PJ, Bennett DJ & Yang JF. (2004). Role of motoneurons in the generation of muscle spasms after spinal cord injury. *Brain* **127,** 2247-2258.

Harvey PJ, Li X, Li Y & Bennett DJ. (2006a). 5-HT2 receptor activation facilitates a persistent sodium current and repetitive firing in spinal motoneurons of rats with and without chronic spinal cord injury. *J Neurophysiol* **96,** 1158-1170.

Harvey PJ, Li Y, Li X & Bennett DJ. (2006b). Persistent sodium currents and repetitive firing in motoneurons of the sacrocaudal spinal cord of adult rats. *J Neurophysiol* **96,** 1141-1157.

Hassan AS, Fajardo ME, Cummings M, McPherson LM, Negro F, Dewald JPA, Heckman CJ & Pearcey GEP. (2021). Estimates of persistent inward currents are reduced in upper limb motor units of older adults. *J Physiol* **599,** 4865-4882.

Heckman CJ, Hyngstrom AS & Johnson MD. (2008). Active properties of motoneurone dendrites: diffuse descending neuromodulation, focused local inhibition. *J Physiol* **586,** 1225-1231.

Heckman CJ & Lee RH. (1999). The role of voltage-sensitive dendritic conductances in generating bistable firing patterns in motoneurons. *J Physiol Paris* **93,** 97-100.

Hounsgaard J, Hultborn H, Jespersen B & Kiehn O. (1988). Bistability of alpha-motoneurones in the decerebrate cat and in the acute spinal cat after intravenous 5-hydroxytryptophan. *J Physiol* **405,** 345-367.

Hyngstrom AS, Johnson MD, Miller JF & Heckman CJ. (2007). Intrinsic electrical properties of spinal motoneurons vary with joint angle. *Nat Neurosci* **10,** 363-369.

Jean-Xavier C, Sharples SA, Mayr KA, Lognon AP & Whelan PJ. (2018). Retracing your footsteps: developmental insights to spinal network plasticity following injury. *J Neurophysiol* **119,** 521-536.

Jensen DB, Kadlecova M, Allodi I & Meehan CF. (2020). Spinal motoneurones are intrinsically more responsive in the adult G93A SOD1 mouse model of amyotrophic lateral sclerosis. *J Physiol* **598,** 4385-4403.

Kernell D. (1965). High-frequency repetitive firing of cat lumbosacral motoneurones stimulated by long-lasting injected currents. *Acta Physiol Scand* **65,** 74-86.

Kiehn O & Eken T. (1997). Prolonged firing in motor units: evidence of plateau potentials in human motoneurons? *J Neurophysiol* **78,** 3061-3068.

Lee RH & Heckman CJ. (1998). Bistability in spinal motoneurons in vivo: systematic variations in persistent inward currents. *J Neurophysiol* **80,** 583-593.

Lee RH & Heckman CJ. (2000). Adjustable amplification of synaptic input in the dendrites of spinal motoneurons in vivo. *J Neurosci* **20,** 6734-6740.

Lee RH, Kuo JJ, Jiang MC & Heckman CJ. (2003). Influence of active dendritic currents on input-output processing in spinal motoneurons in vivo. *J Neurophysiol* **89,** 27-39.

Leroy F, Lamotte d'Incamps B & Zytnicki D. (2015). Potassium currents dynamically set the recruitment and firing properties of F-type motoneurons in neonatal mice. *J Neurophysiol* **114,** 1963-1973.

Li X, Murray K, Harvey PJ, Ballou EW & Bennett DJ. (2007). Serotonin facilitates a persistent calcium current in motoneurons of rats with and without chronic spinal cord injury. *J Neurophysiol* **97,** 1236-1246.

Li Y, Gorassini MA & Bennett DJ. (2004). Role of persistent sodium and calcium currents in motoneuron firing and spasticity in chronic spinal rats. *J Neurophysiol* **91,** 767-783.

McNeil CJ, Doherty TJ, Stashuk DW & Rice CL. (2005). Motor unit number estimates in the tibialis anterior muscle of young, old, and very old men. *Muscle Nerve* **31,** 461-467.

Mizuno N & Itoh H. (2009). Functions and regulatory mechanisms of Gq-signaling pathways. *Neurosignals* **17,** 42-54.

Murray KC, Nakae A, Stephens MJ, Rank M, D'Amico J, Harvey PJ, Li X, Harris RL, Ballou EW, Anelli R, Heckman CJ, Mashimo T, Vavrek R, Sanelli L, Gorassini MA, Bennett DJ & Fouad K. (2010). Recovery of motoneuron and locomotor function after spinal cord injury depends on constitutive activity in 5-HT2C receptors. *Nat Med* **16,** 694-700.

Murray KC, Stephens MJ, Ballou EW, Heckman CJ & Bennett DJ. (2011). Motoneuron excitability and muscle spasms are regulated by 5-HT2B and 5-HT2C receptor activity. *J Neurophysiol* **105,** 731-748.

Negro F, Muceli S, Castronovo AM, Holobar A & Farina D. (2016). Multi-channel intramuscular and surface EMG decomposition by convolutive blind source separation. *J Neural Eng* **13,** 026027.

Nezu A, Kimura S, Uehara S, Kobayashi T, Tanaka M & Saito K. (1997). Magnetic stimulation of motor cortex in children: maturity of corticospinal pathway and problem of clinical application. *Brain Dev* **19,** 176-180.

Oliveira DS, Casolo A, Balshaw TG, Maeo S, Lanza MB, Martin NRW, Maffulli N, Kinfe TM, Eskofier BM, Folland JP, Farina D & Del Vecchio A. (2022). Neural decoding from surface high-density EMG signals: influence of anatomy and synchronization on the number of identified motor units. *J Neural Eng* **19**.

Orssatto LBR, Borg DN, Blazevich AJ, Sakugawa RL, Shield AJ & Trajano GS. (2021). Intrinsic motoneuron excitability is reduced in soleus and tibialis anterior of older adults. *Geroscience* **43,** 2719-2735.

Perrier JF, Rasmussen HB, Christensen RK & Petersen AV. (2013). Modulation of the intrinsic properties of motoneurons by serotonin. *Curr Pharm Des* **19,** 4371-4384.

Petersen TH, Kliim-Due M, Farmer SF & Nielsen JB. (2010). Childhood development of common drive to a human leg muscle during ankle dorsiflexion and gait. *J Physiol* **588,** 4387-4400.

Powers RK, Nardelli P & Cope TC. (2008). Estimation of the contribution of intrinsic currents to motoneuron firing based on paired motoneuron discharge records in the decerebrate cat. *J Neurophysiol* **100,** 292-303.

Quinlan KA, Schuster JE, Fu R, Siddique T & Heckman CJ. (2011). Altered postnatal maturation of electrical properties in spinal motoneurons in a mouse model of amyotrophic lateral sclerosis. *J Physiol* **589,** 2245-2260.

Revill AL, Chu NY, Ma L, LeBlancq MJ, Dickson CT & Funk GD. (2019). Postnatal development of persistent inward currents in rat XII motoneurons and their modulation by serotonin, muscarine and noradrenaline. *J Physiol* **597,** 3183-3201.

Sharples SA & Miles GB. (2021). Maturation of persistent and hyperpolarization-activated inward currents shapes the differential activation of motoneuron subtypes during postnatal development. *Elife* **10**.

Skinner JW, Christou EA & Hass CJ. (2019). Lower Extremity Muscle Strength and Force Variability in Persons With Parkinson Disease. *J Neurol Phys Ther* **43,** 56-62.

Smith CC & Brownstone RM. (2020). Spinal motoneuron firing properties mature from rostral to caudal during postnatal development of the mouse. *J Physiol* **598,** 5467-5485.

Svirskis G & Hounsgaard J. (1997). Depolarization-induced facilitation of a plateau-generating current in ventral horn neurons in the turtle spinal cord. *J Neurophysiol* **78,** 1740-1742.

Taylor CA, Kopicko BH, Negro F & Thompson CK. (2022). Sex differences in the detection of motor unit action potentials identified using high-density surface electromyography. *J Electromyogr Kinesiol* **65,** 102675.

Thompson CK & Hornby TG. (2013). Divergent modulation of clinical measures of volitional and reflexive motor behaviors following serotonergic medications in human incomplete spinal cord injury. *J Neurotrauma* **30,** 498-502.

Wei K, Glaser JI, Deng L, Thompson CK, Stevenson IH, Wang Q, Hornby TG, Heckman CJ & Kording KP. (2014). Serotonin affects movement gain control in the spinal cord. *J Neurosci* **34,** 12690-12700.

Willerslev-Olsen M, Andersen JB, Sinkjaer T & Nielsen JB. (2014). Sensory feedback to ankle plantar flexors is not exaggerated during gait in spastic hemiplegic children with cerebral palsy. *J Neurophysiol* **111,** 746-754.

Wood CL, Lane LC & Cheetham T. (2019). Puberty: Normal physiology (brief overview). *Best Pract Res Clin Endocrinol Metab* **33,** 101265.

Xia Y, Chen D, Xia H, Liao Z, Tang W & Yan Y. (2017). Serotonergic projections to lumbar levels and its plasticity following spinal cord injury. *Neurosci Lett* **649,** 70-77.

Yeo SS, Jang SH & Son SM. (2014). The different maturation of the corticospinal tract and corticoreticular pathway in normal brain development: diffusion tensor imaging study. *Front Hum Neurosci* **8,** 573.

Chapter 3

Introduction

It is well known that muscular force, contractile velocity and muscle power are smaller in children compared to adults; however, muscle size and fibre composition alone cannot account for all of these differences [reviewed in (Dotan *et al.*, 2012)]. In muscles such as the plantarflexors and knee extensors, comparisons between volitional and electrically-evoked force production suggest that children are unable to voluntarily recruit all of their motor units during a maximum effort (Blimkie, 1989; Paasuke *et al.*, 2000; Grosset *et al.*, 2008; O'Brien *et al.*, 2010); additionally, children show reduced fatiguability during matched contractions compared to adults (Paraschos *et al.*, 2007; Armatas *et al.*, 2010). Considering these observations, it has been hypothesized that for some muscle groups, children do not fully recruit all of their fast, fatigue-resistant motor units (Dotan *et al.*, 2012), contributing to the slower and weaker muscle activation compared to adults. Thus, if children must rely more on their weaker type I motor units to produce equivalent amounts of force as adults, one would expect that the firing rates in these activated units would be higher compared to adults to compensate for a reduced recruitment of fast motor units that produce larger amounts of force. In addition, children exhibit greater amounts of agonist-antagonist co-contraction in thigh and lower leg muscles, especially during sub-maximal contractions (Frost *et al.*, 1997; Grosset *et al.*, 2008), requiring more voluntary synaptic drive and faster firing rates in the agonist motor units to produce enough force to overcome the opposing antagonist contraction.

With the advent of non-invasive, multi-electrode surface EMG, higher discharge rates of single motor units have been reported in children compared to adults at forces matched to the percentage of their maximum voluntary contraction (MVC). In the first dorsal interosseus

64

(FDI) muscle, children (~ 9 years old) had higher motor unit firing rates compared to adults (~ 23 years old) at 30% MVC (Miller *et al.*, 2019). In knee extensor motor units, firing rates were consistently (but not significantly) higher in boys aged 9-11 years compared to men aged 18-30 years during a 20 to 80% MVC in one study (Chalchat *et al.*, 2019), although firing rates were higher in adults (~ 21 years old) compared to children (~ 9 years old) in another study (Parra *et al.*, 2020), leaving open the question of whether firing rates change during development in lower limb muscles. Because the TA muscle in young adults (~25 to 30 years) is ~75% type I and 25% type II, (Henriksson-Larsen *et al.*, 1983; Jakobsson *et al.*, 1991), and assuming a similar proportion in children, firing rates of TA motor units in children may be higher compared to adults at matched forces if there is a reduced activation of fast type II motor units. Thus, we examined if the start, maximum and end firing rates of lower limb TA motor units in a young development group (aged 7 to 17 years) were higher compared to a young adult (18 to 28 years) and older adult (32 to 53 years) group. As in *Chapter 2*, we also placed participants taking SSRIs into a separate group given the potential effects serotonin has on motoneuron excitability and firing rates (Harvey *et al.,* 2006a,b).

Another feature of the multiple motor unit recordings described above was the decrease in mean and maximum firing rates as the recruitment threshold of the motor units increased, in both the children and adult participants (Chalchat *et al.*, 2019; Miller *et al.*, 2019; Parra *et al.*, 2020), consistent with other studies in adults with recordings from the FDI, deltoid, vastus lateralis and tibialis anterior (TA) muscles (De Luca *et al.*, 1982; De Luca & Hostage, 2010; Hu *et al.*, 2014). This phenomenon, known as the "onion skin" effect [coined by (De Luca & Erim, 1994)], may be produced by a parallel increase in the firing rate saturation and recruitment threshold of the motoneuron, where firing rates of successively recruited motor units decrease during an increasing synaptic input (Revill & Fuglevand, 2011; Fuglevand *et al.*, 2015). However, an opposite finding has been shown in other adult

studies where the maximum firing rates of FDI (Moritz *et al.*, 2005; Barry *et al.*, 2007), soleus (Oya *et al.*, 2009), TA (Erim *et al.*, 1996; Jesunathadas *et al.*, 2012) and biceps brachii motor units (Gydikov & Kosarov, 1974) *increase* with recruitment threshold of the motor units, consistent with animal studies where small, low-threshold motoneurons have longer AHPs and lower firing rates compared to larger, higher-threshold motoneuorns with shorter AHPs and faster firing rates (Eccles *et al.*, 1958; Burke, 1968; Kernell *et al.*, 1983).

Many of the studies listed above that demonstrated a pronounced onion skin effect used a 5-pin surface array sensor and a Precision Decomposition III algorithm (De Luca *et al.*, 2006) to isolate the firing behaviour of multiple single motor units. In contrast, the studies cited above where maximum firing rates increased with recruitment threshold used visual identification to isolate single motor units from intramuscular needle EMG. Because it is theoretically and experimentally difficult to isolate multiple motor units from a small (< 20) number of surface EMG electrode sites (Farina & Enoka, 2011; Caillet *et al.*, 2023), it has been suggested that the lower firing rates in the higher-threshold units isolated from the 5-pin array and Precision Decomposition algorithm may result from missed spikes, especially at higher levels of contraction where superimposition of multiple motor units occurs more often (Farina & Enoka, 2011; Piotrkiewicz & Türker, 2017). Thus, we reexamined the relationship between maximum firing rates and recruitment threshold of the TA motor units using high density surface EMG (HDsEMG) with 64 electrode sites and blind source decomposition where more stringent validation of motor unit identification has been performed (Holobar *et al.*, 2010; Negro *et al.*, 2016). Because these techniques appear to produce more accurate isolation of motor units at higher forces (Enoka, 2019), we hypothesized that the maximum firing rate of the TA motor units would increase as the recruitment threshold of the motor unit increased, similar to the findings produced from the visual identification of single motor units from intramuscular EMG.

Finally, we examined a third motor unit firing behaviour where the discharge rate decreases during a steady or increasing input. We observed this slowing of firing rate in *Chapter 2,* where during the lower-gain tertiary range, the firing rate of the TA motor units would sometimes decrease just before peak torque even though the dorsiflexion torque, and presumably voluntary synaptic drive, continued to increase. Hence, we termed this the "tertiary sag" range. Because motoneuron firing rates can decrease towards the end of a 10-second increasing current injection into the motoneuron soma (Bennett *et al.*, 2001b; Binder *et al.*, 2020), the decrease in motor unit firing rates during the tertiary sag range may be produced by intrinsic properties of the motoneuron, such as spike frequency adaptation (Sawczuk *et al.*, 1995; Powers & Binder, 1999; Brownstone, 2006; Button *et al.*, 2007). Alternatively, the tertiary sag range may be produced by a selective decrease in voluntary synaptic drive to the TA motoneuron pool while the drive to other motoneuron pools supplying muscles around the ankle and foot that contribute to the dorsiflexion torque continued to increase.

To examine the presence and amplitude of the tertiary sag range, we measured the slope and duration of the third straight line fit to the ascending firing rate profile described in *Chapter 2* but only when the slope of this line was < 0 Hz/s. We hypothesized that a tertiary sag range would be present in children given the early emergence of spike frequency adaptation in developing human motoneurons (Takazawa *et al.*, 2012). We also present the first steps in trying to determine if the tertiary sag range is indeed produced by mechanisms intrinsic to the motoneuron or if it was produced by a decrease in synaptic drive to the TA motoneuron pool. This was examined by measuring if the start of the tertiary sag range occurred at different times across multiple motor units simultaneously measured during the ascending phase of a contraction, which would support an intrinsic mechanism. In contrast, a synchronous start of the tertiary sag range across multiple, simultaneously activated motor

units would likely occur from a decrease in common synaptic drive across the TA

motoneuron pool.

Methods

Ethics and participants

Experiments were approved by the Health Research Ethics Board of the University of Alberta (Protocol 00076790) and conformed to the Declaration of Helsinki. All 50 participants provided written informed consent prior to the experiment, and we grouped the participants as in *Chapter 2*. The young development group had an average age of 12.18 ± 2.69 years (mean $\pm$ standard deviation) with 12 males and 8 females (n = 20), the young adult group had an average age of 22.61 ± 3.60 years with 6 males and 7 females (n = 13) and the older adult group had an average age of 42.38 ± 7.92 years with 3 males and 5 females (n = 8). A separate group of participants between the ages of 11 and 28 years (17.02 ± 5.02 years), with 4 females and 5 males (n = 9), were on selective serotonin reuptake inhibitors (SSRI). This SSRI group was compared to their peers also aged between 11 to 28 years who were not taking SSRIs (18.17 ± 5.32 years, p = 0.584 Mann-Whitney Rank Sum test) and comprised of 12 females and 14 males (n = 26). All participants were excluded for any history of central or peripheral nerve injury or disease. Puberty, menstrual or menopausal status were not recorded. In six of the adult participants, parts of the data were taken from a previous study (Afsharipour *et al.*, 2020).

EMG Recordings

To identify single motor units, flexible high-density surface EMG (HDsEMG) electrodes with 64 recording sites (GR08MM1305; OT Bioelecttronica Inc., Turin, Italy) were placed over the tibialis anterior (TA) muscle. The recordings sites, arranged in a 5 (wide) by 13 (long) grid with an 8 mm spacing, were placed lengthwise about 1 cm lateral to the tibia and 4-5 cm below the lower edge of the patella over the belly of the TA muscle.

Recordings were made in a monopolar configuration with the reference and ground electrode straps (WS2; OT Bioelecttronica Inc.) wrapped around the lower leg just above the ankle and with the ground strap most distal. To reduce impedance, the skin over the TA was first rubbed with an abrasive paste (Nuprep, Weaver and Company, CO) and any excess was removed with a saline or alcohol-soaked gauze. HDsEMG signals were amplified (150 times) and filtered with a 10 Hz high pass and 900 Hz low pass filter using a Quattrocento amplifier (OT Bioelecttronica, 16 bit, Inc., Turin. Italy). A pair of Ag-AgCl surface EMG electrodes (Kendall; Chicopee, MA, USA, 3.2 cm by 2.2 cm) were placed in a bipolar configuration over the soleus muscle to measure antagonist muscle activity during the isometric contractions. All signals were digitized with the Quatrocentro A/D and sampled at a frequency that was set to 2048 Hz.

Experimental protocol

Participants sat in a chair with their knee extended to ~120° and their dominant foot tightly sandwiched between two plates of an adjustable 3D printed foot holder, with the heel on the floor and ankle at ~ 90°. Dorsiflexion torque was measured by an S-shaped strain gauge (150-lb SSM, Interface Force Measurement Solutions, AZ) attached to the bottom of the foot holder directly underneath the metatarsophalangeal joint. The maximum dorsiflexion torque was measured from the largest of two maximum voluntary contractions (MVCs) separated by at least 30 seconds. Participants were then tasked to perform an isometric triangular dorsiflexion at either 10, 20 or 30% of their MVC torque, and match their torque output to a target triangle presented over a computer screen with the exerted torque being displayed from left to right. Each triangular contraction consisted of a 10-second ascending phase and a 10-second descending phase, with 20 seconds between each contraction to avoid frequency-dependent facilitation of motor units (Gorassini *et al.*, 2002b). At least 8 to 10

contraction trials were performed at each level of MVC torque in sets of 4 to 5 contractions, and the 4 best trials were selected for analysis. Participants typically started with a 20 or 30% MVC contraction because these were easier to perform. Only the 30% MVC data were used for this protocol for clarity of presentation and the 10% and 20% MVC data will be presented in a separate paper.

Data Analysis

Decomposition of single motor units: The HDsEMG signals were first converted into a MATLAB file format (MATLAB version R2021b/R2022a) with custom-built functions, and then digitally filtered (4th-order, zero lag Butterworth filter with a bandpass of 10 - 500 Hz and an additional 60-Hz notch). HDsEMG signals with poor signal-to-noise were removed (typically 2-3 of the 64 recorded signals). Blind source separation (Negro *et al.*, 2016) was used to decompose the HDsEMG signals into the contributing single motor units. Only motor unit action potentials with a mean Silhouette (SIL) value of 0.85 or higher were used (Negro *et al.*, 2016). The trains of motor unit action potentials (or pulses) were manually edited to remove or add extra pulses to correct too high or too low firing rates, respectively, with no more than 10% of the motor unit pulses modified in a single firing rate profile. A fifth-order polynomial curve was fit to the firing rate profile of each motor unit for subsequent analysis as described below. Recruitment threshold of the motor units was determined as in *Chapter 2*.

Start, Maximum and End rates: The start, maximum or end firing rate for all units in each contraction were measured from the fit polynomial line using a custom Matlab program. The average value measured from all units in a single contraction was calculated and this value was then averaged across the 4 contractions in each participant and then across participants within a group. The mean start, maximum and end firing rates were also plotted

against the age of the participant in the young development and young adult groups (7 to 28 years) to visualize trends across age.

Onion Skin Effect: As noted in the Introduction, the onion skin effect presents when the maximum firing rate decreases with the recruitment threshold of the motor units (De Luca *et al.*, 1982; De Luca & Hostage, 2010). To determine if this effect occured in the TA motor units for our recording and decomposition protocol, in each participant the maximum firing rate of each motor unit was plotted against its recruitment threshold, grouping data from all four contractions together. A straight line was then fit to the data in steps of ~ 0.5% MVC. The straight line from all participants were plotted together within each group and the average value of the straight line for a given range of recruitment thresholds (binned every 2% MVC) was then averaged across participants within each group.

Piecewise linear fit to the ascending firing rate profile (trilinear analysis): The ascending firing rate profile was iteratively fit with three straight lines to mark the secondary, tertiary and tertiary sag ranges as described in *Chapter 2*. Results from the secondary and tertiary ranges are presented in *Chapter 2* and the results for the tertiary sag range are presented here. Briefly, using Matlab scripts a non-linear parameter search method (fminserach), was used to optimize the best fit of three connected lines to the ascending firing rate profile. We considered the ascending profile to have a tertiary sag range if the slope of the third line after the tertiary range was ≤ 0 Hz/s. In cases where there was no tertiary sag range, the straight line through the tertiary range was fit to data points extending to the peak torque. The proportion of motor units having a tertiary sag range (as described in *Chapter 2*), and the slope and duration of the fit straight line, were plotted against the age of the participants or the recruitment threshold of the motor units as described below.

Analysis according to recruitment threshold of the motor units: To examine if the firing rate and tertiary sag values (slope and duration) varied according to the recruitment

threshold of the motor unit, values from motor units having a recruitment threshold within a given range (e.g., bins of 0-3%, 3-5%, 5-7% … 25-27% MVC) from the 4 contractions were averaged together in each participant. These binned averages were then averaged across participants within each group.

Statistics

Sigma Plot 11.0 software was used for all statistics. Because mean firing rates did not differ between males and females during the 30% MVC contractions, as will be detailed in another paper, the two sexes were collapsed within each group. A Shapiro-Wilk test was used to assess the normality of the data. Unpaired, between-group comparisons for normally distributed data were assessed with Student's t-test and non-parametric data were assessed with the Mann-Whitney-rank-sum test. The relationship between variables (i.e., start, maximum, and end firing rates) and participant age were evaluated with a Pearson product correlation moment (r). Within each group, a one-way ANOVA was performed on normally distributed data and one-way ANOVA on Ranks on non-normally distributed data to compare the effect of motor unit recruitment threshold on firing rates and tertiary sag range variables (e.g., slope and duration). A two-way ANOVA was performed to analyze the effect of group and recruitment threshold on the firing rates and the tertiary sag range variables. Statistical significance for all analyses was defined as $p \leq 0.05$. Data are presented in the text and tables as the mean value $\pm$ standard deviation (SD).

Results

Start, maximum and end firing rates across age

The mean firing rates of the TA motor units activated during a 30% MVC isometric dorsiflexion were often higher in the young development and SSRI groups compared to the adult and SSRI control participants, respectively (Table 1a). As shown for a young development (10-year-old) and SSRI participant (left and right graphs, Fig. 3.1A), the maximum and end firing rates of the various motor units were often higher compared to young adults (e.g., 24-year-old, middle Fig. 3.1A) and older adults (not shown). Across the young development and young adult groups from 7 to 28 years of age, there was a negative correlation between the maximum or end firing rates and age (middle and right graphs, Fig. 3.1B, r and p values Table 3.1b). Moreover, maximum firing rates in the young development group (7 to 17 years) were higher compared to the young adult group (18 to 28 years) and likewise, the end firing rates in the young development group were higher compared to both the young adult and older adult groups (Table 3.1a,c). In contrast, the start rate was not different between groups (left, Fig. 3.1B, Table 3.1a,c), nor was there a correlation to age (Table 3.1b). However, both the start and maximum rates were higher in participants taking SSRIs compared to the age-matched controls (solid red symbols in Fig. 3.1B, Table 3.1a,c).

Table 3.1(a)	Young Dev	Young Adult	Older Adult	SSRI	SSRI Age-matched control
Start rate (Hz)	10.38 ± 1.95	9.36 ± 1.54	9.84 ± 1.98	11.18 ± 1.57	9.64 ± 1.82
Max rate (Hz)	18.32 ± 2.44	16.51 ± 1.75	16.98 ± 3.34	19.02 ± 1.98	17.23 ± 2.26
End rate (Hz)	7.29 ± 1.64	6.13 ± 1.03	6.04 ± 0.85	7.34 ± 1.18	6.48 ± 1.41
	(b) Combo (7-28 years)	**(c)** Young Dev vs Old Dev	Young Dev vs Adult	Old Dev vs Adult	SSRI vs Age-matched control
Start rate (Hz)	r= -0.261 p= 0.142	p= 0.123 (S) t= 1.585	p= 0.519 (S) t= 0.654	p= 0.539 (S) t= 0.626	**P < 0.001 (MW) T= 270.000**
Max rate (Hz)	**r= -0.363 p= 0.038**	**p= 0.028 (S) t= 2.302**	p= 0.248 (S) t= 1.183	P= 0.638 (MW) T= 95.000	**p= 0.042 (S) t= 2.120**
End rate (Hz)	**r= -0.484 p = 0.004**	**p= 0.029 (S) t= 2.287**	**p= 0.050 (S) t= -2.055**	p= 0.834 (S) t= 0.213	p= 0.111 (S) t= -1.638

Table. 3.1. a) Mean (±SD) of start, maximum and end rates for each group. **b):** Pearson's Product (r) and p-values for correlation of the different firing rates vs. age across the combined young developmental and adult groups (Combo). **c)** Results of unpaired comparisons between the various groups using Student's t-tests (S) or Mann-Whitney Rank Sum test (MW). Significant values where p < 0.05 are marked in bold.
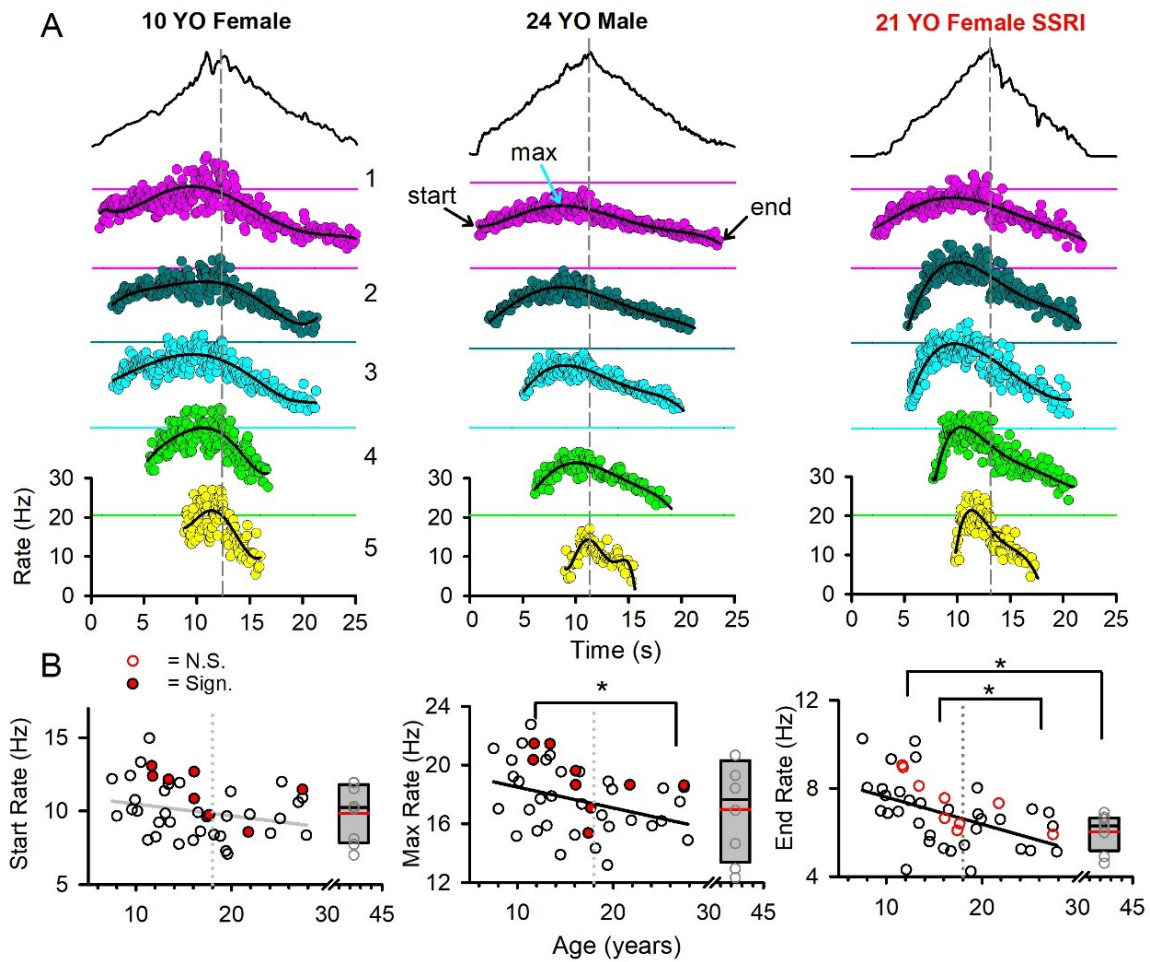
Figure 3.1. **A)** Representative firing rate profiles of motor units used to measure the start, maximum and end firing rates from the fit 5th order polynomial line (black). *Left:* 10-year-old (yo) female; *Middle:* 24-year-old female; *Right*: 24-year-old male taking an SSRI. **B)** Start, maximum and end rates plotted against age for the young development and young adult groups (open circles), the SSRI group (red circles) and older adults (box plot with individual participant data in grey circles, mean red line, median black line). Average age of older adult group is plotted at 42.4 years. Black regression lines indicate there is a significant correlation with age, grey regression lines indicate no correlation (see Table 3.1b for r and p values). Filled red circles = significant difference between the SSRI group and the age-matched controls (11 to 28 years, unpaired Student's t-test with p < 0.05). The dashed vertical line separates the young development and young adult participants. * = significant difference between young development and adult groups with p < 0.05, results of unpaired comparisons are presented in Table 3.1c.

Start, maximum and end firing rates across motor unit recruitment threshold

The start, maximum and end firing rates were further analyzed based on the recruitment threshold of the motor units (Fig. 3.2), similar to the analysis for ΔF in *Chapter 2*. When tested with a one-way ANOVA, there was no main effect of recruitment threshold of the motor units on the start or end firing rates in any in any of the groups (see non-bolded numbers in Table 3.2a). In contrast, a one-way ANOVA on Ranks showed a significant main effect of recruitment threshold on the maximum firing rates in the young adults (* in Fig. 3.2, bolded numbers Table 3.2a). When taking the recruitment threshold of the motor units into account, the higher firing rates in the young development and SSRI groups compared to the adults and age-matched controls, respectively, were more apparent. The two-way ANOVA showed a significant main effect of group on the start, maximum and end rates between the young development and young adult groups and for the maximum and end firing rates between the young development and older adult groups (see solid circles in Fig. 3.2 and bolded values in Table 3.2b). Likewise, the two-way ANOVA showed a significant main effect of group for the start and maximum firing rates between the SSRI and SSRI control groups (solid circles in Fig. 3.2 and bolded numbers in Table 3.2b).
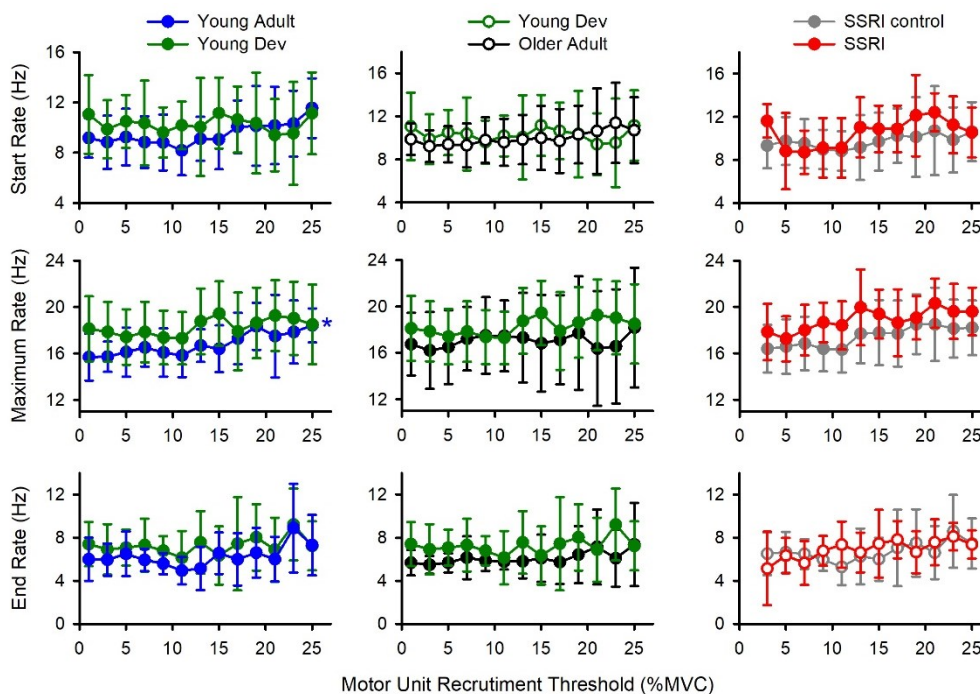
Figure 3.2. The start (top), maximum (middle) and end (bottom) firing rates plotted against the recruitment threshold of the motor units for the young development (green), young adult (blue), older adults (black), SSRI (red) and SSRI-age matched controls (grey). * = significant effect of recruitment threshold on maximum firing rate in the young adult group (bolded numbers in Table 3.2a). Solid symbols indicate significant effect of group on the start, maximum or end rate from a two-way ANOVA (bolded numbers in Table 3.2b). Error bars ± SD.

Table 3.2 a) One-wayANOVA	Young Dev	Young Adult	Older Adult	SSRI
Start	F(12)=0.586 P= 0.852	F(12)=1.424 P= 0.163	H(12)=4.423 P= 0.975	F(11)=1.547 P= 0.126
Maximum	F(12)=1.220 P=0.272	**H(12)=22.850 P=0.029**	H(12)=2.480 P= 0.998	F(11)=1.135 P= 0.346
End	H(12)=12.951 P= 0.373	H(12)=15.674 P= 0.207	H(12)=3.466 P= 0.991	F(11)=0.885 P= 0.566
b) Two-way ANOVA	Young Dev vs Young Adult	Young Dev vs Older Adult	Young Adult vs Older Adult	SSRI vs Age-matched controls
Start Rate Group x RT	F(1,12)=0.718 P= 0.734	F(1,12)=0.593 P= 0.847	F(1,12)=0.326 P= 0.984	F(1,11)=1.415 P= 0.164
Group	**F(1,12) = 7.658 P= 0.006**	F(1,12)=0.309 P= 0.579	F(1,12) = 3.001 P= 0.085	**F(1,11)=7.519 P= 0.006**
RT	F(1,12) = 1.171 P= 0.303	F(1,12)=0.544 P= 0.885	F(1,12) = 1.507 P= 0.124	F(1,11)=1.525 P= 0.121
Maximum Rate Group x RT	F(1,12)=0.562 P= 0.872	F(1,12)=0.368 P= 0.974	F(1,12)=0.381 P= 0.969	F(1,11)=0.265 P= 0.991
Group	**F(1,12)=27.271 P< 0.001**	**F(1,12)=7.535 P= 0.006**	F(1,12) = 0.647 P= 0.422	**F(1,11)=26.418 P< 0.001**
RT	**F(1,12)=1.872 P= 0.037**	F(1,12)=0.333 P= 0.983	F(1,12) = 0.725 P= 0.726	**F(1,11)=2.556 P= 0.004**
End Rate Group x RT	F(1,12)=0.475 P= 0.928	F(1,12)=0.856 P= 0.592	F(1,12)=1.055 P= 0.400	F(1,11)=0.986 P= 0.459
Group	**F(1,12)=16.049 P< 0.001**	**F(1,12)=11.649 P< 0.001**	F(1,12) = 0.135 P= 0.714	F(1,11)=3.479 P= 0.063
RT	**F(1,12)=2.856 P< 0.001**	F(1,12)=0.905 P= 0.543	F(1,12) = 1.210 P= 0.278	F(1,11)=1.214 P= 0.276

Table 3.2. a) Results for one-way ANOVA and one-way ANOVA on Ranks examining effect of recruitment threshold (RT) on the start, maximum and end firing rates for the data plotted in Figure 3.2. **b)** Results of two-way ANOVA comparing group and recruitment threshold (RT) for the data plotted in Figure 3.2.

Maximum firing rate vs recruitment threshold of motor unit

We further investigated the relationship between maximal firing rates and recruitment threshold of the motor units by plotting, in each participant, the maximal firing rate of each motor unit, as measured from the fit polynomial line for all 4 contractions, against the recruitment threshold of the motor unit. A straight line was then fit to the data as shown for an 18-year-old participant in Fig. 3.3A. In most participants, the straight line fit to the data

had a positive slope where the maximal firing rates increased with the recruitment threshold of the motor units as shown for a participant in the SSRI group (thin black line, Fig. 3.3D) whose smoothed firing rate profiles are plotted in Figure 3.3G for a single contraction. In some participants, the slope of the line was negative (e.g., dark blue line, Fig. 3.3E older adult) where some of the higher threshold units recruited near peak torque (dark blue profiles in Fig. 3.3H) had lower firing rates compared to the lower threshold units. When the straight-line fits for each participant were plotted together within each group (grey lines in Figs. 3.3B-F) and a mean line was fit to this data (thick coloured lines), on average there was a positive correlation between the maximum firing rate and the recruitment threshold of the motor units in all groups (see r and p values in Table 3a). Moreover, there were no differences in the median slopes between the various groups (Table 3.3b,c).
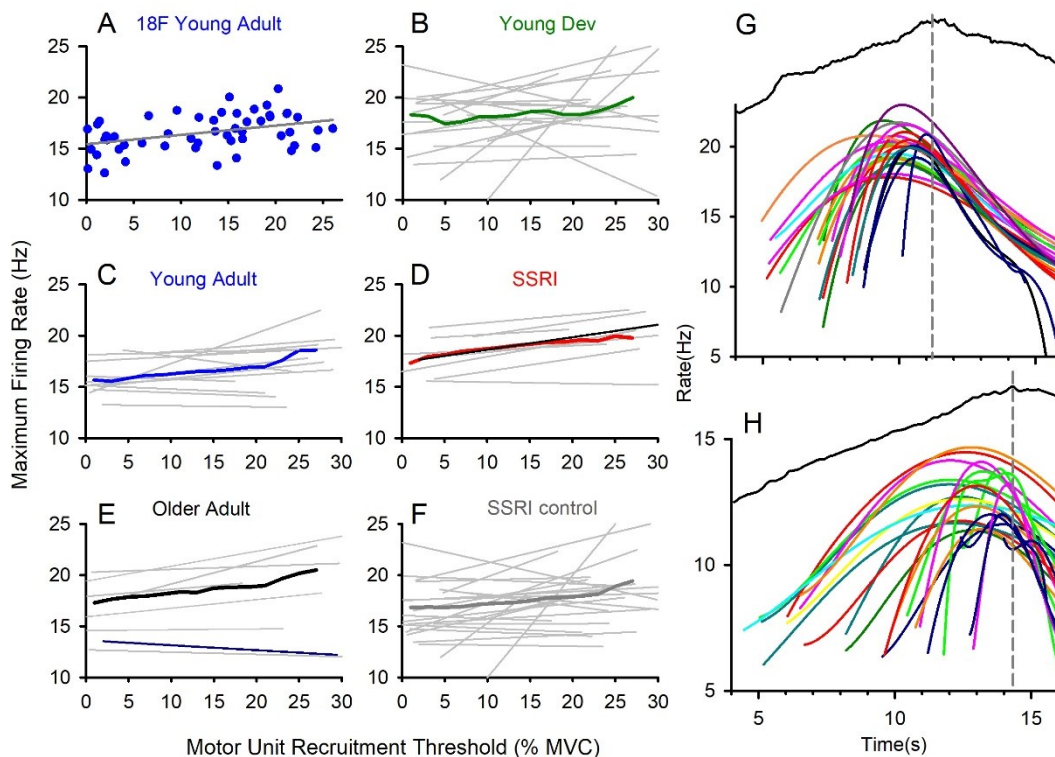
Figure 3.3. A) Straight line (grey) fit through data points representing maximum firing rate plotted against recruitment threshold for all motor units from 4 contractions in an 18-year-old female participant. **B-F)** Straight line fits for each participant (grey) with the average line measured across participants for the **B)** young development (green), **C)** young adult (blue), **D)** SSRI (red), **E)** older adult (black) and **F)** SSRI age-matched controls (dark grey). **G)** Overlay of firing rate profiles for one contraction from a participant in the SSRI group with a positive slope shown in *D* by a black line. **H)** Same as G for an older adult participant with a negative slope shown in *E* by a dark blue line.

Table 3.3	Young Dev	Young Adult	Older Adult	SSRI	SSRI control
a) Correlation max rate vs RT	**r= 0.767, p= 0.001**	**r= 0.926, p < 0.001**	**r= 0.965, p < 0.001**	**r= 0.967, p < 0.001**	**r= 0.934, p < 0.001**
b) Median slope (Hz/%MVC)	0.054 (-0.36 - 0.76)	0.0448 (-0.10 - 0.29)	0.050 (-0.048 - 0.22)	0.082 (-0.013 - 0.15)	0.084 (-0.18 - 0.76)
	Young Dev vs Young Adult	Young Dev vs Older Adult	Young Adult vs Older Adult	SSRI vs Control	
c) unpaired comparisons	P = 0.519 (MW) T= 203.000	P = 0.819 (MW) T= 111.000	p = 0.618 (S) t= -0.507	P = 0.335 (MW) T= 172.000	

Table 3.3. a) Pearson product (r) for the correlation between maximum firing rate and recruitment threshold of units for the averaged straight line fit to the group data in Figure 3.3. Significant values where p < 0.05 are marked in bold. **b)** Median (and range) slope values of individual straight-line fits in each group. **c):** Results of unpaired comparison between the various groups using Mann-Whitney Rank Sum test (MW) or Student's t-test (S).

Tertiary sag range

As shown in *Chapter 2* (Fig. 2.5A), the firing rate profiles during the ascending portion of the triangular 30% MVCs could sometimes be fit with three joined straight lines (replotted here on an expanded time scale in Fig. 3.4A). The first straight line marks the secondary range where we propose the initial activation of the PIC accelerates firing during motor unit recruitment, whereas the second straight line marks the tertiary range where the PIC is fully activated and the motoneuron responds to synaptic inputs at a lower gain (Afsharipour *et al.*, 2020; Binder *et al.*, 2020). Here we examine the slope and duration of the third straight line where during the tertiary range, the firing rate of the motor units decrease even though the torque, and presumably the synaptic drive to the TA motoneuron pool, continue to increase (red lines in Fig. 3.4A). We term this period of decreased firing rate the tertiary sag range. In all groups, around 50% of the motor units with recruitment thresholds between 0 and 15% MVC (Fig. 3.4A, top profiles) had a tertiary sag range. In contrast, the highest threshold units recruited at 25% MVC had ~ 25% of their units with a tertiary sag range (Fig. 3.4B). In the young adult, older adult and SSRI controls, the proportion of motor units with a tertiary sag range was smaller in the highest-threshold units (at 25% MVC)

compared to the lowest-threshold units (at 1% MVC, p < 0.050, Student's t-tests), because the firing rate profiles of the highest-threshold units often became dominated by the secondary range where firing rates continued to increase until peak torque (e.g., Fig. 3.4A, bottom middle unit). Also, the mean proportion of all units with a tertiary sag range was lower in the young development and young adult groups compared to the older adult group but was higher in the SSRI group compared to SSRI controls (Table 3.4a,b).
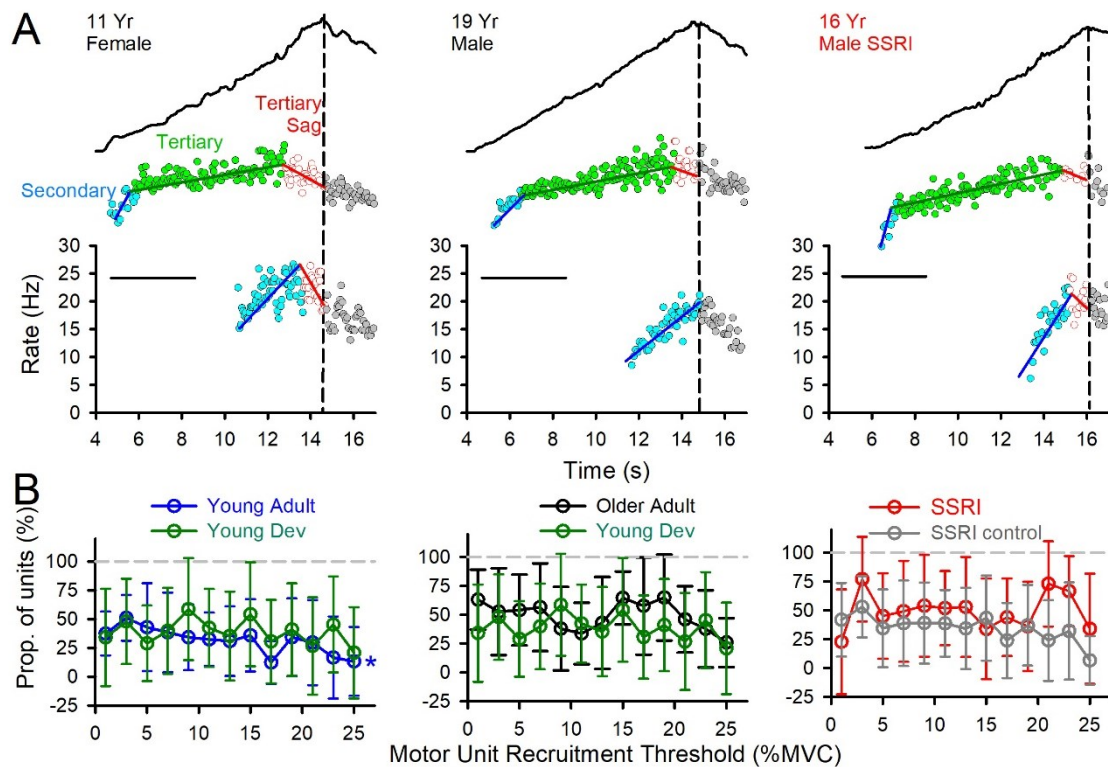
Figure 3.4. A) Representative examples of joined straight-line fits to the secondary (blue), tertiary (green) and tertiary sag (red) ranges (red) for lower threshold (middle) and higher threshold (bottom) motor units (replotted from Figure 2.5 in Chapter 2 on expanded time scale). The vertical dashed line marks peak torque. **B)** Proportion of units having a tertiary sag range plotted against the recruitment threshold of the motor units. Same group pairings as in Figure 3.2. Error bars ± SD.

Table 3.4 Prop. of Tertiary Sag	Young Dev	Young Adult	Adult	SSRI	SSRI control
(a) Mean ± SD %	36.63±10.51	32.43±13.24	49.23±12.30	49.27±16.00	36.33±10.45
	Young Dev vs Young Adult	Young Dev vs Older Adult	Young Adult vs Older Adult	SSRI vs Age-matched controls	
(b) Unpaired comparisons	p= 0.105 (S) t = 1.687	**p= 0.040 (S) t = -2.176**	**p= 0.001 (S) t= -3.703**	**p= 0.012 (S) t = 2.736**	

Table 3.4. a) Mean ± SD of proportion of all motor units with a tertiary sag range in the various groups. **b)** Unpaired comparison of group means from using Student's t-test (S), significant comparisons with p< 0.05 marked in bold.

As with the secondary and tertiary ranges in *Chapter 2*, we also examined if the slope and duration of the tertiary sag range changed with age. The slope, but not duration, of the tertiary sag range was negatively correlated with age across the young development and young adult groups (black line in Fig. 3.5 left graph, bolded numbers in Table 3.5b). However, there were no differences in the mean slope or duration of the tertiary sag range between the young development, young adult and adult groups (Table 3.5a,c). In contrast, the slope of the tertiary sag range was larger by ~ 40% in the SSRI group compared to their age-matched controls (solid circles in left graph of Fig. 3.5, bolded numbers in Table 3.5c).
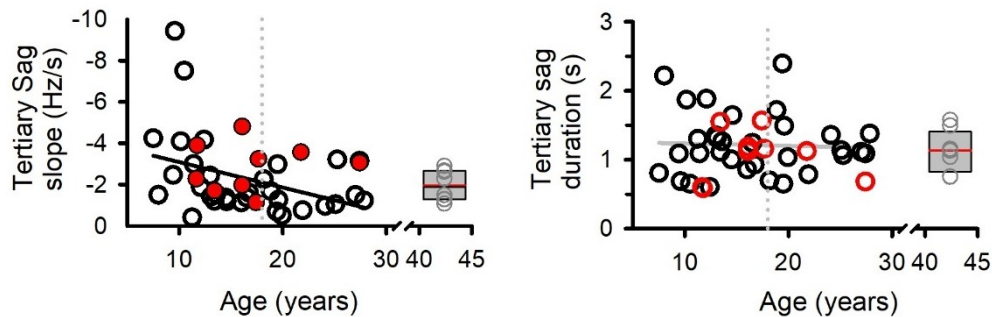
Figure 3.5. Average slope (left) and duration (right) of the tertiary sag range plotted across age for each participant in young development and young adult (open circles) and SSRI (red) groups and for the adults (box plot with individual participant data in grey circles, mean line in red, median line in black) plotted at the mean age of 42.4 years. Black regression lines denote a significant correlation with age. Filled red circles denote significant differences between SSRI and their age-matched controls (results of unpaired comparisons in Table 3.5c).

Table 3.5 Tertiary Sag	Young Dev	Young Adult	Older Adult	SSRI	SSRI age-matched control
(a) Mean slope (Hz/s)	-2.73 ± 2.32	-1.63 ± 0.95	-1.95 ± 0.74	-2.85 ± 1.169	-1.69 ± 0.94
Mean duration (s)	1.20 ± 0.44	1.22 ± 0.46	1.13 ± 0.29	1.06 ± 0.37	1.21 ± 0.39
	(b) Combo (7-28)	**(c)** Young Dev vs Young Adult	Young Dev vs Older Adult	Young Adult vs Older Adult	SSRI vs age-matched control
Tertiary Sag slope (Hz/s)	**r= -0.379, p= 0.033**	P= 0.116 (MW) T= 256.000	P= 0.614 (MW) T= 122.000	P= 0.328 (MW) T= 74.000	**p= 0.005 (S) t= 2.995**
Tertiary Sag duration (s)	r= 0.046, p= 0.803	P= 0.848 (MW) T= 220.000	p= 0.664 (S) t= 0.440	p= 0.621 (S) t= 0.503	p= 0.334 (S) t= -0.980

Table 3.5. a) Mean (±SD) of the slope and duration of the tertiary sag range. **b)** Correlation of the tertiary sag range (slope and duration) across the young development and young adult (Combo) groups. **c)** Results of Student's t-test (S) or Mann-Whitney Rank Sum (MW) comparisons between the various groups. Significant values where $p < 0.05$ are marked in bold.

We also examined if the slope and duration of the tertiary sag range varied with the recruitment threshold of the motor units within and across the different groups. The one-way ANOVA on Ranks showed there was no main effect of motor unit recruitment threshold on the tertiary sag slope or duration in all groups except for the tertiary range sag slope in the young development group (* in Fig. 3.6 top left, Table 3.6a). The two-way ANOVA showed no interaction effect with group and recruitment threshold in all group pairings but there was a main effect of group on the tertiary sag slope between the SSRI and SSRI control groups (solid circles in Fig. 3.6, top right and bolded numbers in Table 3.6b).
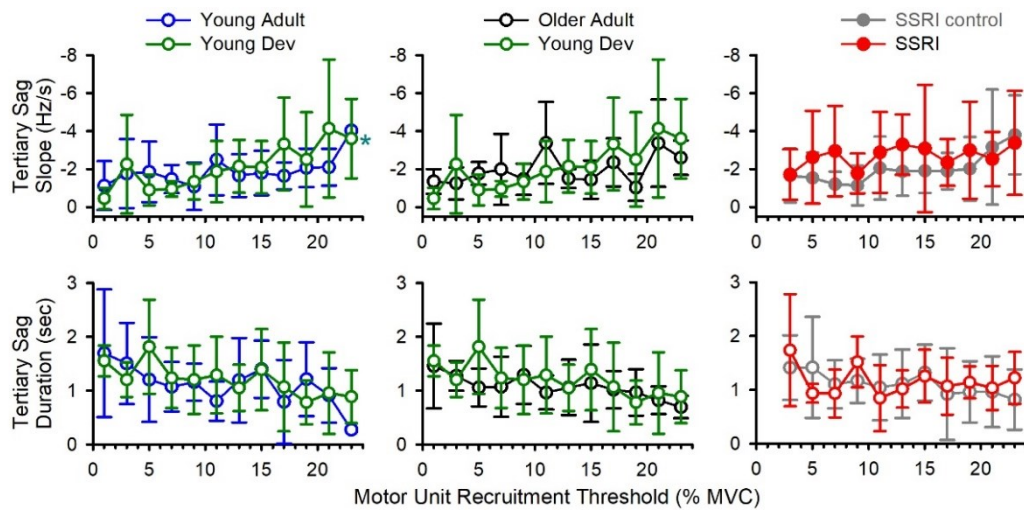
Figure 3.6. Slope (top) and duration (bottom) of the tertiary sag range plotted against recruitment threshold (RT) of the motor units. * = significant effect of RT on tertiary sag slope in young development group. Solid circles = significant effect of group between SSRI and SSRI control groups.

Table 3.6 (a) One-way ANOVA	Young Dev	Young Adult	Older Adult	SSRI
Tertiary sag slope	**H(11)=22.278 P= 0.002**	H(11)=14.150 P= 0.225	H(11)=16.953 P= 0.109	H(10)=3.712 P= 0.959
Tertiary sag duration	H(11)=15.350 P=0.167	H(11)=14.213 P= 0.287	F(11)=0.939 P= 0.511	H(10)=12.657 P= 0.242
(b) Two-way ANOVA	Young Dev vs Young Adult	Young Dev vs Older Adult	Young Adult vs Older Adult	SSRI vs age-matched control
Tertiary sag slope Group x RT	F(1,11)=0.932 P= 0.512	F(1,11)=1.356 P= 0.201	F(1,11)=0.764 P= 0.675	F(1,11)=0.713 P= 0.711
Group	F(1,11)=0.537 P= 0.465	F(1,11)=0.213 P= 0.646	F(1,11)=0.588 P= 0.445	**F(1,11)=6.457 P= 0.012**
RT	**F(1,11)=2.232 P= 0.015**	**F(1,11)=2.790 P= 0.003**	**F(1,11)=2.396 P= 0.010**	F(1,11)=1.640 P= 0.098
Tertiary sag duration Group x RT	F(1,11)=0.947 P= 0.497	F(11)=0.601 P= 0.825	F(1,11)=0.242 P= 0.994	F(1,11)=0.714 P= 0.711
Group	F(1,11)=0.807 P= 0.370	F(11)=1.750 P= 0.188	F(1,11)=0.449 P= 0.504	F(1,11)=0.259 P=0.611
RT	**F(1,11)=1.865 P= 0.048**	F(11)=1570 P= 0.114	F(1,11)=1.681 P= 0.085	**F(1,11)=1.898 P= 0.048**

Table 3.6. a) Results from one-way ANOVA and ANOVA on Ranks examining effect of recruitment threshold on the slope and duration of the tertiary sag range for data plotted in Figure 3.6. **b)** Results from two-way ANOVA comparing effects of group and recruitment threshold on tertiary sag range slope and duration. Significant values where p < 0.05 are marked in bold.

If the decrease in the firing rate of the motor units during the tertiary sag range is due to a decrease in common synaptic drive to the TA motoneuron pool, the start of tertiary sag range would likely be similar across all motor units. In contrast, if the start of the tertiary sag range was different across all motor units, it may be due to an intrinsic property of the motoneuron, such as late spike frequency adaptation (Brownstone, 2006), since each motoneuron may be independent of one another. To compare the start of the tertiary sag range across the different motor units, the time of onset of the tertiary sag range to the time of peak torque (length of pink arrow in Fig. 3.7A upper left graph) was measured. Since the time of peak torque was constant across all motor units, the duration of the tertiary sag range provided a proxy of its start time. For example, the shorter the duration of the tertiary sag range, the later it started in relation to the time of peak torque. Motor units with no tertiary sag range (e.g., middle bottom unit in Fig. 3.4A) were given a duration of 0 seconds. We compared the duration (i.e., start) of the tertiary sag range in a group of eight young and older adults having a large (≥ 20) number of decomposed motor units per contraction (Fig. 3.7A).
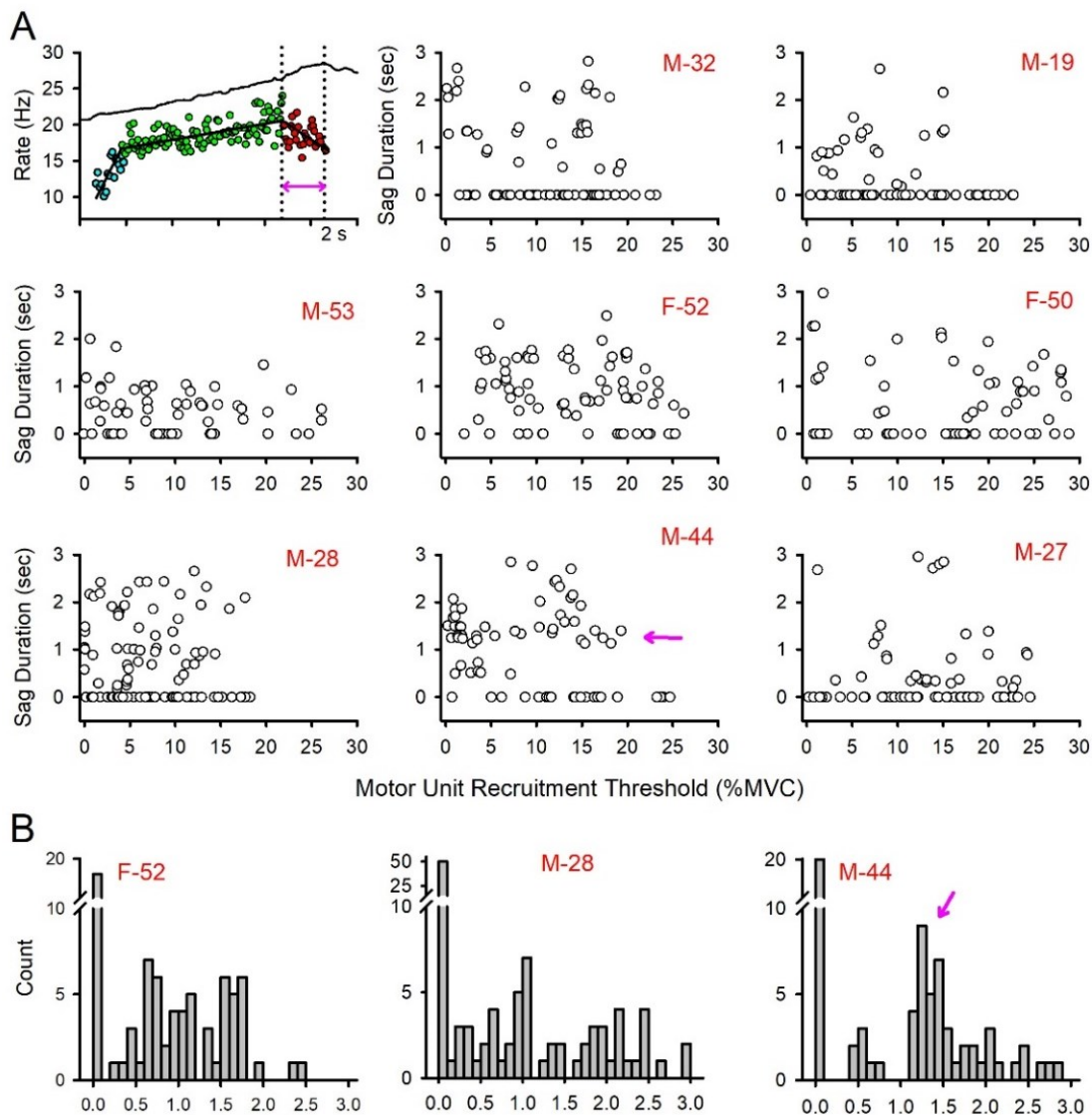
Figure 3.7. A) Top left: Duration of tertiary sag range measured from the start of the tertiary sag range to the peak of the dorsiflexion torque (length of pink arrow). **M-32 to M-44**: duration of the tertiary sag range plotted against recruitment threshold of the motor unit for all four contractions in each participant. Participant code (sex male (M), female (F)-age). **B)** Example histogram counts of tertiary sag range durations for participants F-52 and M-32 without a single peak and for participant M-44 with a single peak near 1.35 seconds.

As shown for these eight participants (Fig. 3.7A, M-32 to M-27), the duration of the tertiary sag range was quite variable across motor units of different recruitment thresholds. Around 50% of the motor units did *not* have a tertiary sag range (i.e., 0 s duration, see also Fig. 3.5), even in the low threshold motor units, consistent with their not being a decrease in synaptic drive to the TA motoneuron pool during the ascending phase of the triangular

contraction. For motor units of similar recruitment threshold *with* a tertiary sag firing range, the start (duration) varied between 0 to 3 seconds, indicating that although these motor units were recruited together, the tertiary sag range started at different times during the ascending phase of the contraction. When plotting the distribution of tertiary sag durations in each participant, typically there was no single distinct peak, besides at 0 ms, indicating a lack of common tertiary sag range start times across the motor units, as shown for participants F-52 and M-28 in Figure 3.7B. However, in one participant (M-44, bottom middle Fig. 3.7A), several motor units with different recruitment thresholds had a similar tertiary sag duration (at pink arrow) that resulted in a prominent single peak at 1.35 seconds (pink arrow, Fig. 3.7B, right graph), which could reflect a common decrease in synaptic drive across these units at this time. However, there were several motor units with similar recruitment thresholds that had tertiary sag start times above and below 1.35 seconds (Fig. 3.7A, M-44), consistent with their not being a common decrease in synaptic drive at this time.

The same analysis was performed for all nine participants in the SSRI group (F-16 to F27, Fig. 3.8) where the tertiary sag slope was steeper compared to the age-matched controls (Table 3.5a,c). Similar to the combined young and older adult group, there were many motor units without a tertiary sag range (0 ms duration, Fig. 3.8 top graphs for each participant). The start of the tertiary sag range was also variable across motor units of similar recruitment thresholds, without a marked peak in the corresponding histograms except for at 0 ms (Fig. 3.8 bottom graphs). These findings are consistent with a lack of a common decreasing synaptic drive to the TA motoneuron pool contributing to tertiary sag range.
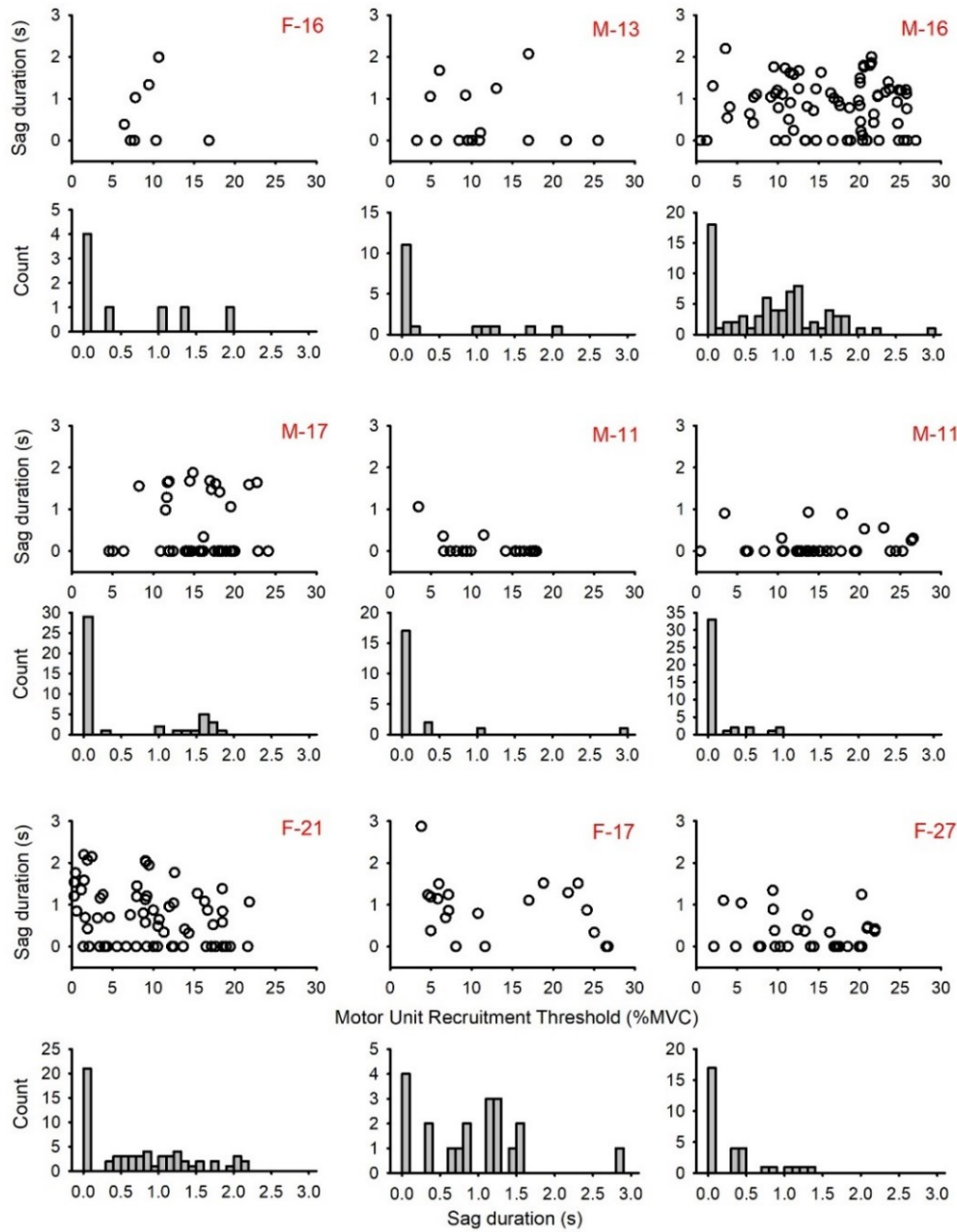
Figure 3.8. Same as Figure 3.7. **Top graphs:** duration of the tertiary sag range plotted against the recruitment threshold for all motor units from the four contractions in each participant taking SSRIs. **Bottom graphs:** Corresponding histograms counts of tertiary sag range durations.

Discussion

General Summary

Our results demonstrate that the firing behaviour of TA motor units during a matched, moderate dorsiflexion changes from child to adulthood, and in response to oral intake of SSRIs. For example, in children and adolescents between 7 and 17 years of age, the start, maximum and/or end firing rates are ~10% higher compared to young and older adults. Similarly, in participants taking SSRIs, start and maximum firing rates are ~15% higher compared to their age-matched controls. As we discuss below, developmental changes in the magnitude of synaptic drive and/or the intrinsic properties of the motoneurons likely contribute to the higher firing rates in the young development and SSRI groups. One common feature in all groups was the increase in maximum firing rates as the recruitment threshold of the motor units increased. This result is different compared to studies using 5-pin surface EMG and may be related to the more accurate identification of single motor units by the 64-electrode HDsEMG employed here. Finally, when present, the rate of decrease in firing rates before peak torque (i.e., slope of the tertiary sag range) slows with age across development and likewise, is faster in participants taking SSRIs compared to their age-matched controls. We provide initial evidence that this decrease in firing rate may result from an intrinsic property of the motoneuron, such as spike frequency adaptation, which may undergo developmental changes with age and be influenced by facilitation of motoneuron PICs from serotonin.

Higher firing rates in young development and SSRI participants

Previous reports have suggested that firing rates in prepubescent children are higher compared to adults at matched levels of MVC force to compensate for the inability to activate fast, type II motor units (Dotan *et al.*, 2012; Miller *et al.*, 2019). We show here that the

maximum and end firing rates decrease with age from 7 to 28 years with the young development group having higher rates compared to the young adult and/or older adult groups. The higher firing rates in the young development group may be produced by a higher synaptic drive needed to reach a comparable level of 30% MVC torque compared to the older adult groups if not as many large, fast motor units with higher force generation were recruited. Alternatively, or in addition, the amount of coactivation of the antagonist triceps surae muscles may be larger in the young development group so that a stronger voluntary drive is needed to counteract the opposing antagonist contraction (Frost *et al.*, 1997; Grosset *et al.*, 2008), as will be examined in the future (*Chapter 4*). The higher firing rates in the young development group may also be matched to faster twitch contraction times of the TA muscle since it progressively slows in dorsiflexors from 20 to 100 years of age (Vandervoort & McComas, 1986). However, twitch contraction times in the TA have not been measured in participants less than 20 years of age, leaving open the question if it is shorter in the young development group.

When taking the recruitment thresholds of the motor units into account, the start rates in the young development and SSRI groups were higher compared to the adult and SSRI control groups, respectively. Interestingly, the motor units in these two groups also have a steeper and shorter secondary range (*Chapter 2*), where a more rapidly activating PIC at recruitment could produce the observed higher start rates. The maximum firing rates were also higher in the SSRI group compared to the age-matched controls, consistent with 5-HT increasing the input resistance of the motoneuron (Harvey *et al.*, 2006a), facilitating the NaPIC and shortening the AHP (Harvey *et al.*, 2006b) to possibly produce higher rates of initial and steady firing rates.

Increasing maximum firing rates with recruitment threshold of the motor units

Studies utilizing intramuscular EMG and visual motor unit identification have shown that low threshold motor units peak at lower rates and forces compared to higher threshold motor units where firing rates continue to increase up to 100% MVC (Gydikov & Kosarov, 1974; Moritz *et al.*, 2005; Barry *et al.*, 2007; Oya *et al.*, 2009; Jesunathadas *et al.*, 2012). This pattern of firing rate discharge is logical for efficient muscle force production because low threshold motor units achieve peak tetanic forces at lower firing rates compared to higher threshold units given the slower twitch contraction times in the former [reviewed in (Piotrkiewicz & Türker, 2017)]. Thus, the low firing rates in lower threshold motor units keep the maximum firing rates tuned to their slower contraction times, potentially preventing unnecessary high firing rates and energy expenditure (Burke, 1968). Similarly, we also observe a positive relationship between maximum firing rates and recruitment threshold of the motor units isolated with HDsEMG and blind source decomposition where several motor units can be simultaneously identified during a single contraction. However, in some cases, the firing rates of the highest threshold motor units recruited near peak torque were less than the lower threshold motor units (e.g., dark blue profiles in Fig. 3.6G,H). This may be produced by a reduced availability of increasing suprathreshold current near the 30% MVC peak torque to drive the firing rates higher (Powers & Heckman, 2017). Future experiments will examine if the firing rates of these motor units can be driven higher by larger synaptic inputs during contractions that are > 30% MVC.

How are these results reconciled with other studies which show a decrease in maximum firing rates as the recruitment threshold of the motor unit increases to produce an onion skin effect? As mentioned in the Introduction, previous studies showing an onion skin effect in the TA at comparable contraction intensities (20 to 50% MVC) were decomposed using 5-pin surface arrays and a Precision Decomposition technique (De Luca & Hostage,

2010; Nawab *et al.*, 2010). This technique is prone to a greater probability of missing spikes from the superimposition of motor units during stronger contraction intensities (Farina & Enoka, 2011). Thus, missed spikes in the higher threshold units at higher forces would artificially produce lower firing rates. (Nawab *et al.*, 2010). Precision Decomposition also selects motor unit activation times based on the unit's local predicted firing rate, potentially producing artificially higher firing rates in the lower threshold units as well. In contrast, motor units visually isolated from intramuscular EMG or from 64-electrode HDsEMG and blind source decomposition may be less susceptible to missed spikes and forced firing rate profiles, and thus, show higher firing rates in progressively activated motor units (Farina & Enoka, 2011; Caillet *et al.*, 2023). Further studies using HDsEMG and blind source decomposition at higher contractions are needed to determine if increases in maximum firing rates with recruitment threshold is still maintained, as occurs with contractions up to 90% MVC for TA motor units visually identified from intramuscular EMG (Jesunathadas *et al.*, 2012).

Tertiary sag range

Half of the lower threshold motor units exhibited decreasing firing rates during the increasing dorsiflexion torque that could occur over a few seconds until peak torque was reached. This early decrease in firing rate, which forms the tertiary sag range, could result from a selective decrease in synaptic drive to the TA motoneuron pool while the synaptic drive to other synergistic muscles around the ankle and foot increased, contributing to an increase in net dorsiflexion torque. If the common synaptic drive to the TA motoneuron pool decreased, then the firing rate of all simultaneously activated motor units would likely have decreased at the same time. However, in some of the young and older adults where it was possible to examine the simultaneous firing behaviour of at least 20 or more motor units, the

start of the tertiary sag range was variable (up to 3 seconds), with some units of similar recruitment thresholds not exhibiting a tertiary sag range at all (Fig. 3.7). The variable onset of the tertiary sag firing range is consistent with a variable onset of spike frequency adaptation across the different motoneurons, a property that is intrinsic to the motoneuron (Brownstone, 2006). Likewise, a lack of a tertiary sag range in half of the motor units is consistent with a lack of decreasing synaptic drive during the ascending torque profile, especially for the lower threshold units firing in their tertiary range where firing rates should be linearly related to synaptic drive (Bennett *et al.*, 1998). Lastly, electromechanical delay (EMD), which is the time lag between muscle activation and the resulting production of muscle force (Schmid *et al.*, 2019), may also contribute to the decrease in firing rates before a decrease in joint torque was measured. However, the EMD for the TA muscle ranges from 30-50 ms (Go *et al.*, 2018) and is likely too short to appreciably contribute to the tertiary sag range which can start, on average, 1.2 seconds before peak torque.

If the tertiary sag range is indeed mediated by spike frequency adaptation, possible mechanisms include a hyperpolarizing SK_L current activated by calcium entering the L-type Ca channels mediating the PIC (Hallworth *et al.*, 2003; Li & Bennett, 2007), increases in the in Na^+- K^+ pump which removes 3 Na^+ ions and brings in 2 K^+ ions to produce a net hyperpolarization of the cell (Sawczuk *et al.*, 1997) or inactivation of Na^+ channels so motoneurons cannot keep up with higher rates of firing (Powers *et al.*, 1999; Powers & Heckman, 2017). It is interesting that motoneurons with large PICs have reduced spike frequency adaptation, potentially due to a reduced inactivation of the NaPIC that facilitates repetitive firing (Harvey *et al.*, 2006b; Button *et al.*, 2007). Thus, it was surprising that the SSRI group had a steeper tertiary range slope compared to the age-matched controls even though the SSRI group had larger estimates of PICs based on the ΔF and secondary range slope (*Chapter 2*). However, if larger PICs also produce a greater amount of calcium

91

activation of SK_L currents (Li & Bennett, 2007), this may also produce greater amounts of spike frequency activation to help clamp high firing rates. Further animal experiments and motoneuron modelling are needed to determine if any or all these mechanisms contribute to the tertiary sag range and how they may change with development or SSRI intake.

It was interesting that the proportion of motor units displaying a tertiary sag range was lower in higher threshold motor units compared to the lowest threshold units (Fig. 3.4). It may be that the highest threshold motor units recruited for just a few seconds before the synaptic drive began to decrease did not have enough calcium entering the PIC to activate SK_L currents and spike frequency adaptation. Moreover, the firing rate acceleration of these higher threshold units during the simultaneous activation of the PIC likely helped to increase the firing rates until peak torque. Thus, we need to determine in future experiments if prolonging the activation of these higher threshold units by continuing the contraction beyond 30% MVC would eventually produce a flattening or even decrease in firing rates, potentially allowing enough time to activate or inactivate conductances responsible for producing firing rate adaptation (see *Chapter 4*).

Conclusions and future directions

Our results show that the firing rates and/or spike frequency adaptation of TA motor units are different during development and in response to oral intake of SSRIs when tested at a moderate contraction of 30% MVC. Based on muscle and nerve histology from cadavers, it is estimated that the TA is comprised of 445 motor units (Feinstein *et al.*, 1955) [although potentially fewer in the older participants (McNeil *et al.*, 2005)], with 70% of all TA motor units being recruited at 30% of MVC (Feiereisen *et al.*, 1997). When HDsEMG was used to measure conduction velocity across multiple (~40) motor units in the TA, motor units recruited at 30% MVC were in the middle of the full range of conduction velocities and

estimated fiber diameters (Del Vecchio *et al.*, 2018). Although we likely sampled motor units up to the midrange of conduction velocities and motoneuron size, we potentially did not recruit the largest and fastest motoneurons, which may have different firing behaviours from the highest threshold motor units described here. Thus, further studies at contraction levels up to 100% MVC are needed to compare the full firing behaviour of motor units across development and in response to SSRIs. As detailed in *Chapter 4*, contractions stronger than 30% MVC will better characterize the firing rate saturation of the TA motor units to determine if the tertiary sag range is mediated by intrinsic properties of the motoneuron compared to a selective decrease in synaptic drive to the TA motoneuron pool. Finally, examining joints that are controlled by a single muscle, such as the FDI, should produce a closer match between the voluntary synaptic drive to the motoneuron pool of that muscle and the resulting joint torque to better dissociate intrinsic versus synaptic properties contributing to motor unit firing behaviour.

References for Chapter 3

Afsharipour B, Manzur N, Duchcherer J, Fenrich KF, Thompson CK, Negro F, Quinlan KA, Bennett DJ & Gorassini MA. (2020). Estimation of self-sustained activity produced by persistent inward currents using firing rate profiles of multiple motor units in humans. *J Neurophysiol* **124,** 63-85.

Armatas V, Bassa E, Patikas D, Kitsas I, Zangelidis G & Kotzamanidis C. (2010). Neuromuscular differences between men and prepubescent boys during a peak isometric knee extension intermittent fatigue test. *Pediatr Exerc Sci* **22,** 205-217.

Barry BK, Pascoe MA, Jesunathadas M & Enoka RM. (2007). Rate coding is compressed but variability is unaltered for motor units in a hand muscle of old adults. *J Neurophysiol* **97,** 3206-3218.

Bennett DJ, Li Y & Siu M. (2001). Plateau potentials in sacrocaudal motoneurons of chronic spinal rats, recorded in vitro. *J Neurophysiol* **86,** 1955-1971.

Binder MD, Powers RK & Heckman CJ. (2020). Nonlinear Input-Output Functions of Motoneurons. *Physiology (Bethesda)* **35,** 31-39.

Blimkie CJ. (1989). Age- and sex-associated variation in strength during childhood: Anthropometric, morphologic, neurologic, biomechanical, endocrinologic, genetic, and physical activity correlates., ed. Gisolfi C, editor, pp. 99-163. Benchmark Press, Indianapolis, IN.

Brownstone RM. (2006). Beginning at the end: repetitive firing properties in the final common pathway. *Prog Neurobiol* **78,** 156-172.

Burke RE. (1968). Firing patterns of gastrocnemius motor units in the decerebrate cat. *J Physiol* **196,** 631-654.

Button DC, Kalmar JM, Gardiner K, Cahill F & Gardiner PF. (2007). Spike frequency adaptation of rat hindlimb motoneurons. *J Appl Physiol (1985)* **102,** 1041-1050.

Caillet AH, Avrillon S, Kundu A, Yu T, Phillips ATM, Modenese L & Farina D. (2023). Larger and denser: an optimal design for surface grids of EMG electrodes to identify greater and more representative samples of motor units. *bioRxiv*.

Chalchat E, Piponnier E, Bontemps B, Julian V, Bocock O, Duclos M, Ratel S & Martin V. (2019). Characteristics of motor unit recruitment in boys and men at maximal and submaximal force levels. *Exp Brain Res* **237,** 1289-1302.

De Luca CJ, Adam A, Wotiz R, Gilmore LD & Nawab SH. (2006). Decomposition of surface EMG signals. *J Neurophysiol* **96,** 1646-1657.

De Luca CJ & Erim Z. (1994). Common drive of motor units in regulation of muscle force. *Trends Neurosci* **17,** 299-305.

De Luca CJ & Hostage EC. (2010). Relationship between firing rate and recruitment threshold of motoneurons in voluntary isometric contractions. *J Neurophysiol* **104,** 1034-1046.

De Luca CJ, LeFever RS, McCue MP & Xenakis AP. (1982). Behaviour of human motor units in different muscles during linearly varying contractions. *J Physiol* **329,** 113-128.

Del Vecchio A, Negro F, Felici F & Farina D. (2018). Distribution of muscle fibre conduction velocity for representative samples of motor units in the full recruitment range of the tibialis anterior muscle. *Acta Physiol (Oxf)* **222**.

Dotan R, Mitchell C, Cohen R, Klentrou P, Gabriel D & Falk B. (2012). Child-adult differences in muscle activation--a review. *Pediatr Exerc Sci* **24,** 2-21.

Eccles JC, Eccles RM & Lundberg A. (1958). The action potentials of the alpha motoneurones supplying fast and slow muscles. *J Physiol* **142,** 275-291.

Enoka RM. (2019). Physiological validation of the decomposition of surface EMG signals. *J Electromyogr Kinesiol* **46,** 70-83.

Erim Z, De Luca CJ, Mineo K & Aoki T. (1996). Rank-ordered regulation of motor units. *Muscle Nerve* **19,** 563-573.

Farina D & Enoka RM. (2011). Surface EMG decomposition requires an appropriate validation. *J Neurophysiol* **105,** 981-982; author reply 983-984.

Feiereisen P, Duchateau J & Hainaut K. (1997). Motor unit recruitment order during voluntary and electrically induced contractions in the tibialis anterior. *Exp Brain Res* **114,** 117-123.

Feinstein B, Lindegard B, Nyman E & Wohlfart G. (1955). Morphologic studies of motor units in normal human muscles. *Acta Anat (Basel)* **23,** 127-142.

Frost G, Dowling J, Dyson K & Bar-Or O. (1997). Cocontraction in three age groups of children during treadmill locomotion. *J Electromyogr Kinesiol* **7,** 179-186.

Fuglevand AJ, Lester RA & Johns RK. (2015). Distinguishing intrinsic from extrinsic factors underlying firing rate saturation in human motor units. *J Neurophysiol* **113,** 1310-1322.

Go SA, Litchy WJ, Evertz LQ & Kaufman KR. (2018). Evaluating skeletal muscle electromechanical delay with intramuscular pressure. *J Biomech* **76,** 181-188.

Gorassini M, Yang JF, Siu M & Bennett DJ. (2002). Intrinsic activation of human motoneurons: reduction of motor unit recruitment thresholds by repeated contractions. *J Neurophysiol* **87,** 1859-1866.

Grosset JF, Mora I, Lambertz D & Pérot C. (2008). Voluntary activation of the triceps surae in prepubertal children. *J Electromyogr Kinesiol* **18,** 455-465.

Gydikov A & Kosarov D. (1974). Some features of different motor units in human biceps brachii. *Pflugers Arch* **347,** 75-88.

Hallworth NE, Wilson CJ & Bevan MD. (2003). Apamin-sensitive small conductance calcium-activated potassium channels, through their selective coupling to voltage-gated calcium channels, are critical determinants of the precision, pace, and pattern of action potential generation in rat subthalamic nucleus neurons in vitro. *J Neurosci* **23,** 7525-7542.

Harvey PJ, Li X, Li Y & Bennett DJ. (2006a). 5-HT2 receptor activation facilitates a persistent sodium current and repetitive firing in spinal motoneurons of rats with and without chronic spinal cord injury. *J Neurophysiol* **96,** 1158-1170.

Harvey PJ, Li X, Li Y & Bennett DJ. (2006b). Endogenous monoamine receptor activation is essential for enabling persistent sodium currents and repetitive firing in rat spinal motoneurons. *J Neurophysiol* **96,** 1171-1186.

Henriksson-Larsen KB, Lexell J & Sjostrom M. (1983). Distribution of different fibre types in human skeletal muscles. I. Method for the preparation and analysis of cross-sections of whole tibialis anterior. *Histochem J* **15,** 167-178.

Holobar A, Minetto MA, Botter A, Negro F & Farina D. (2010). Experimental analysis of accuracy in the identification of motor unit spike trains from high-density surface EMG. *IEEE Trans Neural Syst Rehabil Eng* **18,** 221-229.

Hu X, Rymer WZ & Suresh NL. (2014). Control of motor unit firing during step-like increases in voluntary force. *Front Hum Neurosci* **8,** 721.

Jakobsson F, Edstrom L, Grimby L & Thornell LE. (1991). Disuse of anterior tibial muscle during locomotion and increased proportion of type II fibres in hemiplegia. *J Neurol Sci* **105,** 49-56.

Jesunathadas M, Klass M, Duchateau J & Enoka RM. (2012). Discharge properties of motor units during steady isometric contractions performed with the dorsiflexor muscles. *J Appl Physiol (1985)* **112,** 1897-1905.

Kernell D, Eerbeek O & Verhey BA. (1983). Relation between isometric force and stimulus rate in cat's hindlimb motor units of different twitch contraction time. *Exp Brain Res* **50,** 220-227.

Li X & Bennett DJ. (2007). Apamin-sensitive calcium-activated potassium currents (SK) are activated by persistent calcium currents in rat motoneurons. *J Neurophysiol* **97,** 3314-3330.

McNeil CJ, Doherty TJ, Stashuk DW & Rice CL. (2005). Motor unit number estimates in the tibialis anterior muscle of young, old, and very old men. *Muscle Nerve* **31,** 461-467.

Miller JD, Sterczala AJ, Trevino MA, Wray ME, Dimmick HL & Herda TJ. (2019). Motor unit action potential amplitudes and firing rates during repetitive muscle actions of the first dorsal interosseous in children and adults. *Eur J Appl Physiol* **119,** 1007-1018.

Moritz CT, Barry BK, Pascoe MA & Enoka RM. (2005). Discharge rate variability influences the variation in force fluctuations across the working range of a hand muscle. *J Neurophysiol* **93,** 2449-2459.

Nawab SH, Chang SS & De Luca CJ. (2010). High-yield decomposition of surface EMG signals. *Clin Neurophysiol* **121,** 1602-1615.

Negro F, Muceli S, Castronovo AM, Holobar A & Farina D. (2016). Multi-channel intramuscular and surface EMG decomposition by convolutive blind source separation. *J Neural Eng* **13,** 026027.

O'Brien TD, Reeves ND, Baltzopoulos V, Jones DA & Maganaris CN. (2010). In vivo measurements of muscle specific tension in adults and children. *Exp Physiol* **95,** 202-210.

Oya T, Riek S & Cresswell AG. (2009). Recruitment and rate coding organisation for soleus motor units across entire range of voluntary isometric plantar flexions. *J Physiol* **587,** 4737-4748.

Paasuke M, Ereline J & Gapeyeva H. (2000). Twitch contraction properties of plantar flexor muscles in pre- and post-pubertal boys and men. *Eur J Appl Physiol* **82,** 459-464.

Paraschos I, Hassani A, Bassa E, Hatzikotoulas K, Patikas D & Kotzamanidis C. (2007). Fatigue differences between adults and prepubertal males. *Int J Sports Med* **28,** 958-963.

Parra ME, Miller JD, Sterczala AJ, Trevino MA, Dimmick HL & Herda TJ. (2020). Differences in the firing rate versus recruitment threshold relationships of the vastus lateralis in children ages 7-10 years and adults. *Hum Mov Sci* **72,** 102650.

Piotrkiewicz M & Türker KS. (2017). Onion Skin or Common Drive? *Front Cell Neurosci* **11,** 2.

Powers RK & Binder MD. (1999). Models of spike encoding and their use in the interpretation of motor unit recordings in man. *Prog Brain Res* **123,** 83-98.

Powers RK & Heckman CJ. (2017). Synaptic control of the shape of the motoneuron pool input-output function. *J Neurophysiol* **117,** 1171-1184.

Powers RK, Sawczuk A, Musick JR & Binder MD. (1999). Multiple mechanisms of spike-frequency adaptation in motoneurones. *J Physiol Paris* **93,** 101-114.

Revill AL & Fuglevand AJ. (2011). Effects of persistent inward currents, accommodation, and adaptation on motor unit behaviour: a simulation study. *J Neurophysiol* **106,** 1467-1479.

Sawczuk A, Powers RK & Binder MD. (1995). Spike frequency adaptation studied in hypoglossal motoneurons of the rat. *J Neurophysiol* **73,** 1799-1810.

Sawczuk A, Powers RK & Binder MD. (1997). Contribution of outward currents to spike-frequency adaptation in hypoglossal motoneurons of the rat. *J Neurophysiol* **78,** 2246-2253.

Schmid L, Klotz T, Siebert T & Rohrle O. (2019). Characterization of Electromechanical Delay Based on a Biophysical Multi-Scale Skeletal Muscle Model. *Front Physiol* **10,** 1270.

Takazawa T, Croft GF, Amoroso MW, Studer L, Wichterle H & Macdermott AB. (2012). Maturation of spinal motor neurons derived from human embryonic stem cells. *PLoS One* **7,** e40154.

Vandervoort AA & McComas AJ. (1986). Contractile changes in opposing muscles of the human ankle joint with aging. *J Appl Physiol (1985)* **61,** 361-367.

Chapter 4

Final discussion and conclusions

Intrinsic conductances in motoneurons undergo developmental changes as animals and humans age, which can alter their transduction of synaptic inputs and ultimately, firing behaviour. To investigate these changes, we performed HDs-EMG recordings on the TA muscle of 50 neurologically intact participants between the ages of 7 and 53, including 9 individuals taking selective serotonin reuptake inhibitors (SSRI). Using the firing rate profiles of multiple, simultaneously identified single motor units and the ΔF technique (Afsharipour *et al.*, 2020), we analyzed the contribution of PICs (and potentially I_{CaNs}) to the self-sustained firing of TA motoneurons. Additionally, we investigated the non-linear firing behaviour of TA motor units during a gradually increasing isometric dorsiflexion to 30% MVC by measuring the slope and duration of the secondary, tertiary and tertiary sag ranges and comparing them between age groups, in participants taking oral SSRIs and across motor units of increasing recruitment thresholds.

Our findings in *Chapter 2* show that the young development group aged 7-18 years of age exhibit higher self-sustained activity and steeper secondary range slopes than the young adult (18-28 years) and older adult (32-53 years) groups that could be mediated by a larger amplitude and lower threshold PICs, respectively. Furthermore, the SSRI group had steeper secondary range slopes and larger ΔF values compared to the age-matched controls, consistent with elevated levels of spinal serotonin decreasing the threshold and increasing the amplitude, respectively, of motoneuron PICs. The ΔF values were significantly correlated to the slope of the secondary range, suggesting that both the amplitude and threshold of the PIC may covary. Moreover, torque steadiness increased as the ΔF and secondary slope decreased

99

during development, suggesting that large, low threshold PICs may make controlling

dorsiflexion force more challenging in children with underdeveloped corticospinal tracts.

In *Chapter 3*, we also measured the start, maximum and end firing rates of the motor

units in the same 50 participants. Younger participants between 7 to 18 years and those taking

SSRIs have higher rates of firing compared to participants 18 years and older and to controls

of a similar age group, respectively. A potential explanation for the higher rates observed in

younger participants is a stronger synaptic drive to the TA motoneuron pool. This could be

due to their inability to recruit fast, higher threshold units that produce larger forces so that

the slower motor units must compensate and fire faster, or from greater antagonist muscle

contractions that they must contract against. Higher firing rates in the SSRI group could be

mediated by serotonin decreasing the duration of the afterhyperpolarization (Miles *et al.*,

2007). We also observed that in most participants from all groups, the maximum firing rates

during the 30% MVC increased with the recruitment threshold of the motor unit. This pattern

is efficient for muscle force production because lower threshold motor units with slower

twitch contraction times can reach their peak force at lower firing rates compared to higher

threshold units. To prevent unnecessary energy expenditure, the firing rates of lower

threshold motor units are kept in check by firing rate saturation, which is tuned to their

slower contraction times (Eccles *et al.*, 1958; Burke, 1968), whereas higher threshold units

have less rate saturation to reach higher firing rates to match their shorter twitch contraction

times. Finally, in about half of the motor units despite an increasing effort and presumably

synaptic drive, the firing rate of the motor units began to decrease within 3 seconds or less

before peak torque, producing a tertiary sag range. The slope of the tertiary sag range appears

to decrease with age and increases in participants taking oral SSRIs. The steeper tertiary sag

slope compared to the age matched controls was not expected considering PICs, which are

larger in these groups, decrease spike frequency adaptation in animal studies (Harvey *et al.*,

2006b; Button *et al.*, 2007). While the origin of the tertiary sag range may be mediated by intrinsic conductances, a reduction in common synaptic drive to the TA motoneurons may also contribute to this phenomenon. However, initial findings indicate that the onset of the tertiary sag range is variable across the multiple, simultaneously recorded motor units, which suggests that a decrease in common synaptic drive to the TA motoneuron pool is not the sole cause of the tertiary sag range. An alternative explanation is that the sag is intrinsically mediated, possibly through the hyperpolarizing CaPIC-mediated SK_L current (Hallworth *et al.*, 2003; Li & Bennett, 2007). Further research is needed to confirm these findings and to better understand the underlying mechanisms of the tertiary sag range. Furthermore, the proportion of motor units having a tertiary sag firing range decreased in higher-threshold units, potentially because the prominent secondary ranges in these units kept the firing rate of the motoneurons accelerating until peak torque was reached.

Overall, our study provides new insights into the intricate relationship between motoneuron intrinsic properties, age, and motor unit firing profiles, highlighting the possible mechanisms that influence motoneuron firing behaviour and force unsteadiness.

Additional considerations

The lack of children under the age of 7 years represents a significant limitation in the scope of our investigation into the development of intrinsic motoneuron properties. This age range is critical for motor skill development, and as such, the exclusion of this age range limits our ability to fully understand the full developmental trajectories of motoneurons from newborn to adulthood. We were unable to conduct these recordings because children within this age range find it very difficult to match their ankle torque to the target triangle. This task was at the ability limit for children aged 7 to 10 years as shown by the large CoV in torque steadiness compared to older participants. Furthermore, the 64 electrode HDsEMG and blind
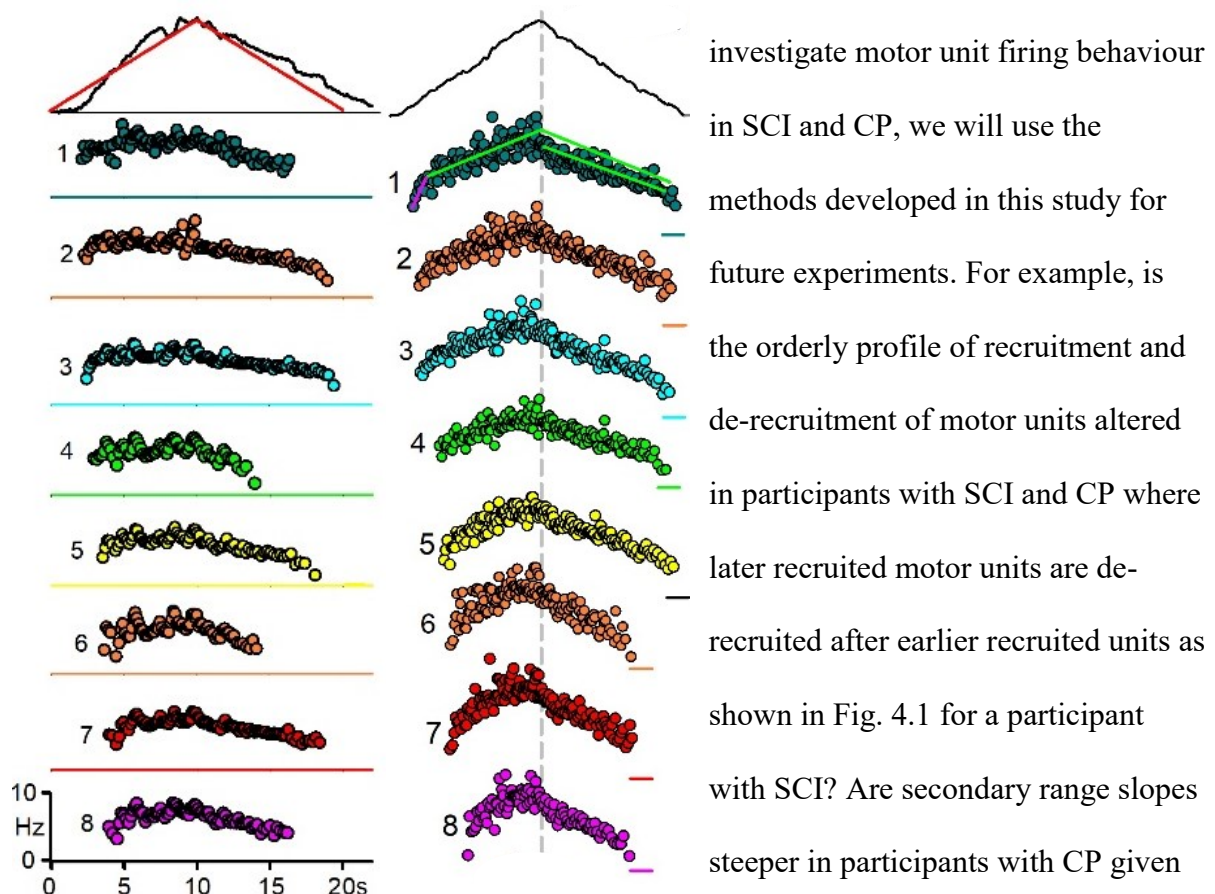
source separation method was unable to accurately decompose a large number of units in this age group, typically only yielding around 3-8 units per contraction. HDsEMG surface arrays with 256 electrodes produce twice the number of decomposed motor units in adults compared to the 64 electrode array (Caillet *et al.*, 2023) and should be tried in children to increase motor unit numbers. Animal experiments can also be a valuable tool for understanding the mechanisms that regulate motoneuron development, although both cervical and lumbar spinal cords tend to not survive in vitro past three weeks (Glazova *et al.*, 2015). However, experiments on the rodent sacral spinal cord, which survives *in vitro* into adulthood (Bennett *et al.*, 2004), can provide important insights into developmental changes in motoneurons after 3 weeks as rodents enter phases of sexual maturity and further motor skill development. Additionally, *in vivo* experiments using decerebrate cats and rats can also be used to examine developmental changes in motoneurons after 3 weeks to early adulthood (Meehan *et al.*, 2012). In conjunction with animal and human experiments, computer modelling can simulate the impact of different intrinsic conductances on motoneuron firing profiles (Powers & Heckman, 2015). By combining findings from animal experiments, computer modelling and our study, we can gain a more comprehensive understanding of the development of motoneurons and their relationship with synaptic inputs and intrinsic properties.

Our lack of assessment to determine if participants were pre-, pubertal or post-pubertal across the young development and young adult groups represents another limitation of our study. Future studies with larger sample sizes and assessment of sexual development may provide the opportunity to examine the effect of puberty on motoneuron development in more detail, allowing for a more comprehensive understanding of the relationship between age, puberty, and motoneuron development.

Future directions

Motor unit firing behaviour in neurotrauma

The firing behaviour of motoneurons observed in individuals with spinal cord injury (SCI) and cerebral palsy (CP) can vary significantly compared to age-matched, neurologically intact participants (Hounsgaard *et al.*, 1988; Powers & Binder, 2001; Rank *et al.*, 2011; D'Amico *et al.*, 2014; Condliffe *et al.*, 2016). Specifically, preliminary findings show that individuals with SCI have lower firing rates and shallower tertiary range slopes at matched levels of MVC, in addition to increased self-sustained activity (Fig 4.1) (D'Amico *et al.*, 2014). Such changes may be due to alterations in ion channel expression and synaptic input, resulting in heightened PICs that contribute to spasticity, a common symptom in both SCI and CP (Li *et al.*, 2004; Murray *et al.*, 2010). The altered balance of excitatory and inhibitory inputs to the motoneuron, with larger PICs and decreased postsynaptic inhibition, can also lead to involuntary spasms (D'Amico *et al.*, 2014; Trompetto *et al.*, 2014). To further investigate motor unit firing behaviour in SCI and CP, we will use the methods developed in this study for future experiments. For example, is the orderly profile of recruitment and de-recruitment of motor units altered in participants with SCI and CP where later recruited motor units are de-recruited after earlier recruited units as shown in Fig. 4.1 for a participant with SCI? Are secondary range slopes steeper in participants with CP given

that in animal studies, the threshold for PICs is hyperpolarized in spastic animals subjected to prenatal hypoxia/ischemia compared to sham controls, potentially due to higher levels of spinal serotonin (Li *et al.*, 2007)?

Figure 4.1. Comparison of Firing profiles in SCI and control participants. Dorsiflexion torque (top trace) and firing rate profile of 8 decomposed TA motor units during a triangular 20% maximum voluntary contraction (MVC) plotted from top to bottom in order of recruitment threshold. Left: firing profiles of a SCI patient. Right: firing profiles of a control participant.

Role of antagonist muscle activation

Future analysis from this thesis will include measuring the differences in antagonist soleus muscle activity in the different groups of participants. The role of antagonist soleus muscle activity on maximum firing rates needs to be measured to examine if enhanced soleus activity may be associated with greater firing rates in the agonist TA muscle in young children and SSRI participants (Reece & Herda, 2021). These investigations could provide a more comprehensive understanding of the factors contributing to motor performance in young individuals and those taking SSRIs, which could have important clinical implications for optimizing treatment and intervention strategies.

Contraction magnitude

In addition to 30% MVC, we recorded data for 10% and 20% MVC during the same experiment for all participants. We aim to compare these results with the 30% MVC data to observe any changes in the outcomes with lower intensities of contraction and if there are any differences in males versus females that we did not observe at 30% MVC (Alexandra Yacyshyn, personal communication).

Tertiary sag firing range

We plan to continue our investigation of the tertiary sag range. To ensure the accuracy and reliability of our findings, we will focus on analyzing data from participants who have at least 20 or more decomposed motor units per contraction. This is particularly important given that only ~ 50% of units exhibit a tertiary sag range, and participants with a low number of units may introduce sampling errors in the results. By carefully examining the data with this in mind, we aim to strengthen the validity of our conclusions that tertiary sag is produced from an intrinsic property of the motoneuron.

To investigate whether the tertiary sag is mediated by an intrinsic property of the motoneuron or if it is due to a decrease in common synaptic drive to the TA motoneuron pool, we examined the onset of the tertiary sag range across motor units of different recruitment thresholds in participants with a high number of units, primarily young adult and older adult participants (see Figure 3.7). First, we observed that 50% of motor units spanning all recruitment thresholds did not have a tertiary sag range, consistent with a lack of descending synaptic drive across the TA motoneuron pool during the ascending phase of the contraction. Second, we observed a variable onset (duration) of tertiary sag in relation to the time of peak torque across motor units of different recruitment thresholds, suggesting that the tertiary sag may have an intrinsic origin rather than being due to a decrease in synaptic drive as it is not happening at the same time in all units. However, in a few participants, we observed that the onset of the tertiary sag range occurred around the same time in a group of motor units, possibly indicating a decrease in the common synaptic drive to the motor units. We plan to conduct additional experiments to further examine the contributions of intrinsic properties and synaptic drive to the tertiary sag range. For example, we will perform voluntary contractions at higher levels of force, such as 50% MVC, to observe whether the results differ from those obtained with 30% MVC experiments. If a decrease in firing rate is

observed during a 50% MVC at the same level of torque as during a 30% MVC, it would

suggest the presence of spike frequency adaptation, where the firing rate of the motoneuron

cannot keep up with the increase in synaptic drive. On the other hand, if the firing rates of the

motor units continue to increase to 50% MVC, then the decreases we observed just before

peak torque at 30% MVC may be due to a decrease in synaptic drive. Moreover, if higher

threshold units that previously did not exhibit sag (Fig. 4.2B), start to display sag at higher

force levels (Fig. 4.2A), this indicates that the motoneuron needs to remain active for a longer
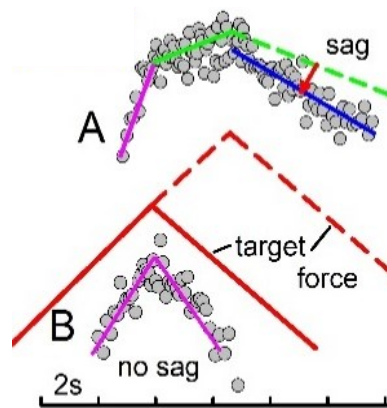
duration to develop sag.

Figure 4.2. Designed experiment to investigate sag in firing profiles. Tertiary sag is measured in 30% MVC and a high intensity contraction like 50% MVC. A) Secondary and tertiary region is shown with purple and green traces, respectively. The dashed green line is the reflected tertiary region in the descending phase and the blue line is fit to the descending phase. B) The dashed force line shows the higher intensity contraction compared to 30% MVC force profile shown with the red trace.

To provide a more complete comparison of tertiary sag firing, we will also measure

the tertiary sag range during the descending phase of the contraction. Specifically, we will

quantify the area of reduced firing rate below a predicted line (hatched lines in Fig. 4.3),

which is extrapolated from the ascending tertiary range slope and mirrored onto the

descending phase of the contraction (Fig 4.3). Thus, this is the predicted symmetrical firing

rate profile in the absence of any tertiary sag firing. By doing so, we will be able to make a

better comparison of the tertiary sag firing range between the participants with and without

injury and assess any changes that occur with recruitment threshold. These studies will also be complimented with animal studies using pharmacology to identify ion channels or exchangers that might be involved in spike frequency adaptation and with computer modelling which can modify conductances that cannot be specifically blocked with pharmacology, such as the SK_L current.
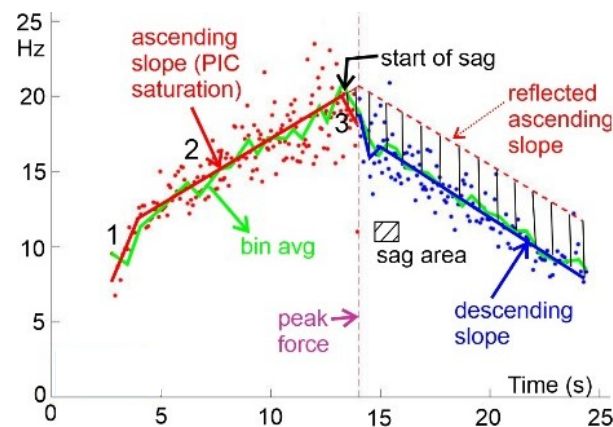
Figure 4.3. Quantifying tertiary sag range using the descending phase of the contraction. Sag is quantified by measuring the area between the tertiary range slope that is reflected and mirrored to descending phase and the descending firing rate (blue lines). Three continuous lines are fit to the ascending and descending phase, shown with red and blue traces, respectively. The green trace shows the average, binned firing profile (500 ms bins). Peak torque which separates the ascending and descending phase of the contraction is marked with the dashed pink line.

In summary, this thesis provides initial results demonstrating that intrinsic motoneuron properties change with development and in response to oral intake of SSRIs. Further studies are needed to examine earlier periods of development and the mechanisms contributing to the higher firing rates in the young development group and the underlying mechanisms producing spike frequency adaptation. These findings will be useful to compare to children with neurodevelopmental and motoneuron disorders.

References for Chapter 4

Afsharipour B, Manzur N, Duchcherer J, Fenrich KF, Thompson CK, Negro F, Quinlan KA, Bennett DJ & Gorassini MA. (2020). Estimation of self-sustained activity produced by persistent inward currents using firing rate profiles of multiple motor units in humans. *J Neurophysiol* **124,** 63-85.

Bennett DJ, Sanelli L, Cooke CL, Harvey PJ & Gorassini MA. (2004). Spastic long-lasting reflexes in the awake rat after sacral spinal cord injury. *J Neurophysiol* **91,** 2247-2258.

Burke RE. (1968). Firing patterns of gastrocnemius motor units in the decerebrate cat. *J Physiol* **196,** 631-654.

Button DC, Kalmar JM, Gardiner K, Cahill F & Gardiner PF. (2007). Spike frequency adaptation of rat hindlimb motoneurons. *J Appl Physiol (1985)* **102,** 1041-1050.

Caillet AH, Avrillon S, Kundu A, Yu T, Phillips ATM, Modenese L & Farina D. (2023). Larger and denser: an optimal design for surface grids of EMG electrodes to identify greater and more representative samples of motor units. *bioRxiv*.

Condliffe EG, Jeffery DT, Emery DJ & Gorassini MA. (2016). Spinal inhibition and motor function in adults with spastic cerebral palsy. *J Physiol* **594,** 2691-2705.

D'Amico JM, Condliffe EG, Martins KJ, Bennett DJ & Gorassini MA. (2014). Recovery of neuronal and network excitability after spinal cord injury and implications for spasticity. *Front Integr Neurosci* **8,** 36.

Eccles JC, Eccles RM & Lundberg A. (1958). The action potentials of the alpha motoneurones supplying fast and slow muscles. *J Physiol* **142,** 275-291.

Glazova MV, Pak ES & Murashov AK. (2015). Neurogenic potential of spinal cord organotypic culture. *Neurosci Lett* **594,** 60-65.

Hallworth NE, Wilson CJ & Bevan MD. (2003). Apamin-sensitive small conductance calcium-activated potassium channels, through their selective coupling to voltage-gated calcium channels, are critical determinants of the precision, pace, and pattern of action potential generation in rat subthalamic nucleus neurons in vitro. *J Neurosci* **23,** 7525-7542.

Harvey PJ, Li X, Li Y & Bennett DJ. (2006). Endogenous monoamine receptor activation is essential for enabling persistent sodium currents and repetitive firing in rat spinal motoneurons. *J Neurophysiol* **96,** 1171-1186.

Hounsgaard J, Hultborn H, Jespersen B & Kiehn O. (1988). Bistability of alpha-motoneurones in the decerebrate cat and in the acute spinal cat after intravenous 5-hydroxytryptophan. *J Physiol* **405,** 345-367.

Li X & Bennett DJ. (2007). Apamin-sensitive calcium-activated potassium currents (SK) are activated by persistent calcium currents in rat motoneurons. *J Neurophysiol* **97,** 3314-3330.

Li X, Murray K, Harvey PJ, Ballou EW & Bennett DJ. (2007). Serotonin facilitates a persistent calcium current in motoneurons of rats with and without chronic spinal cord injury. *J Neurophysiol* **97,** 1236-1246.

Li Y, Gorassini MA & Bennett DJ. (2004). Role of persistent sodium and calcium currents in motoneuron firing and spasticity in chronic spinal rats. *J Neurophysiol* **91,** 767-783.

Meehan CF, Grondahl L, Nielsen JB & Hultborn H. (2012). Fictive locomotion in the adult decerebrate and spinal mouse in vivo. *J Physiol* **590,** 289-300.

Miles GB, Hartley R, Todd AJ & Brownstone RM. (2007). Spinal cholinergic interneurons regulate the excitability of motoneurons during locomotion. *Proc Natl Acad Sci U S A* **104,** 2448-2453.

Murray KC, Nakae A, Stephens MJ, Rank M, D'Amico J, Harvey PJ, Li X, Harris RL, Ballou EW, Anelli R, Heckman CJ, Mashimo T, Vavrek R, Sanelli L, Gorassini MA, Bennett DJ & Fouad K. (2010). Recovery of motoneuron and locomotor function after spinal cord injury depends on constitutive activity in 5-HT2C receptors. *Nat Med* **16,** 694-700.

Powers RK & Binder MD. (2001). Input-output functions of mammalian motoneurons. *Rev Physiol Biochem Pharmacol* **143,** 137-263.

Powers RK & Heckman CJ. (2015). Contribution of intrinsic motoneuron properties to discharge hysteresis and its estimation based on paired motor unit recordings: a simulation study. *J Neurophysiol* **114,** 184-198.

Rank MM, Murray KC, Stephens MJ, D'Amico J, Gorassini MA & Bennett DJ. (2011). Adrenergic receptors modulate motoneuron excitability, sensory synaptic transmission and muscle spasms after chronic spinal cord injury. *J Neurophysiol* **105,** 410-422.

Reece TM & Herda TJ. (2021). An examination of a potential organized motor unit firing rate and recruitment scheme of an antagonist muscle during isometric contractions. *J Neurophysiol* **125,** 2094-2106.

Trompetto C, Marinelli L, Mori L, Pelosin E, Curra A, Molfetta L & Abbruzzese G. (2014). Pathophysiology of spasticity: implications for neurorehabilitation. *Biomed Res Int* **2014,** 354906.

Bibliography

Afsharipour B, Manzur N, Duchcherer J, Fenrich KF, Thompson CK, Negro F, Quinlan KA, Bennett DJ & Gorassini MA. (2020). Estimation of self-sustained activity produced by persistent inward currents using firing rate profiles of multiple motor units in humans. *J Neurophysiol* **124,** 63-85.

Armatas V, Bassa E, Patikas D, Kitsas I, Zangelidis G & Kotzamanidis C. (2010). Neuromuscular differences between men and prepubescent boys during a peak isometric knee extension intermittent fatigue test. *Pediatr Exerc Sci* **22,** 205-217.

Barrett JN & Crill WE. (1974). Influence of dendritic location and membrane properties on the effectiveness of synapses on cat motoneurones. *J Physiol* **239,** 325-345.

Barrientos RM, Brunton PJ, Lenz KM, Pyter L & Spencer SJ. (2019). Neuroimmunology of the female brain across the lifespan: Plasticity to psychopathology. *Brain Behav Immun* **79,** 39-55.

Barry BK, Pascoe MA, Jesunathadas M & Enoka RM. (2007). Rate coding is compressed but variability is unaltered for motor units in a hand muscle of old adults. *J Neurophysiol* **97,** 3206-3218.

Beauchamp JA, Pearcey GEP, Khurram OU, Chardon M, Wang YC, Powers RK, Dewald JPA & Heckman CJ. (2023). A geometric approach to quantifying the neuromodulatory effects of persistent inward currents on individual motor unit discharge patterns. *J Neural Eng* **20**.

Belanger AY & McComas AJ. (1989). Contractile properties of human skeletal muscle in childhood and adolescence. *Eur J Appl Physiol Occup Physiol* **58,** 563-567.

Bennett DJ, Hultborn H, Fedirchuk B & Gorassini M. (1998a). Short-term plasticity in hindlimb motoneurons of decerebrate cats. *J Neurophysiol* **80,** 2038-2045.

Bennett DJ, Hultborn H, Fedirchuk B & Gorassini M. (1998b). Synaptic activation of plateaus in hindlimb motoneurons of decerebrate cats. *J Neurophysiol* **80,** 2023-2037.

Bennett DJ, Li Y, Harvey PJ & Gorassini M. (2001a). Evidence for plateau potentials in tail motoneurons of awake chronic spinal rats with spasticity. *J Neurophysiol* **86,** 1972-1982.

Bennett DJ, Li Y & Siu M. (2001b). Plateau potentials in sacrocaudal motoneurons of chronic spinal rats, recorded in vitro. *J Neurophysiol* **86,** 1955-1971.

Bennett DJ, Sanelli L, Cooke CL, Harvey PJ & Gorassini MA. (2004). Spastic long-lasting reflexes in the awake rat after sacral spinal cord injury. *J Neurophysiol* **91,** 2247-2258.

Binder MD, Powers RK & Heckman CJ. (2020). Nonlinear Input-Output Functions of Motoneurons. *Physiology (Bethesda)* **35,** 31-39.

Blimkie CJ. (1989). Age- and sex-associated variation in strength during childhood: Anthropometric, morphologic, neurologic, biomechanical, endocrinologic, genetic, and physical activity correlates., ed. Gisolfi C, editor, pp. 99-163. Benchmark Press, Indianapolis, IN.

Bos R, Drouillas B, Bouhadfane M, Pecchi E, Trouplin V, Korogod SM & Brocard F. (2021). Trpm5 channels encode bistability of spinal motoneurons and ensure motor control of hindlimbs in mice. *Nat Commun* **12,** 6815.

Bos R, Harris-Warrick RM, Brocard C, Demianenko LE, Manuel M, Zytnicki D, Korogod SM & Brocard F. (2018). Kv1.2 Channels Promote Nonlinear Spiking Motoneurons for Powering Up Locomotion. *Cell Rep* **22,** 3315-3327.

Bouchant A, Martin V, Maffiuletti NA & Ratel S. (2011). Can muscle size fully account for strength differences between children and adults? *J Appl Physiol (1985)* **110,** 1748-1749.

Bregman BS. (1987). Development of serotonin immunoreactivity in the rat spinal cord and its plasticity after neonatal spinal cord lesions. *Brain Res* **431,** 245-263.

Brown MC, Jansen JK & Van Essen D. (1976). Polyneuronal innervation of skeletal muscle in new-born rats and its elimination during maturation. *J Physiol* **261,** 387-422.

Brownstone RM. (2006). Beginning at the end: repetitive firing properties in the final common pathway. *Prog Neurobiol* **78,** 156-172.

Buller AJ, Eccles JC & Eccles RM. (1960). Differentiation of fast and slow muscles in the cat hind limb. *J Physiol* **150,** 399-416.

Burke RE. (1967). Composite nature of the monosynaptic excitatory postsynaptic potential. *J Neurophysiol* **30,** 1114-1137.

Burke RE. (1968). Firing patterns of gastrocnemius motor units in the decerebrate cat. *J Physiol* **196,** 631-654.

Button DC, Gardiner K, Marqueste T & Gardiner PF. (2006). Frequency-current relationships of rat hindlimb alpha-motoneurones. *J Physiol* **573,** 663-677.

Button DC, Kalmar JM, Gardiner K, Cahill F & Gardiner PF. (2007). Spike frequency adaptation of rat hindlimb motoneurons. *J Appl Physiol (1985)* **102,** 1041-1050.

Caillet AH, Avrillon S, Kundu A, Yu T, Phillips ATM, Modenese L & Farina D. (2023). Larger and denser: an optimal design for surface grids of EMG electrodes to identify greater and more representative samples of motor units. *bioRxiv*.

Carlin KP, Jones KE, Jiang Z, Jordan LM & Brownstone RM. (2000). Dendritic L-type calcium currents in mouse spinal motoneurons: implications for bistability. *Eur J Neurosci* **12,** 1635-1646.

Carrascal L, Nieto-Gonzalez JL, Cameron WE, Torres B & Nunez-Abades PA. (2005). Changes during the postnatal development in physiological and anatomical characteristics of rat motoneurons studied in vitro. *Brain Res Brain Res Rev* **49,** 377-387.

Chalchat E, Piponnier E, Bontemps B, Julian V, Bocock O, Duclos M, Ratel S & Martin V. (2019). Characteristics of motor unit recruitment in boys and men at maximal and submaximal force levels. *Exp Brain Res* **237,** 1289-1302.

Cheng Y, Song N, Ge R & Dai Y. (2021). Serotonergic Modulation of Persistent Inward Currents in Serotonergic Neurons of Medulla in ePet-EYFP Mice. *Front Neural Circuits* **15,** 657445.

Condliffe EG, Jeffery DT, Emery DJ & Gorassini MA. (2016). Spinal inhibition and motor function in adults with spastic cerebral palsy. *J Physiol* **594,** 2691-2705.

Cushing S, Bui T & Rose PK. (2005). Effect of nonlinear summation of synaptic currents on the input-output properties of spinal motoneurons. *J Neurophysiol* **94,** 3465-3478.

D'Amico JM, Condliffe EG, Martins KJ, Bennett DJ & Gorassini MA. (2014). Recovery of neuronal and network excitability after spinal cord injury and implications for spasticity. *Front Integr Neurosci* **8,** 36.

D'Amico JM, Murray KC, Li Y, Chan KM, Finlay MG, Bennett DJ & Gorassini MA. (2013). Constitutively active 5-HT2/α1 receptors facilitate muscle spasms after human spinal cord injury. *J Neurophysiol* **109,** 1473-1484.

De Luca CJ, Adam A, Wotiz R, Gilmore LD & Nawab SH. (2006). Decomposition of surface EMG signals. *J Neurophysiol* **96,** 1646-1657.

De Luca CJ & Erim Z. (1994). Common drive of motor units in regulation of muscle force. *Trends Neurosci* **17,** 299-305.

De Luca CJ & Hostage EC. (2010). Relationship between firing rate and recruitment threshold of motoneurons in voluntary isometric contractions. *J Neurophysiol* **104,** 1034-1046.

De Luca CJ, LeFever RS, McCue MP & Xenakis AP. (1982). Behaviour of human motor units in different muscles during linearly varying contractions. *J Physiol* **329,** 113-128.

Del Vecchio A, Holobar A, Falla D, Felici F, Enoka RM & Farina D. (2020a). Tutorial: Analysis of motor unit discharge characteristics from high-density surface EMG signals. *J Electromyogr Kinesiol* **53,** 102426.

Del Vecchio A, Negro F, Felici F & Farina D. (2018). Distribution of muscle fibre conduction velocity for representative samples of motor units in the full recruitment range of the tibialis anterior muscle. *Acta Physiol (Oxf)* **222**.

Del Vecchio A, Sylos-Labini F, Mondì V, Paolillo P, Ivanenko Y, Lacquaniti F & Farina D. (2020b). Spinal motoneurons of the human newborn are highly synchronized during leg movements. *Sci Adv* **6**.

Di Matteo V, Pierucci M, Esposito E, Crescimanno G, Benigno A & Di Giovanni G. (2008). Serotonin modulation of the basal ganglia circuitry: therapeutic implication for Parkinson's disease and other motor disorders. *Prog Brain Res* **172,** 423-463.

Dotan R, Mitchell C, Cohen R, Klentrou P, Gabriel D & Falk B. (2012). Child-adult differences in muscle activation--a review. *Pediatr Exerc Sci* **24,** 2-21.

Dwyer JB & Bloch MH. (2019). Antidepressants for Pediatric Patients. *Curr Psychiatr* **18,** 26-42F.

Eccles JC, Eccles RM & Lundberg A. (1958). The action potentials of the alpha motoneurones supplying fast and slow muscles. *J Physiol* **142,** 275-291.

El Oussini H, Bayer H, Scekic-Zahirovic J, Vercruysse P, Sinniger J, Dirrig-Grosch S, Dieterle S, Echaniz-Laguna A, Larmet Y, Muller K, Weishaupt JH, Thal DR, van Rheenen W, van Eijk K, Lawson R, Monassier L, Maroteaux L, Roumier A, Wong PC, van den Berg LH, Ludolph AC, Veldink JH, Witting A & Dupuis L. (2016). Serotonin 2B receptor slows disease progression and prevents degeneration of spinal cord mononuclear phagocytes in amyotrophic lateral sclerosis. *Acta Neuropathol* **131,** 465-480.

Enoka RM. (2019). Physiological validation of the decomposition of surface EMG signals. *J Electromyogr Kinesiol* **46,** 70-83.

Erim Z, De Luca CJ, Mineo K & Aoki T. (1996). Rank-ordered regulation of motor units. *Muscle Nerve* **19,** 563-573.

Falk B, Usselman C, Dotan R, Brunton L, Klentrou P, Shaw J & Gabriel D. (2009). Child-adult differences in muscle strength and activation pattern during isometric elbow flexion and extension. *Appl Physiol Nutr Metab* **34,** 609-615.

Farina D & Enoka RM. (2011). Surface EMG decomposition requires an appropriate validation. *J Neurophysiol* **105,** 981-982; author reply 983-984.

Feiereisen P, Duchateau J & Hainaut K. (1997). Motor unit recruitment order during voluntary and electrically induced contractions in the tibialis anterior. *Exp Brain Res* **114,** 117-123.

Feinstein B, Lindegard B, Nyman E & Wohlfart G. (1955). Morphologic studies of motor units in normal human muscles. *Acta Anat (Basel)* **23,** 127-142.

Frost G, Dowling J, Dyson K & Bar-Or O. (1997). Cocontraction in three age groups of children during treadmill locomotion. *J Electromyogr Kinesiol* **7,** 179-186.

Fuglevand AJ, Lester RA & Johns RK. (2015). Distinguishing intrinsic from extrinsic factors underlying firing rate saturation in human motor units. *J Neurophysiol* **113,** 1310-1322.

Gao BX & Ziskind-Conhaim L. (1998). Development of ionic currents underlying changes in action potential waveforms in rat spinal motoneurons. *J Neurophysiol* **80,** 3047-3061.

Geertsen SS, Willerslev-Olsen M, Lorentzen J & Nielsen JB. (2017). Development and aging of human spinal cord circuitries. *J Neurophysiol* **118,** 1133-1140.

Gilfarb RA & Leuner B. (2022). GABA System Modifications During Periods of Hormonal Flux Across the Female Lifespan. *Front Behav Neurosci* **16,** 802530.

Glazova MV, Pak ES & Murashov AK. (2015). Neurogenic potential of spinal cord organotypic culture. *Neurosci Lett* **594,** 60-65.

Go SA, Litchy WJ, Evertz LQ & Kaufman KR. (2018). Evaluating skeletal muscle electromechanical delay with intramuscular pressure. *J Biomech* **76,** 181-188.

Goodlich BI, Del Vecchio A, Horan SA & Kavanagh JJ. (2023). Blockade of 5-HT(2) receptors suppress motor unit firing and estimates of persistent inward currents during voluntary muscle contraction in humans. *J Physiol*.

Gorassini M, Bennett DJ, Kiehn O, Eken T & Hultborn H. (1999). Activation patterns of hindlimb motor units in the awake rat and their relation to motoneuron intrinsic properties. *J Neurophysiol* **82,** 709-717.

Gorassini M, Yang JF, Siu M & Bennett DJ. (2002a). Intrinsic activation of human motoneurons: possible contribution to motor unit excitation. *J Neurophysiol* **87,** 1850-1858.

Gorassini M, Yang JF, Siu M & Bennett DJ. (2002b). Intrinsic activation of human motoneurons: reduction of motor unit recruitment thresholds by repeated contractions. *J Neurophysiol* **87,** 1859-1866.

Gorassini MA, Knash ME, Harvey PJ, Bennett DJ & Yang JF. (2004). Role of motoneurons in the generation of muscle spasms after spinal cord injury. *Brain* **127,** 2247-2258.

Gregory CM & Bickel CS. (2005). Recruitment patterns in human skeletal muscle during electrical stimulation. *Phys Ther* **85,** 358-364.

Grosset JF, Mora I, Lambertz D & Pérot C. (2008). Voluntary activation of the triceps surae in prepubertal children. *J Electromyogr Kinesiol* **18,** 455-465.

Gydikov A & Kosarov D. (1974). Some features of different motor units in human biceps brachii. *Pflugers Arch* **347,** 75-88.

Hallworth NE, Wilson CJ & Bevan MD. (2003). Apamin-sensitive small conductance calcium-activated potassium channels, through their selective coupling to voltage-gated calcium channels, are critical determinants of the precision, pace, and pattern of action potential generation in rat subthalamic nucleus neurons in vitro. *J Neurosci* **23,** 7525-7542.

Harvey PJ, Li X, Li Y & Bennett DJ. (2006a). 5-HT2 receptor activation facilitates a persistent sodium current and repetitive firing in spinal motoneurons of rats with and without chronic spinal cord injury. *J Neurophysiol* **96,** 1158-1170.

Harvey PJ, Li X, Li Y & Bennett DJ. (2006b). Endogenous monoamine receptor activation is essential for enabling persistent sodium currents and repetitive firing in rat spinal motoneurons. *J Neurophysiol* **96,** 1171-1186.

Harvey PJ, Li Y, Li X & Bennett DJ. (2006c). Persistent sodium currents and repetitive firing in motoneurons of the sacrocaudal spinal cord of adult rats. *J Neurophysiol* **96,** 1141-1157.

Hassan AS, Fajardo ME, Cummings M, McPherson LM, Negro F, Dewald JPA, Heckman CJ & Pearcey GEP. (2021). Estimates of persistent inward currents are reduced in upper limb motor units of older adults. *J Physiol* **599,** 4865-4882.

Heckman CJ, Hyngstrom AS & Johnson MD. (2008a). Active properties of motoneurone dendrites: diffuse descending neuromodulation, focused local inhibition. *J Physiol* **586,** 1225-1231.

Heckman CJ, Johnson M, Mottram C & Schuster J. (2008b). Persistent inward currents in spinal motoneurons and their influence on human motoneuron firing patterns. *Neuroscientist* **14,** 264-275.

Heckman CJ & Lee RH. (1999). The role of voltage-sensitive dendritic conductances in generating bistable firing patterns in motoneurons. *J Physiol Paris* **93,** 97-100.

Heckman CJ, Lee RH & Brownstone RM. (2003). Hyperexcitable dendrites in motoneurons and their neuromodulatory control during motor behavior. *Trends Neurosci* **26,** 688-695.

Henriksson-Larsen KB, Lexell J & Sjostrom M. (1983). Distribution of different fibre types in human skeletal muscles. I. Method for the preparation and analysis of cross-sections of whole tibialis anterior. *Histochem J* **15,** 167-178.

Holobar A, Minetto MA, Botter A, Negro F & Farina D. (2010). Experimental analysis of accuracy in the identification of motor unit spike trains from high-density surface EMG. *IEEE Trans Neural Syst Rehabil Eng* **18,** 221-229.

Hounsgaard J, Hultborn H, Jespersen B & Kiehn O. (1988). Bistability of alpha-motoneurones in the decerebrate cat and in the acute spinal cat after intravenous 5-hydroxytryptophan. *J Physiol* **405,** 345-367.

Hu X, Rymer WZ & Suresh NL. (2014). Control of motor unit firing during step-like increases in voluntary force. *Front Hum Neurosci* **8,** 721.

Hultborn H, Denton ME, Wienecke J & Nielsen JB. (2003). Variable amplification of synaptic input to cat spinal motoneurones by dendritic persistent inward current. *J Physiol* **552,** 945-952.

Hyngstrom AS, Johnson MD, Miller JF & Heckman CJ. (2007). Intrinsic electrical properties of spinal motoneurons vary with joint angle. *Nat Neurosci* **10,** 363-369.

Jakobsson F, Edstrom L, Grimby L & Thornell LE. (1991). Disuse of anterior tibial muscle during locomotion and increased proportion of type II fibres in hemiplegia. *J Neurol Sci* **105,** 49-56.

Jean-Xavier C, Sharples SA, Mayr KA, Lognon AP & Whelan PJ. (2018). Retracing your footsteps: developmental insights to spinal network plasticity following injury. *J Neurophysiol* **119,** 521-536.

Jensen DB, Kadlecova M, Allodi I & Meehan CF. (2020). Spinal motoneurones are intrinsically more responsive in the adult G93A SOD1 mouse model of amyotrophic lateral sclerosis. *J Physiol* **598,** 4385-4403.

Jesunathadas M, Klass M, Duchateau J & Enoka RM. (2012). Discharge properties of motor units during steady isometric contractions performed with the dorsiflexor muscles. *J Appl Physiol (1985)* **112,** 1897-1905.

Kanehisa H, Ikegawa S, Tsunoda N & Fukunaga T. (1994). Strength and cross-sectional area of knee extensor muscles in children. *Eur J Appl Physiol Occup Physiol* **68,** 402-405.

Kernell D. (1965). High-frequency repetitive firing of cat lumbosacral motoneurones stimulated by long-lasting injected currents. *Acta Physiol Scand* **65,** 74-86.

Kernell D, Eerbeek O & Verhey BA. (1983). Relation between isometric force and stimulus rate in cat's hindlimb motor units of different twitch contraction time. *Exp Brain Res* **50,** 220-227.

Kiehn O & Eken T. (1997). Prolonged firing in motor units: evidence of plateau potentials in human motoneurons? *J Neurophysiol* **78,** 3061-3068.

Kim EH, Wilson JM, Thompson CK & Heckman CJ. (2020). Differences in estimated persistent inward currents between ankle flexors and extensors in humans. *J Neurophysiol* **124,** 525-535.

Kluka V, Martin V, Vicencio SG, Jegu AG, Cardenoux C, Morio C, Coudeyre E & Ratel S. (2015). Effect of muscle length on voluntary activation level in children and adults. *Med Sci Sports Exerc* **47,** 718-724.

Larsson L, Grimby G & Karlsson J. (1979). Muscle strength and speed of movement in relation to age and muscle morphology. *J Appl Physiol Respir Environ Exerc Physiol* **46,** 451-456.

Lee RH & Heckman CJ. (1998). Bistability in spinal motoneurons in vivo: systematic variations in persistent inward currents. *J Neurophysiol* **80,** 583-593.

Lee RH & Heckman CJ. (2000). Adjustable amplification of synaptic input in the dendrites of spinal motoneurons in vivo. *J Neurosci* **20,** 6734-6740.

Lee RH, Kuo JJ, Jiang MC & Heckman CJ. (2003). Influence of active dendritic currents on input-output processing in spinal motoneurons in vivo. *J Neurophysiol* **89,** 27-39.

Leroy F, Lamotte d'Incamps B & Zytnicki D. (2015). Potassium currents dynamically set the recruitment and firing properties of F-type motoneurons in neonatal mice. *J Neurophysiol* **114,** 1963-1973.

Li X & Bennett DJ. (2007). Apamin-sensitive calcium-activated potassium currents (SK) are activated by persistent calcium currents in rat motoneurons. *J Neurophysiol* **97,** 3314-3330.

Li X, Murray K, Harvey PJ, Ballou EW & Bennett DJ. (2007). Serotonin facilitates a persistent calcium current in motoneurons of rats with and without chronic spinal cord injury. *J Neurophysiol* **97,** 1236-1246.

Li Y, Gorassini MA & Bennett DJ. (2004). Role of persistent sodium and calcium currents in motoneuron firing and spasticity in chronic spinal rats. *J Neurophysiol* **91,** 767-783.

Lloyd RS, Faigenbaum AD, Stone MH, Oliver JL, Jeffreys I, Moody JA, Brewer C, Pierce KC, McCambridge TM, Howard R, Herrington L, Hainline B, Micheli LJ, Jaques R, Kraemer WJ, McBride MG, Best TM, Chu DA, Alvar BA & Myer GD. (2014). Position statement on youth resistance training: the 2014 International Consensus. *Br J Sports Med* **48,** 498-505.

Maffiuletti NA, Aagaard P, Blazevich AJ, Folland J, Tillin N & Duchateau J. (2016). Rate of force development: physiological and methodological considerations. *Eur J Appl Physiol* **116,** 1091-1116.

Martin V, Kluka V, Garcia Vicencio S, Maso F & Ratel S. (2015). Children have a reduced maximal voluntary activation level of the adductor pollicis muscle compared to adults. *Eur J Appl Physiol* **115,** 1485-1491.

McNeil CJ, Doherty TJ, Stashuk DW & Rice CL. (2005). Motor unit number estimates in the tibialis anterior muscle of young, old, and very old men. *Muscle Nerve* **31,** 461-467.

Meehan CF, Grondahl L, Nielsen JB & Hultborn H. (2012). Fictive locomotion in the adult decerebrate and spinal mouse in vivo. *J Physiol* **590,** 289-300.

Meehan CF, Sukiasyan N, Zhang M, Nielsen JB & Hultborn H. (2010). Intrinsic properties of mouse lumbar motoneurons revealed by intracellular recording in vivo. *J Neurophysiol* **103,** 2599-2610.

Merton PA. (1954). Voluntary strength and fatigue. *J Physiol* **123,** 553-564.

Miles GB, Hartley R, Todd AJ & Brownstone RM. (2007). Spinal cholinergic interneurons regulate the excitability of motoneurons during locomotion. *Proc Natl Acad Sci U S A* **104,** 2448-2453.

Miller JD, Sterczala AJ, Trevino MA, Wray ME, Dimmick HL & Herda TJ. (2019). Motor unit action potential amplitudes and firing rates during repetitive muscle actions of the first dorsal interosseous in children and adults. *Eur J Appl Physiol* **119,** 1007-1018.

Mizuno N & Itoh H. (2009). Functions and regulatory mechanisms of Gq-signaling pathways. *Neurosignals* **17,** 42-54.

Moritz CT, Barry BK, Pascoe MA & Enoka RM. (2005). Discharge rate variability influences the variation in force fluctuations across the working range of a hand muscle. *J Neurophysiol* **93,** 2449-2459.

Murray KC, Nakae A, Stephens MJ, Rank M, D'Amico J, Harvey PJ, Li X, Harris RL, Ballou EW, Anelli R, Heckman CJ, Mashimo T, Vavrek R, Sanelli L, Gorassini MA, Bennett DJ & Fouad K. (2010). Recovery of motoneuron and locomotor function after spinal cord injury depends on constitutive activity in 5-HT2C receptors. *Nat Med* **16,** 694-700.

Murray KC, Stephens MJ, Ballou EW, Heckman CJ & Bennett DJ. (2011). Motoneuron excitability and muscle spasms are regulated by 5-HT2B and 5-HT2C receptor activity. *J Neurophysiol* **105,** 731-748.

Nakanishi ST & Whelan PJ. (2010). Diversification of intrinsic motoneuron electrical properties during normal development and botulinum toxin-induced muscle paralysis in early postnatal mice. *J Neurophysiol* **103,** 2833-2845.

Nawab SH, Chang SS & De Luca CJ. (2010). High-yield decomposition of surface EMG signals. *Clin Neurophysiol* **121,** 1602-1615.

Negro F, Muceli S, Castronovo AM, Holobar A & Farina D. (2016). Multi-channel intramuscular and surface EMG decomposition by convolutive blind source separation. *J Neural Eng* **13,** 026027.

Nezu A, Kimura S, Uehara S, Kobayashi T, Tanaka M & Saito K. (1997). Magnetic stimulation of motor cortex in children: maturity of corticospinal pathway and problem of clinical application. *Brain Dev* **19,** 176-180.

O'Brien TD, Reeves ND, Baltzopoulos V, Jones DA & Maganaris CN. (2010). In vivo measurements of muscle specific tension in adults and children. *Exp Physiol* **95,** 202-210.

O'Brien TD, Reeves ND, Baltzopoulos V, Jones DA & Maganaris CN. (2012). Commentary on child-adult differences in muscle activation--a review. *Pediatr Exerc Sci* **24,** 22-25.

Oliveira DS, Casolo A, Balshaw TG, Maeo S, Lanza MB, Martin NRW, Maffulli N, Kinfe TM, Eskofier BM, Folland JP, Farina D & Del Vecchio A. (2022). Neural decoding from surface high-density EMG signals: influence of anatomy and synchronization on the number of identified motor units. *J Neural Eng* **19**.

Orssatto LBR, Borg DN, Blazevich AJ, Sakugawa RL, Shield AJ & Trajano GS. (2021). Intrinsic motoneuron excitability is reduced in soleus and tibialis anterior of older adults. *Geroscience* **43,** 2719-2735.

Oya T, Riek S & Cresswell AG. (2009). Recruitment and rate coding organisation for soleus motor units across entire range of voluntary isometric plantar flexions. *J Physiol* **587,** 4737-4748.

Paasuke M, Ereline J & Gapeyeva H. (2000). Twitch contraction properties of plantar flexor muscles in pre- and post-pubertal boys and men. *Eur J Appl Physiol* **82,** 459-464.

Paraschos I, Hassani A, Bassa E, Hatzikotoulas K, Patikas D & Kotzamanidis C. (2007). Fatigue differences between adults and prepubertal males. *Int J Sports Med* **28,** 958-963.

Parmiggiani F & Stein RB. (1981). Nonlinear summation of contractions in cat muscles. II. Later facilitation and stiffness changes. *J Gen Physiol* **78,** 295-311.

Parra ME, Miller JD, Sterczala AJ, Trevino MA, Dimmick HL & Herda TJ. (2020). Differences in the firing rate versus recruitment threshold relationships of the vastus lateralis in children ages 7-10 years and adults. *Hum Mov Sci* **72,** 102650.

Perrier JF, Alaburda A & Hounsgaard J. (2002). Spinal plasticity mediated by postsynaptic L-type Ca2+ channels. *Brain Res Brain Res Rev* **40,** 223-229.

Perrier JF & Cotel F. (2008). Serotonin differentially modulates the intrinsic properties of spinal motoneurons from the adult turtle. *J Physiol* **586,** 1233-1238.

Perrier JF, Rasmussen HB, Christensen RK & Petersen AV. (2013). Modulation of the intrinsic properties of motoneurons by serotonin. *Curr Pharm Des* **19,** 4371-4384.

Petersen TH, Kliim-Due M, Farmer SF & Nielsen JB. (2010). Childhood development of common drive to a human leg muscle during ankle dorsiflexion and gait. *J Physiol* **588,** 4387-4400.

Piotrkiewicz M & Türker KS. (2017). Onion Skin or Common Drive? *Front Cell Neurosci* **11,** 2.

Powers RK & Binder MD. (1999). Models of spike encoding and their use in the interpretation of motor unit recordings in man. *Prog Brain Res* **123,** 83-98.

Powers RK & Binder MD. (2001). Input-output functions of mammalian motoneurons. *Rev Physiol Biochem Pharmacol* **143,** 137-263.

Powers RK & Heckman CJ. (2015). Contribution of intrinsic motoneuron properties to discharge hysteresis and its estimation based on paired motor unit recordings: a simulation study. *J Neurophysiol* **114,** 184-198.

Powers RK & Heckman CJ. (2017). Synaptic control of the shape of the motoneuron pool input-output function. *J Neurophysiol* **117,** 1171-1184.

Powers RK, Nardelli P & Cope TC. (2008). Estimation of the contribution of intrinsic currents to motoneuron firing based on paired motoneuron discharge records in the decerebrate cat. *J Neurophysiol* **100,** 292-303.

Powers RK, Sawczuk A, Musick JR & Binder MD. (1999). Multiple mechanisms of spike-frequency adaptation in motoneurones. *J Physiol Paris* **93,** 101-114.

Quinlan KA, Schuster JE, Fu R, Siddique T & Heckman CJ. (2011). Altered postnatal maturation of electrical properties in spinal motoneurons in a mouse model of amyotrophic lateral sclerosis. *J Physiol* **589,** 2245-2260.

Rank MM, Murray KC, Stephens MJ, D'Amico J, Gorassini MA & Bennett DJ. (2011). Adrenergic receptors modulate motoneuron excitability, sensory synaptic transmission and muscle spasms after chronic spinal cord injury. *J Neurophysiol* **105,** 410-422.

Reece TM & Herda TJ. (2021). An examination of a potential organized motor unit firing rate and recruitment scheme of an antagonist muscle during isometric contractions. *J Neurophysiol* **125,** 2094-2106.

Revill AL, Chu NY, Ma L, LeBlancq MJ, Dickson CT & Funk GD. (2019). Postnatal development of persistent inward currents in rat XII motoneurons and their modulation by serotonin, muscarine and noradrenaline. *J Physiol* **597,** 3183-3201.

Revill AL & Fuglevand AJ. (2011). Effects of persistent inward currents, accommodation, and adaptation on motor unit behavior: a simulation study. *J Neurophysiol* **106,** 1467-1479.

Rose PK & Neuber-Hess M. (1991). Morphology and frequency of axon terminals on the somata, proximal dendrites, and distal dendrites of dorsal neck motoneurons in the cat. *J Comp Neurol* **307,** 259-280.

Sawczuk A, Powers RK & Binder MD. (1995). Spike frequency adaptation studied in hypoglossal motoneurons of the rat. *J Neurophysiol* **73,** 1799-1810.

Sawczuk A, Powers RK & Binder MD. (1997). Contribution of outward currents to spike-frequency adaptation in hypoglossal motoneurons of the rat. *J Neurophysiol* **78,** 2246-2253.

Schmid L, Klotz T, Siebert T & Rohrle O. (2019). Characterization of Electromechanical Delay Based on a Biophysical Multi-Scale Skeletal Muscle Model. *Front Physiol* **10,** 1270.

Schwindt PC & Crill WE. (1982). Factors influencing motoneuron rhythmic firing: results from a voltage-clamp study. *J Neurophysiol* **48,** 875-890.

Scott W, Stevens J & Binder-Macleod SA. (2001). Human skeletal muscle fiber type classifications. *Phys Ther* **81,** 1810-1816.

Sharples SA & Miles GB. (2021). Maturation of persistent and hyperpolarization-activated inward currents shapes the differential activation of motoneuron subtypes during postnatal development. *Elife* **10**.

Shield A & Zhou S. (2004). Assessing voluntary muscle activation with the twitch interpolation technique. *Sports Med* **34,** 253-267.

Skinner JW, Christou EA & Hass CJ. (2019). Lower Extremity Muscle Strength and Force Variability in Persons With Parkinson Disease. *J Neurol Phys Ther* **43,** 56-62.

Smith CC & Brownstone RM. (2020). Spinal motoneuron firing properties mature from rostral to caudal during postnatal development of the mouse. *J Physiol* **598,** 5467-5485.

Svirskis G & Hounsgaard J. (1997). Depolarization-induced facilitation of a plateau-generating current in ventral horn neurons in the turtle spinal cord. *J Neurophysiol* **78,** 1740-1742.

Takazawa T, Croft GF, Amoroso MW, Studer L, Wichterle H & Macdermott AB. (2012). Maturation of spinal motor neurons derived from human embryonic stem cells. *PLoS One* **7,** e40154.

Taylor CA, Kopicko BH, Negro F & Thompson CK. (2022). Sex differences in the detection of motor unit action potentials identified using high-density surface electromyography. *J Electromyogr Kinesiol* **65,** 102675.

Thompson CK & Hornby TG. (2013). Divergent modulation of clinical measures of volitional and reflexive motor behaviors following serotonergic medications in human incomplete spinal cord injury. *J Neurotrauma* **30,** 498-502.

Thorstensson A, Grimby G & Karlsson J. (1976). Force-velocity relations and fiber composition in human knee extensor muscles. *J Appl Physiol* **40,** 12-16.

Trompetto C, Marinelli L, Mori L, Pelosin E, Curra A, Molfetta L & Abbruzzese G. (2014). Pathophysiology of spasticity: implications for neurorehabilitation. *Biomed Res Int* **2014,** 354906.

Ulfhake B & Cullheim S. (1988). Postnatal development of cat hind limb motoneurons. III: Changes in size of motoneurons supplying the triceps surae muscle. *J Comp Neurol* **278,** 103-120.

Ulfhake B, Cullheim S & Franson P. (1988). Postnatal development of cat hind limb motoneurons. I: Changes in length, branching structure, and spatial distribution of dendrites of cat triceps surae motoneurons. *J Comp Neurol* **278,** 69-87.

Vandenberk MS & Kalmar JM. (2014). An evaluation of paired motor unit estimates of persistent inward current in human motoneurons. *J Neurophysiol* **111,** 1877-1884.

Vandervoort AA & McComas AJ. (1986). Contractile changes in opposing muscles of the human ankle joint with aging. *J Appl Physiol (1985)* **61,** 361-367.

Vinay L, Brocard F & Clarac F. (2000). Differential maturation of motoneurons innervating ankle flexor and extensor muscles in the neonatal rat. *Eur J Neurosci* **12,** 4562-4566.

Wei K, Glaser JI, Deng L, Thompson CK, Stevenson IH, Wang Q, Hornby TG, Heckman CJ & Kording KP. (2014). Serotonin affects movement gain control in the spinal cord. *J Neurosci* **34,** 12690-12700.

Willerslev-Olsen M, Andersen JB, Sinkjaer T & Nielsen JB. (2014). Sensory feedback to ankle plantar flexors is not exaggerated during gait in spastic hemiplegic children with cerebral palsy. *J Neurophysiol* **111,** 746-754.

Wood CL, Lane LC & Cheetham T. (2019). Puberty: Normal physiology (brief overview). *Best Pract Res Clin Endocrinol Metab* **33,** 101265.

Xia Y, Chen D, Xia H, Liao Z, Tang W & Yan Y. (2017). Serotonergic projections to lumbar levels and its plasticity following spinal cord injury. *Neurosci Lett* **649,** 70-77.

Yeo SS, Jang SH & Son SM. (2014). The different maturation of the corticospinal tract and corticoreticular pathway in normal brain development: diffusion tensor imaging study. *Front Hum Neurosci* **8,** 573.